AD 285 356

COGNITIVE SYSTEMS RESEARCH PROGRAM

CORNELL UNIVERSITY ITHACA, N. Y.

REPORT NO. 3

ANALOGUE MEMORY MECHANISMS FOR NEURAL NETS

BY

GEORGE NAGY

August 31, 1962

Prepared Under Contract No. NONR 401 (40)

CSRP

COGNITIVE SYSTEMS RESEARCH PROGRAM

Cornell University Ithaca, New York

Report No. 3

Analogue Memory Mechanisms for Neural Nets

by

George Nagy

August 31, 1962

Prepared under Contract No. NONR 401 (40). Reproduction, translation, publication, use and disposal in whole or in part by or for the United States Government is permitted. This thesis was accepted by the Graduate Faculty of Cornell University in partial fulfillment of the requirements for the degree of Doctor of Philosophy.

SUMMARY

The need for a component capable of simulating semi-permanent changes in biological neurons, suitable for inclusion in brain models, and in perceptrons in particular, is discussed. Various devices intended for this purpose are reviewed and evaluated. A novel method of flux integration, using a permalloy wire as the flux storing medium, and the voltage induced in a search coil as the result of magnetostriction in the wire for readout, is described in detail. The design procedure for the complete memory of an audio-perceptron, Tobermory, based on the magnetostrictive readout integrator, is outlined. Modifications in the integrator, intended to render it suitable for larger and topologically more sophisticated models, are anticipated.

ACKNOWLEDGEMENTS

The author's primary debt of gratitude is due to Dr. Charles Rosen, of the Stanford Research Institute, who originated the idea of the magnetostrictive readout flux integrator, and to George Forsen, also of the Stanford Research Institute, whose advice on many points materially speeded progress.

The author is also deeply indebted to Dr. Frank Rosenblatt, the Director of the Cognitive Systems Research Program, especially for his help in the early phases of the work described, as well as to the other members of the Staff, who were never to busy to offer advice or lend a ready hand with the measurements.

Finally, the author wishes to express his appreciation for the patronage of the Office of Naval Research, whose financial assistance has supported the project from its inception.

TABLE OF CONTENTS

LIST OF FIGURES

LIST OF FIGURES (continued)

LIST OF FIGURES (continued)

TABLES

I. INTRODUCTION

When the Ancients discovered, after a few tentative post-mortems during the time of Hippocrates, that the origins of Thought--whether in the brain or in the abodomen--were unfathomable, they postulated the existence of the Mind.

The chief tenet of the Mind hypothesis was that the Mind has no physical attributes, hence introspection furnishes the sole means of studying its properties. Accordingly, in the next two or three thousand years a great deal of effort was devoted to meditation and contemplation, with most of the energy directed towards attempting to determine whether the Mind was endowed with one particularly elusive quality, that of immortality.

The investigation of this thorny problem was the cynosure of scientific endeavour until the middle of the Eighteenth Century, when dissectionists once more resumed the task abandoned by their Greek colleagues. This time progress was swift: by the end of the Nineteenth Century, fairly extensive information was available on the anatomy of the nervous system, and staining techniques were rapidly coming into their own to permit detailed study of the structure of the brain itself. It was only then that the full complexity of the Mind problem came to light: even early estimates placed the number of nerve cells, or neurons, within the Central Nervous System, at upwards of five billion!

Ramon y Cajal (1852-1934) was the first to establish beyond doubt--beyond reasonable doubt, that is--that the neurons are the primary functional units of the brain. Subsequent workers discovered numerous

properties of the neuron: some of these will be briefly described in the next section.

Medical circles, on the other hand, were more interested in the gross properties of the brain; functional localization, effects of cortical lesions, connectivity, and related experiments. That this interest was not misplaced, is evidenced by the amount of brain surgery performed today; nevertheless it contributed only indirectly towards a fuller understanding of the principles involved in the neuronal networks.

As the body of knowledge increased, it became more and more difficult to formulate hypotheses concerning the Mind which would satisfactorily explain the known results of innumerable psychological experiments without conflicting with established biological facts. Several of the hypotheses in general circulation will be presented in Section 1.2, as a preliminary to a more detailed description of perceptrons in Section 1.3.

Following this somewhat exegetic material, the discussion will narrow down to analogue memory mechanisms, which form the proper subject matter of this dissertation. Memory devices which have been incorporated in brain models, or tested with a view towards such applications, will be reviewed in Chapter II, while the magnetostrictive read-out integrator--a device developed in conjunction with a particular perceptron, Tobermory,[1] at Cornell University--forms the topic of Chapter III. Tobermory itself will be described in Chapter IV, while speculation concerning its successors will be entertained in the concluding chapter, Chapter V.

1.1. Properties of the Nerve Cell

It would be helpful, while studying the nerve cell in preparation for theorizing about brain function, to be able to separate the properties which are essential for the operation of the system from those which are merely an incidental consequence of the organic nature of the brain. Such an a priori distinction would, however, prejudice the cause from the very start; the decision as to which properties to ignore must be postponed as long as possible. It will be seen that not all of the properties enumerated in this section, far from exhaustive as the list is bound to be, are taken into account by any of the models described in the next two sections; responsibility for this must in each case be assigned to the modeller.

A typical nerve cell in the associative area of the brain[2] is depicted in Figure 1. The main body of the cell (soma) contains the nucleus, which in turn surrounds the nucleolus. From the soma emerge numerous processes; one of these is the axon--usually smooth and without branches except at the very end--while the rest are dendrites. The axon may or may not be enveloped by a myelin sheath, and is capable of transmitting a potential wave along its length.

The potential wave, called the action potential, actually consists of a depolarization of the cell membrane along the axon. For a given cell, it is always approximately of the same amplitude--60 to 100 millivolts--and of the same width--0.5 to 2.0 milliseconds, depending on the diameter of the axon.

The action potential is usually initiated by other axonal impulses impinging on the soma or on the dendrites--which apparently merely serve to increase the surface area of the cell body. The juncture

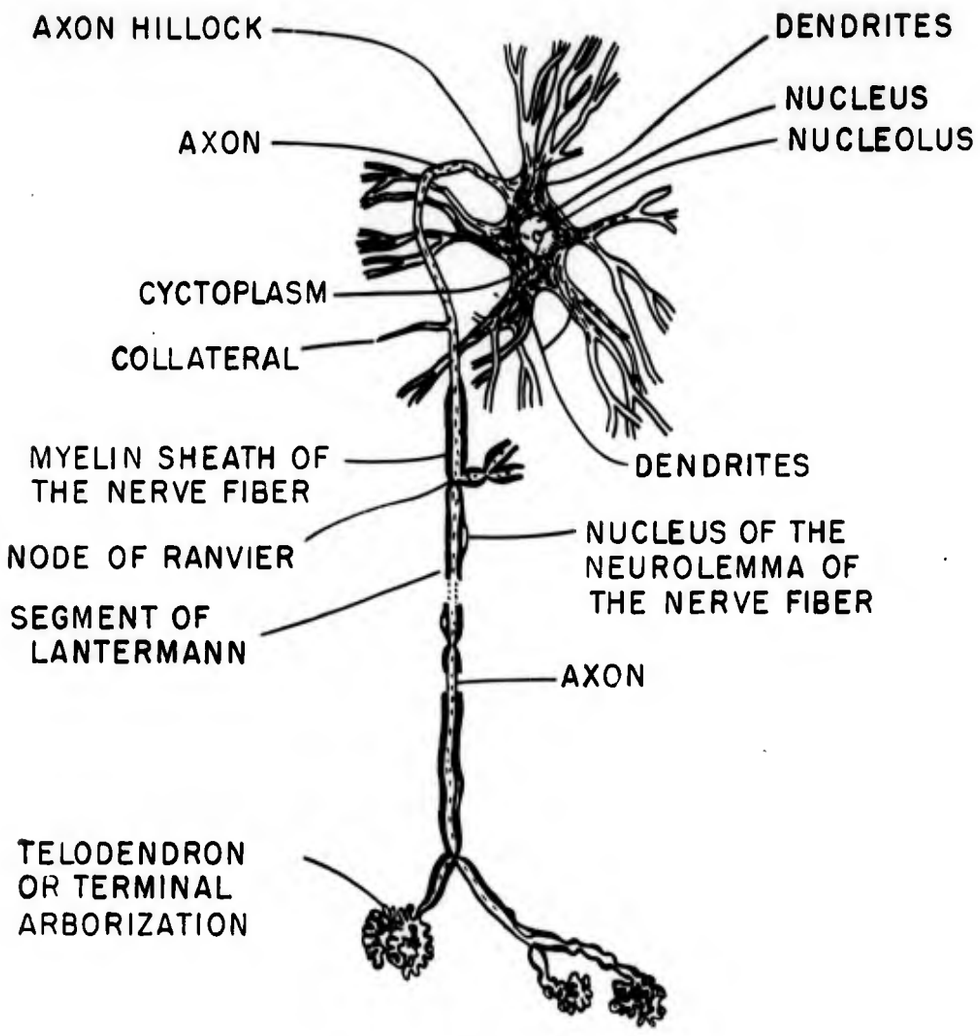

Figure 1. Diagram of a Neuron

between an incoming (afferent) axon and the cell body or dendrite is called a synapse. Synaptic transmission involves a threshold effect, as well as spatial and temporal summation. If the single afferent impulse is insufficient to trigger the action potential, several impulses closely succeeding each other at different synapses of the same cell will likely do so. Not all synapses, however, are excitatory: some have an inhibitory effect. Furthermore, after a cell has been fired, an "absolute refractory period" ensues while the cell is incapable of being fired no matter what the stimulation; this is followed by a "relative refractory period," during which the threshold is higher than normal. Thus a cell responds to increased stimulation, not with larger spikes, but with an increased frequency of discharge.

The mechanism of synaptic transmission is by no means clearly understood; it is believed that both electric and chemical effects are involved. According to one grossly oversimplified hypothesis, a transmitter substance, such as acetylcholine, is released from the end-bulbs of the afferent axon by the action potential, and temporarily depolarizes a portion of the cell membrane. If the depolarization is sufficient in magnitude and extent, a spike potential is initiated.

There is some evidence demonstrating adaptive features in the neuron, particularly on a short time basis. Repeated firing may change the threshold of a cell, or it may increase its rate of response to constant excitation. These properties could evidently hold the key to the nature of the memory trace, which still presents one of the most puzzling enigmas in neurophysiology.

The constraints imposed on brain models by the available body of data are as follows: to perform the function of the human brain there

are available approximately 10^{10} threshold units connected by means of 10^{13} synaptic junctions. The maximum frequency to be found in the system is of the order of one kilocycle per second. These figures admittedly give the theorist considerable latitude; some of the models evolved will now be examined.

1.2. Brain Models

Most of the initial work in this area was concentrated on reducing the known properties of individual nerve cells to a form suitable for mathematical treatment. Among the resultant "model neurons," one which has remained particularly popular to this day is the McCulloch-Pitts neuron.[3]

The McCulloch cell (Figure 2) is characterized by a fixed threshold and complete structural staticity. Transmission of signals is instantaneous, with delays occurring only at the synapses. Inhibitory synapses are absolute: when an inhibitory signal is present, the nerve cannot fire no matter how many excitatory impulses are trying to activate it. Thus the condition for the emission of a unit signal by some neuron at time t is that at time $t-1$ it had received a number of excitatory signals equal to its threshold, and no inhibitory signal.

The most attractive feature about the McCulloch neuron is that nets composed solely of such devices may be analyzed in a straightforward manner according to the rules of boolean algebra. Another noteworthy aspect is the universality of such nets: according to a well known theorem of Turing,[4] binary devices of this type may be interconnected to compute any desired logical function of the input.

Logic: Cell $N_i(\theta)$ is activated at time t if at $t - 1$ the sum of the excitatory inputs to it exceeds or equals θ, and there is no inhibitory input present.

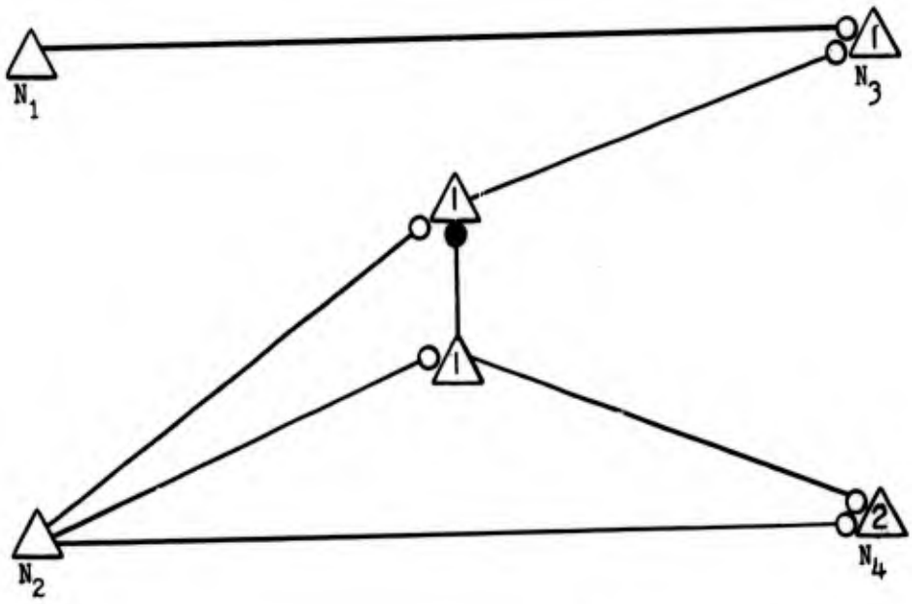

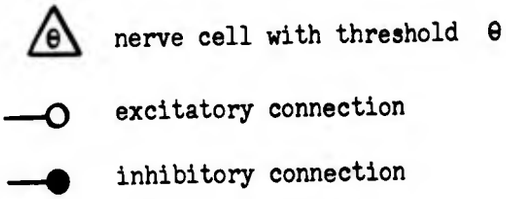

Example of 6-cell network

$$N_3(t) \equiv N_1(t-1) \vee N_2(t-2) \cdot \overline{N_2(t-3)}$$

$$N_4(t) \equiv N_2(t-1) \cdot N_2(t-2)$$

Figure 2. McCulloch-Pitts Neurons

Culbertson[5] actually designed neuron configurations using McCulloch neurons for a number of common functions, such as ordinary arithmetic, timing, and image abstraction. While some of these nets are extremely ingenious, the neurons involved in a given circuit are seldom used for more than one task, and it can be shown easily that for performance approaching the complexity of the human brain far more than ten billion neurons would be required for the appropriate nets. Such "monotypic" models are further open to the criticism that the destruction of a single unit may well put the whole system out of commission; this clearly is not the case with biological organisms.

A theory far less specific in nature is advanced by Hayek in the Sensory Order.[6] "Mind" according to Hayek, is "a particular order of a set of events taking place in some organism and in some manner related to, but not identical with, the physical order of events in the environment." A scheme of hierarchical classification is postulated, with the classes becoming more and more general as one ascends in the "sensory order." No hypothesis is put forth to clarify the physiological operation of the memory mechanism, although some evidence favouring the existence of two kinds of memory, one static and one dynamic (map and model) is examined.

Distant derivatives of Hayek's model include implementations of Bayes nets by Uttley,[7] Buhr,[8] and Gamba.[9] All three of these machines are essentially binary conditional probability computers, testing hypotheses according to Bayes' maximum likelihood formula. They differ among themselves, apart from the electronic design, in the order of the conditional probabilities which are taken into consideration in making a decision.

An ecological approach to the problem is favoured by Ashby. The homeostat, described in Design for a Brain,[10] seeks equilibrium in multidimensional phase space: at equilibrium, all of the system's "essential variables" are within certain specified bounds. The search through phase space is not completely random; if it were, the probability of a random walk ever reaching the region of the space labelled "equilibrium" would be very slim indeed. Experiments have not yet been conducted on a homeostatic machine large enough to yield significant results.

The theories listed so far all seem somewhat clumsy and artificial when compared to the scheme advocated by Hebb in The Organization of Behaviour.[11] Hebb's chief neurophysiological assumption reads as follows: "When an axon A is near enough to excite a cell B and repeatedly or persistently takes part in firing it, some growth process or metabolic change takes place in one or both cells such that A's efficiency, as one of the cells firing B, is increased." From this postulate Hebb builds up the concepts of the cell assembly and the phase sequence, concepts whose versatility he then proceeds to demonstrate by producing plausible explanations of such diverse phenomena as set and attention, learning, gestalt perception, physiological nystagmus, and certain well known electrocorticogram patterns.

While this theory is already appealing in its general form--perhaps partly at least because of Hebb's exceptionally elegant exposition--certain questions arise as to the quantitative aspect of the processes outlined. How many neurons are required to perform a specific "subroutine"? What is the average density of the connections? What are the temporal dimensions involved in the formation of the cell assemblies and the phase sequences?

Rochester[12] and his associates attempted to answer these, and other, questions by simulating Hebb's connection schemes on a digital computer. Their failure to produce clearcut answers is due, at least partly, to the fact that Hebb omitted to explicitly postulate inhibitory connections, and the resultant positive feedback is likely to result in an unstable system.

A much more ambitious program of theoretical analysis, computer simulation, and hardware implementation of a wide class of neural networks was undertaken in 1956 by Rosenblatt.[13] Since the present undertaking is an integral part of this program, some of the nerve nets studied by Rosenblatt--called perceptrons--will now be described in detail.

1.3. Perceptrons

While rigorous definitions are applicable as a rule only to particular subclasses of perceptrons,[13] perceptrons in general may be described as a "class of minimally constrained nerve nets consisting of logically simplified neural elements." These nerve nets have been shown to be capable of adaptive or self-organizing behavior; their primary purpose is "to shed some light on the problem of explaining brain function in terms of brain structure." It is also possible that certain types of perceptrons may find technological application as pattern recognition devices: the development of such devices is not, however, the main purpose of the program.

Although the design of Tobermory (Chapter IV) forms, perhaps, an exception to the overall philosophy of the program, it should be stressed that as a rule Rosenblatt's approach consists of specifying

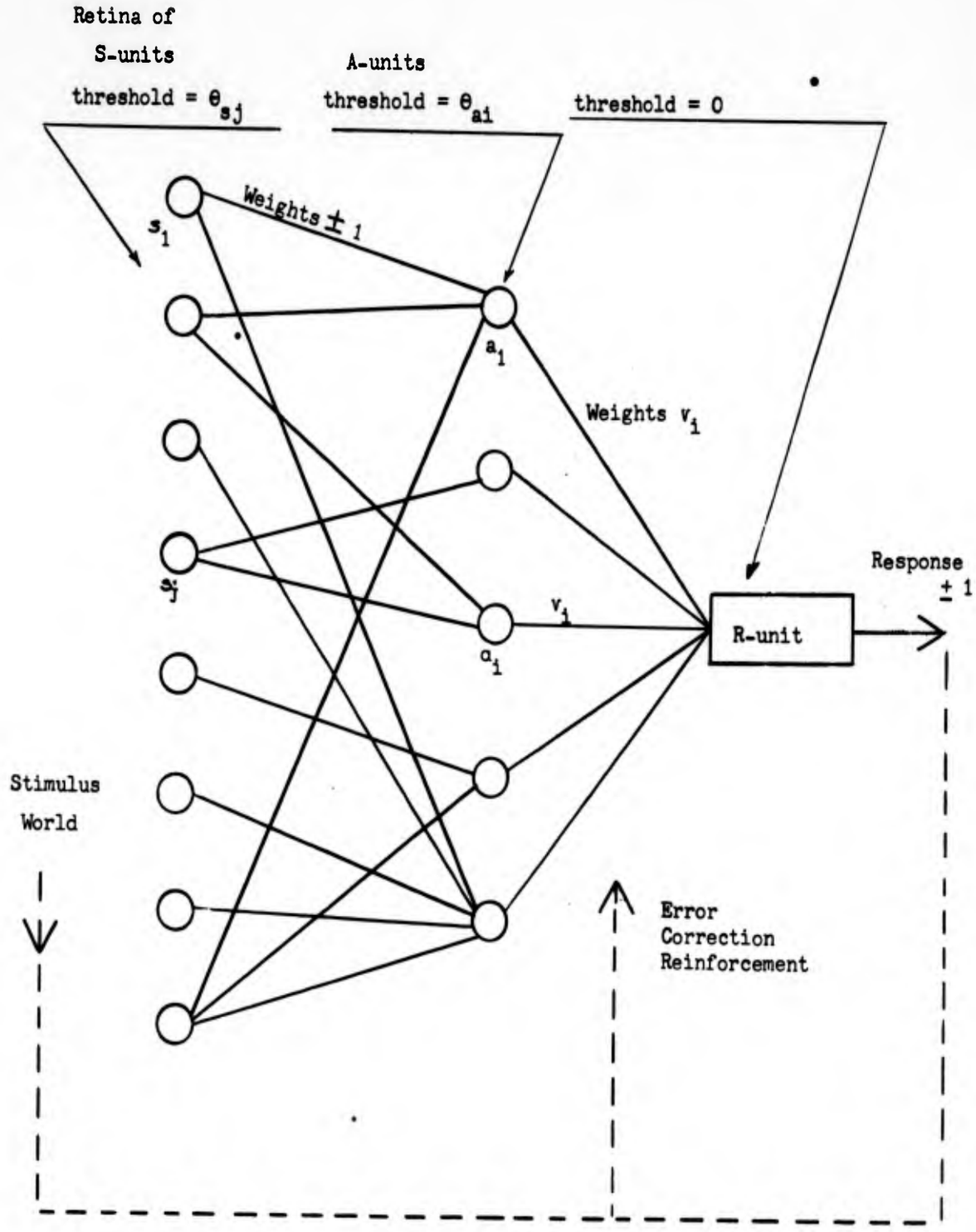

Figure 3. An Elementary Perceptron

a nerve net or perceptron of some biological plausibility, then investigating its properties by the most appropriate means. By concentrating attention on the perceptrons displaying the most brain-like characteristics, it is hoped that new psychological and physiological hypotheses may be formulated, to be tested by experiment; only by the prediction of novel effects and hitherto unobserved phenomena can the perceptron program be fully justified.

Perceptrons may in general be described in terms of a) topological properties (connectivity); b) signal propagation functions; and, c) memory functions (training rules). During the past six years perceptrons of numerous types, with various schemes of interconnections--with and without internal feed-back--and subject to many different types of training rules, have been investigated.[14] For the purpose of this paper, it will fortunately be sufficient to consider only a very simple perceptron, the three layer, series connected, elementary perceptron, and its immediate derivatives, such as Tobermory.

The universe of an elementary perceptron consists of stimuli S_i, some of which are in the positive class, and some in the negative class. The task set to the perceptron is to separate the stimuli, when presented in random order, into the correct classes, i.e., perform a dichotomy.

The elementary perceptron itself (Figure 3) comprises three layers of threshold devices: a layer of sensory (S) units (e.g. light sensitive photocells, or a bank of acoustic filters), a layer of association (A) units, and a single response (R) unit. Random connections from the S to the A layer are many to many, and may have transmission functions of 1 or -1 (excitatory or inhibitory connections). Each of the A-units a_i is connected to the R-unit by a link of value (gain) v_i, and these

may be varied in the course of an "error correction" training sequence as follows.

When the stimulus is presented, some of the S-units go "on". Consequently, some of the A-units, whose thresholds have been exceeded by the algebraic summation of signals from the "on" S-units, also become activated. The input to the R-unit consists of the sum of the unit outputs of the active A-units, each multiplied by the corresponding v_i. If the sum of these is positive, the R-unit signals "positive class." Should this indeed be the correct classification of the stimulus on the retina, we proceed to the next stimulus. If, however, the response is erroneous, then all the values associated with active A-units are decremented in order to decrease the signal to the R-unit. Thus the weight associated with an A-unit is just the time-integral of the reinforcement received by that A-unit during the training sequence.

It may be shown[15] that if the perceptron is inherently capable of finding a solution to the problem, i.e., if there exists a set of weights v_i which results in the correct classification of all the stimuli, then this state will be reached after a finite number of training sessions. Other theorems establish necessary and sufficient conditions for the existence of solutions to given problems in particular elementary perceptrons, and yield upper bounds to the number of training cycles required.

Tobermory,[16] the audio perceptron presently under construction by the Cognitive Systems Research Program, differs from the elementary perceptron described above chiefly in having twelve R-units instead of one. Thus each one of Tobermory's 1000 A-units is connected to each of twelve R-units. This scheme theoretically permits classification of

stimuli into $2^{12} = 4,096$ classes. The universe of Tobermory will consist of short--one or two syllable--words. It is hoped that the machine will learn to classify correctly at least several hundred of these, even when pronounced by different speakers. The input to the associative system will be the amplitude-frequency-time domain analysis of each word, obtained by sampling the word at intervals of a few milliseconds by a bank of 72 frequency and 8 amplitude filters. A more detailed description of the input end of the system is postponed until Chapter IV. The next section contains an outline of the requirements for the components to be used in Tobermory's 12,000 unit memory, as well as in the topologically more complicated machines now in prospect.

1.4. Requirements for Tobermory's Memory

As just shown, the memory of an elementary three-layer perceptron consists essentially of the gain (or attenuation) associated with each of the A-unit to R-unit connections. These weights, it was assumed, could be changed from minus infinity to plus infinity by the addition (or subtraction) of equal increments.

It may be proved without much difficulty that, under very broad conditions, a given perceptron will converge to a solution even if the range of its weights is relatively small (see Neurodynamics:[14] Chapter IX, bounded value perceptron). In typical simulation problems, individual weights seldom exceed ten times the unit of incrementation; thus a range of about twenty to one should suffice for a typical memory unit.[17] Of course, for a given problem, the variation required for a single link is a function of the number of A-units; with enough A-units, an equivalent logic could be devised using only binary links.

The training cycle in a perceptron constitutes a self-correcting negative feedback loop; hence it may also be shown that the addition of random noise to the increments does not preclude a solution from being attained. Thus equal step size is not essential, though it is desirable in as much as the required number of training cycles increases with the random noise added to the corrective increments. The summation of the A-unit signals at the R-units effectively averages the step size, and in a system of the size of Tobermory it is estimated that a variation of three to one in step size could be tolerated. Since an audio input of the type destined for Tobermory is very difficult to simulate on a digital computer, the reliability of this, and other estimates relating to the values of the weights in the final state, the average number of active A-units, and the speed of convergence, is not known for certain. To test these predictions, as well as the functioning of a real-time memory system, is in fact one of the principle reasons for building Tobermory.

The logical design of the system imposes the not too stringent requirement that reinforcement should not take longer than about one-fiftieth of a second. A more difficult problem is raised by the need for long term stability:[17] it should be possible for the machine to retain information for several days. After the testing associated with a given problem has been completed, there should also be some way of erasing from the memory all previous knowledge, and leaving it in a non-biased condition, preferably with all the weights at, or near, zero.

While the requirements outlined here are indeed rather loose, the additional limitation on cost excludes most of the conventional devices which would be normally used in a smaller system. For Tobermory, an upper limit of $1.50 per integrator has been set, but for larger systems this figure would have to be substantially reduced.

II. SURVEY OF PROPOSED ANALOGUE MEMORY SCHEMES

One may gain some idea of the staggering variety of processes which may be potentially harnessed to fulfill perceptron memory functions by considering the number of physical phenomena characterized by a first order differential equation. Since the requirements for a perceptron memory device are rather loosely formulated, the choice between the various approaches available is not an easy one; a quantitative evaluation, based on performance curves and cost, would be a major project in itself.

It should be noted that the advantages or disadvantages of a particular memory device may be reflected in the design of the rest of the perceptron; thus full optimization of the choice between the different types of available devices would require a very complete analysis of perceptron performance.

In this chapter an attempt will be made to review the more salient features of some of the memory schemes proposed to date. It is hoped that even such a superficial survey may be of some help to brain model designers.

2.1. Electromechanical Integrators

The chief virtue of the electromechanical integrator consists of its inherent stability. The "weight" of a given connection is represented by a mechanical displacement, hence it is not subject to variation due to ambient changes or fluctuations in power supply level.

The design incorporated in the Mark I perceptron,[18,19] (400 S-units, 512 A-units) consists of a double potentiometer mounted on a single shaft gear driven by a two watt (input) direct current motor, as shown on

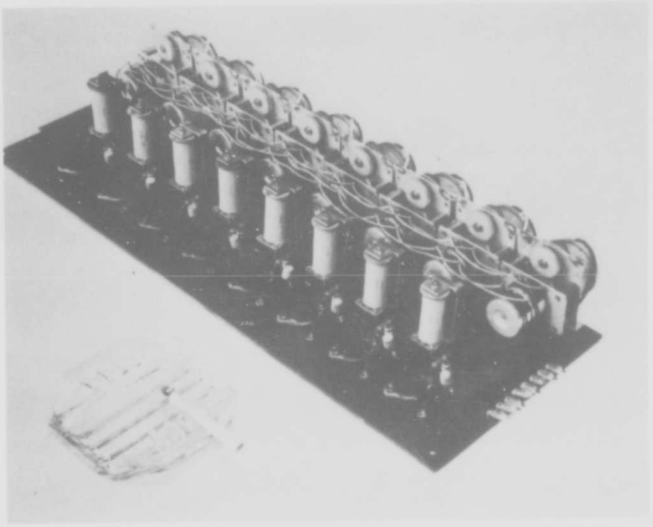

Figure 4. Mark I Integrator Board

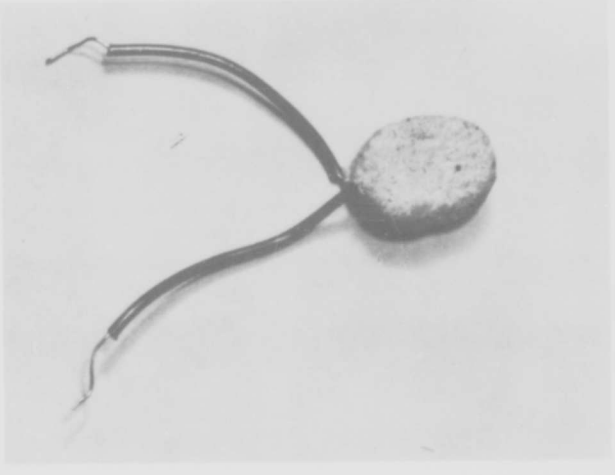

Figure 6. Thermistor

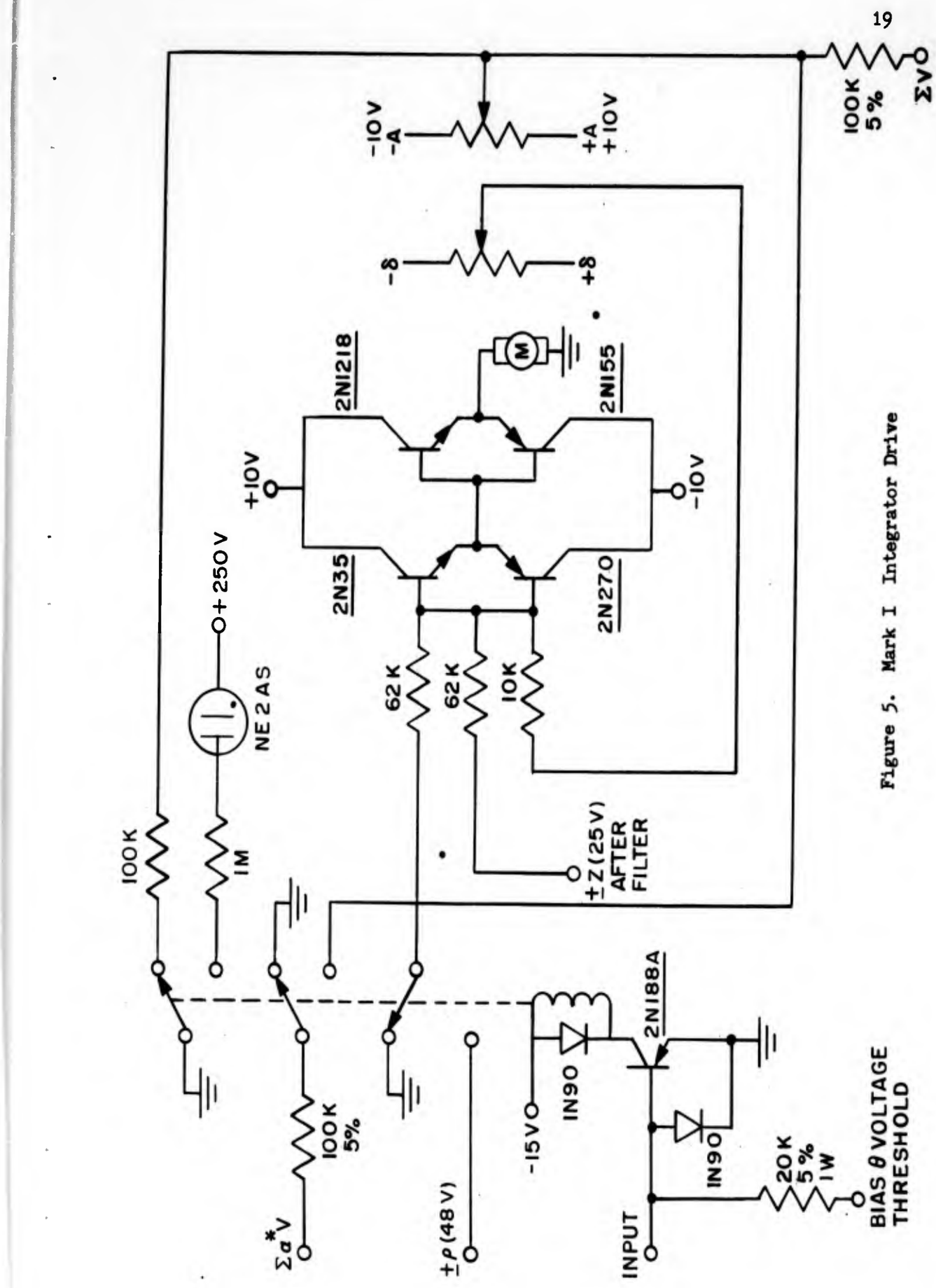

Figure 5. Mark I Integrator Drive

Figure 4. The voltage at the arm of one of the potentiometers is a measure of the corresponding weight while the other provides a local feedback loop to allow decay in the A-unit proportional to its present value. The second potentiometer is used in most experiments only to reset the A-units to some arbitrary zero (say mid-range) after completion of the experiment. It is to be noted that changing the voltage applied to the 512 potentiometer terminals (which are connected in parallel) merely scales the weights by a constant factor, and does not affect convergence.

The gear-head motors are driven by two power transistors (Figure 5), one for each direction of rotation. The bias to these is supplied by two inexpensive switching transistors, which are in turn controlled by the A-unit logic and the reinforcement mechanism.[18] Since the potentiometer arms move very slowly (0.1 rpm) the resolution of the system is limited only by the finite diameter of the resistance wire in the potentiometer windings. The number of steps attainable is about 520, but the length of the reinforcement period is seldom, if ever, made short enough to take advantage of the maximum resolution.

The chief drawbacks of this system are its size and costs. The packing density in the Mark I is only of the order of 10 A-units per cubic foot, and each unit runs upwards of $40 (in the quantities purchased for the Mark I).

R. Venezky has suggested that in a larger system cost and space requirements could be cut down considerably by mounting a number of the potentiometers--possibly as many as 40 or 50--on a common shaft. In a two-phase system all the shafts could be geared together, and driven first forward, then in the reverse direction, by a common driving unit.

Appropriate potentiometers could be clamped to the shaft by a magnetic clutch arrangement during either phase of the reinforcement cycle. The small currents required by a magnetic clutch would allow it to be controlled by a single, not very large, power transistor, while the second potentiometer of each A-unit could be eliminated at the expense of an additional phase.

Although these improvements may be sufficient to extend the range of application of electromechanical integrators to large video systems, in audio perceptrons operating in real time, the fifty cps. reinforcement rate would tax severely even the lowest inertia magnetic clutches. A similar system using an escapement or a ratchet mechanism with a solenoid plunger may have a somewhat higher frequency range, nevertheless none of these devices is simple enough to include in really large (upwards of 100,000 variable weights) perceptrons operating at rates approaching that of biological systems.

2.2. Thermistors

A small perceptron (16 S-units, 20 A-units), using thermistors (Figure 6) for variable weights, was built at Cornell University by A. Arking and H. Y. Chiu.[36]

The currents that flow through a thermistor raise its temperature through ohmic dissipation, and the temperature characteristics of the device are such that its conductance is thereby increased. If the thermistor can be maintained in this non-equilibrium state it will be able to pass larger current for succeeding stimuli.

The nature of this weighting device obviates the need for any auxiliary circuitry: only weights belonging to "active" A-units carry

current and are consequently reinforced. Unfortunately reinforcement is strictly monopolar. A further drawback is the short "half-memory" of thermistors: it is only of the order of three to four minutes. Nevertheless, it is conceivable that the simplicity and low cost of the device may render it useful in large cross-coupled systems; the integrator requirements of such systems will be discussed in more detail in section 2.6.

2.3. Photochromic Integrators

The photochromic integrator, as presently developed by the Armour Research Foundation,[21] is not really an integrator in the previously described sense, since it implements an "exponential" weighting scheme. In such a system, the magnitude of the reinforcement is proportional to the value of the connection at the time reinforcement occurs.

The characteristic curves of the photochromic or phototropic film on which the device is based are displayed in Figure 7. The unique property of this film--developed largely by the National Cash Register Company--is that its transmission near the center of the visible spectrum may be reversibly altered by exposure to high intensity radiation in the borderline regions. Curve A shows the transmissivity of the film after it has been exposed to a flash of light of the spectral composition indicated by curve C (yellow filter), while curve B shows transmissivity after an "erase" pulse through blue filter D. Curve E describes the "read" filter which has been found to interfere least with the condition of the film. Reading is, of course, performed at relatively much lower intensities than reinforcement; the overall transmissivity varies from about 0.3 to 0.8. The material is not too unstable: at room temperature

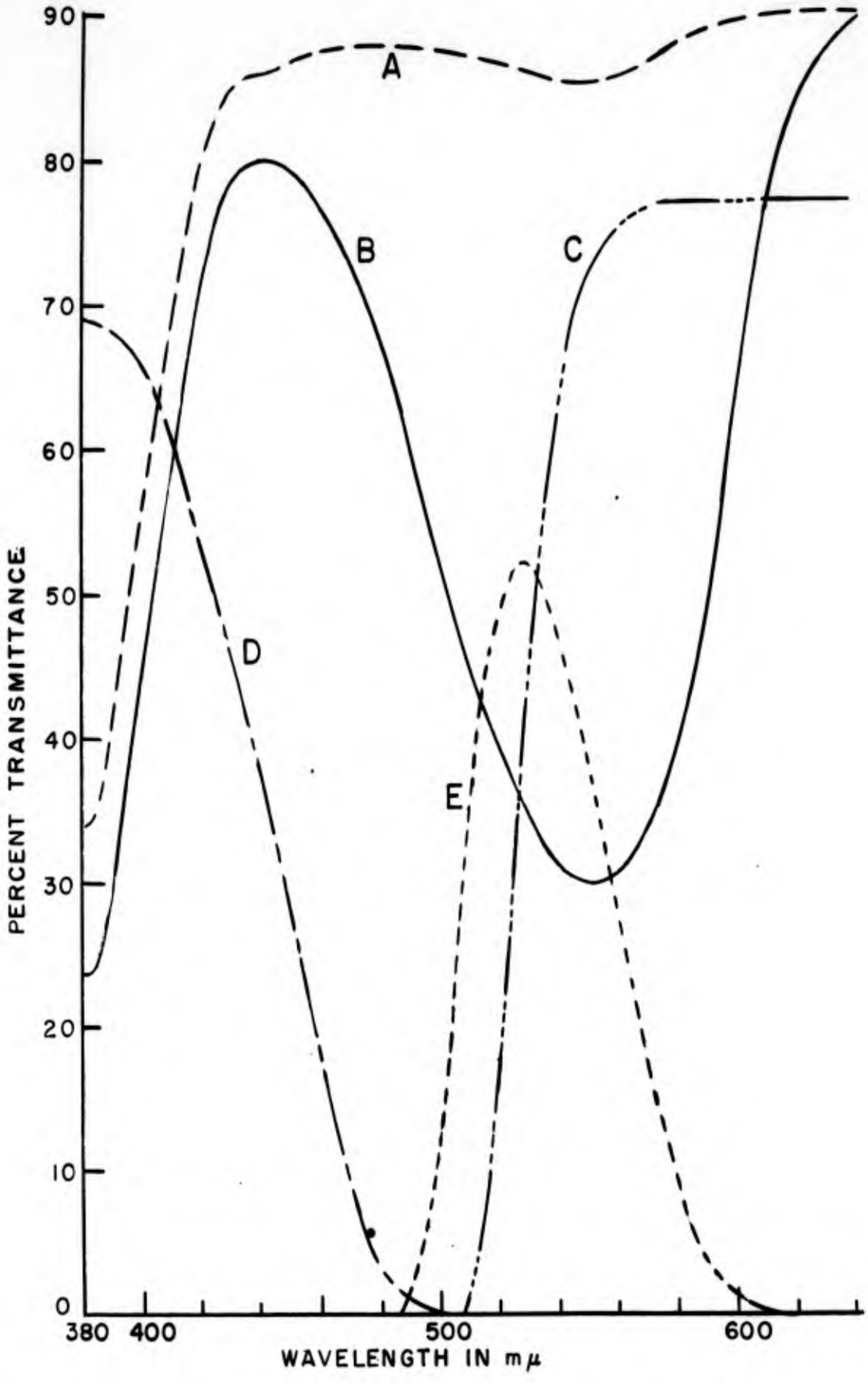

Figure 7. Photochromic Characteristics

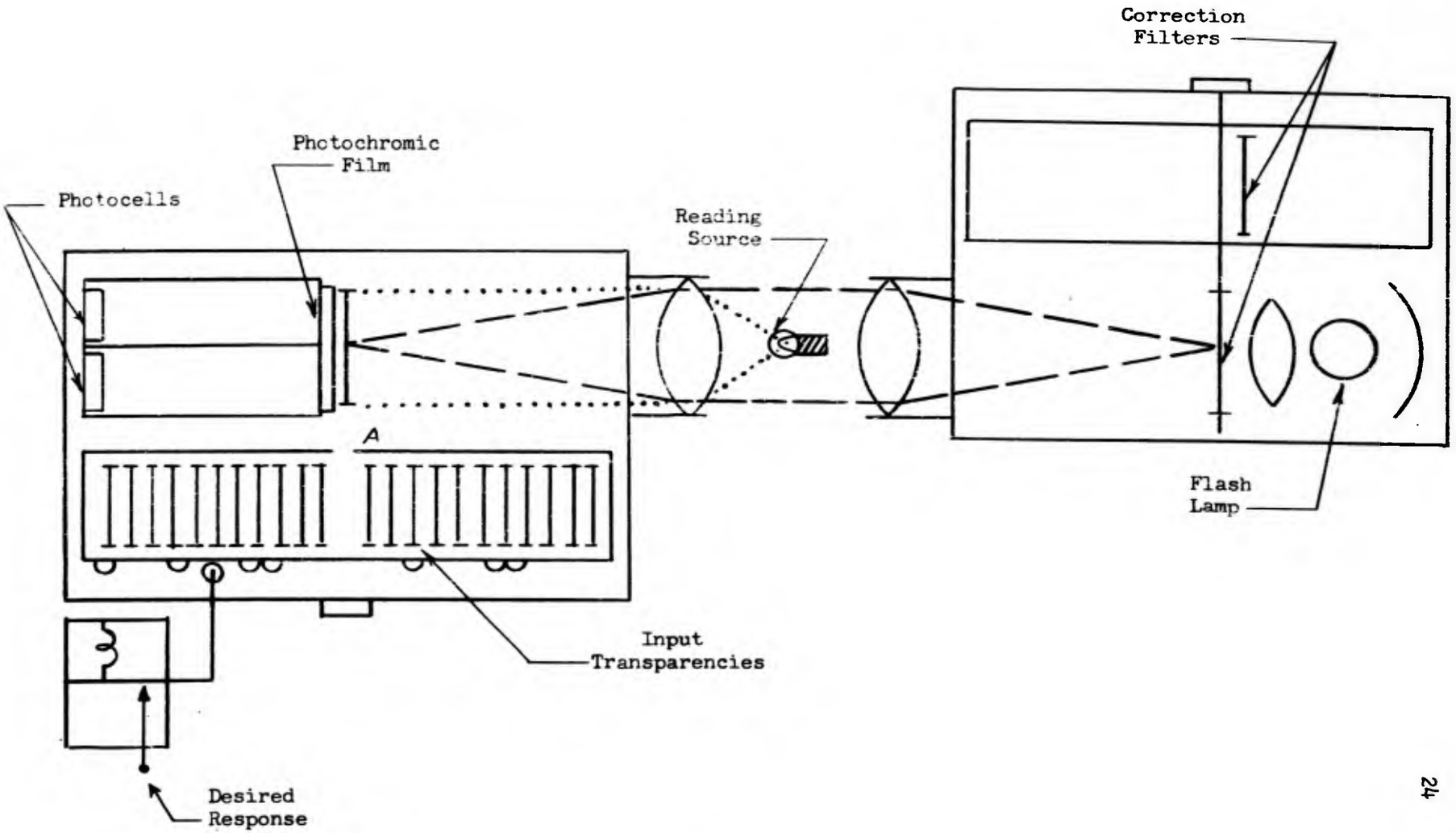

Figure 8 . Photochromic Pattern Recognition Machine

it decays towards an equilibrium point with a time constant of several hours.

A rather elegant photochromic device, built by Scott H. Cameron, is illustrated in Figure 8. The input transparency is introduced into the optical path through slit A, mechanically actuating a switching arrangement which "senses" whether the pattern is to be classified into the positive or the negative class. The picture consists of two side-by-side versions of the same pattern.

After the transparency has been superimposed on the photochromic film, a reading source directs a uniform collimated beam through both halves of the picture. The flux through each section is collected at two photoresistors which form the ratio arms of a bridge detector. The sign of the bridge output corresponds to the input of a perceptron R-unit. If the signal is of the correct sign, the next slide is inserted, while if an "error" is indicated, a high-energy gas discharge lamp collimated through a filter of the correct type, inserted by the mechanical linkage, is fired before the transparency is withdrawn. At each reinforcement, one of the segments of the photochromic film is flooded with blue light, the other with yellow, depending on the nature of the desired response. It is claimed[21] that this structure leads to an error correcting exponential adaptive strategy.

The machine itself is highly automated: it is designed to run through the sequence of slides in its magazine until it stops making mistakes. Unfortunately, technical difficulties with the photoresistors and shutter design have so far impeded experimentation, and to the time of writing no significant results have been attained.

If the very extensive development program required is discounted, the photochromic principle is likely to prove extremely economical even in systems of only moderate size. While the optics involved tend to restrict the range of the device--it is difficult to see, for example, how it could be applied to cross-coupled perceptrons--the idea certainly seems attractive as far as two layer pattern recognizers are concerned. Future applications will probably be technological in nature, with machines such as map-readers and particle-trackers in prospect.

2.4. The Transpolarizer

The transpolarizer,[22,23] an electrostatic analogue of the transfluxor described in section 2.5, consists of two capacitors with a crystalline ferroelectric dielectric and a nearly rectangular hysteresis loop. The basic circuit is shown in Figure 9, and the mode of operation is as follows.

One of the capacitors, say C_1, is maintained in a polarized state by means of a d.c. bias. Then the transpolarizer is said to be in the unblocked state if C_2 is polarized in the same direction as C_1. In this case the two capacitors in series behave essentially as a single ferroelectric element, and present a low impedance to a small a.c. sensing signal. If, however, C_2 is polarized opposite to C_1 then any attempt to switch C_1 would result in C_2 being driven further into saturation. Hence no switching occurs, and the transpolarizer is said to be in the blocked state. The combination acts as a small linear capacitor, and therefore has a relatively high impedance at the driving frequency.

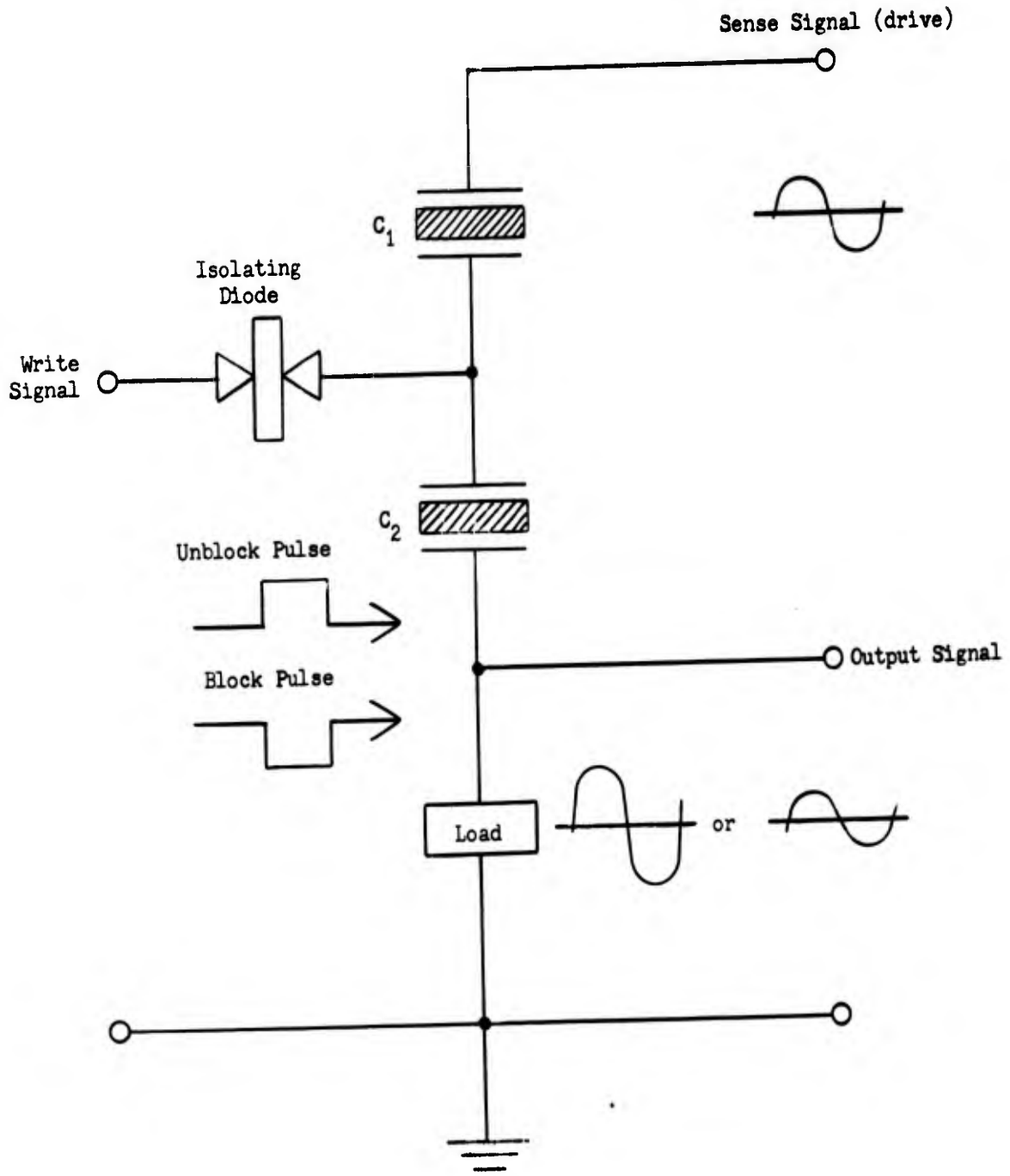

Figure 9. Basic Circuit of a Transpolarizer

The transpolarizer may also be operated in the partially blocked state. Then its impedance is intermediate between the extremes designated above. In dynamic operation, short pulses of either polarity may be applied to set the polarization to the desired level.

With recently developed materials, such as tri-glycine sulfate (TGS) and tri-glycine fluoberyllate (TGFB) extremely stable operation may be attained, and sensing voltages several times as large as the coercive voltage may be safely applied. Sensing may be performed with either sinusoidal or pulse wave shapes.

H. Y. Chiu has conducted experiments on Barium Titanate ($BaTiO_3$) crystals with a view to determining the suitability of transpolarizers as perceptron weighting elements.[24] He was able to obtain about 30 discrete levels, although the output was far from linear. The high input impedance of the crystal offers the advantage of requiring very small amounts of control power, but necessitates a very high output impedance source (c.100 megohms). A large number of transpolarizers could be controlled by means of an accurately focussed electron gun; timing presents no problem, since the setting time is of the order of 1 microsecond.

In conclusion, transpolarizers do not appear to be really suitable for perceptrons about to be built. They may, however, become competitive once electron beam techniques have been developed to the point where whole memory matrices may be deposited on thin films of ferroelectric material.

2.5. Flux Integration

Modelled on the core memories so widely used in digital computers, flux integrators use the partial switching of the domain in a toroidal core under a current impulse as the basic increment. While the mechanics of the process cannot be rigorously explained without a quantum mechanical

model, some quantitative understanding may be gained by consideration of the dynamic hysteresis loop of the core material. The characteristics of a dynamic hysteresis loop will be discussed in somewhat more detail in conjunction with the magnetostrictive integrator; here only a brief description is given.

Suppose a core is in a partially saturated condition (Figure 10) which corresponds to point a' on the hysteresis loop of Figure 11. Inside the circular (or cylindrical) boundary a, all the domains are lined up circumferentially, while outside this boundary chaos reigns. If now a magnetomotive force is set up in the direction of the previous magnetization by appropriately pulsing the toroidal winding, the domains most affected by the pulse will be the ones in the region immediately surrounding the boundary of magnetization. The domains inside cannot line up any further, while among the unaligned domains the ones subject to the greatest magnetizing force will be those for which the path length is shortest (m.m.f. = total ampere-turns per path length). Therefore, if we make the pulse sufficiently short--and, at the same time, of sufficient amplitude to switch at least some of the domains completely--then we will have succeeded in effecting a small radial movement of the boundary of magnetization. This corresponds to an increase in the stored flux to point d' on the hysteresis curve. A quantitative measure of the flux increase may be obtained by equating the area a'b'c'd' of the hysteresis curve to the area under the volt-second curve of the pulse. This equation represents the energy irreversibly transferred from the source to the core.

Two aspects of the process deserve special consideration: the linearity of the flux increase with respect to the number of input pulses, and the necessity of providing a non-destructive read-out. With regard

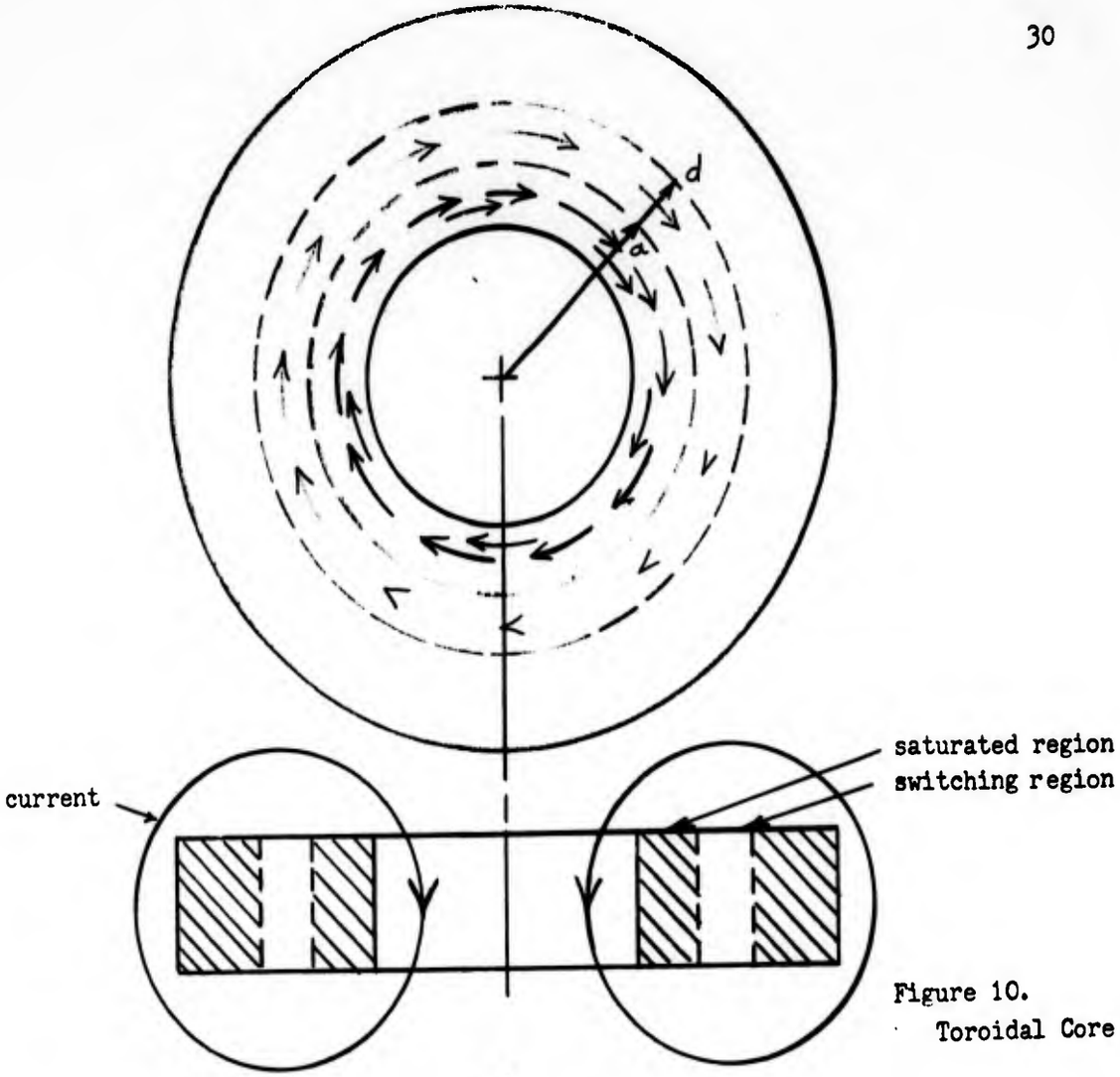

Figure 10.
Toroidal Core

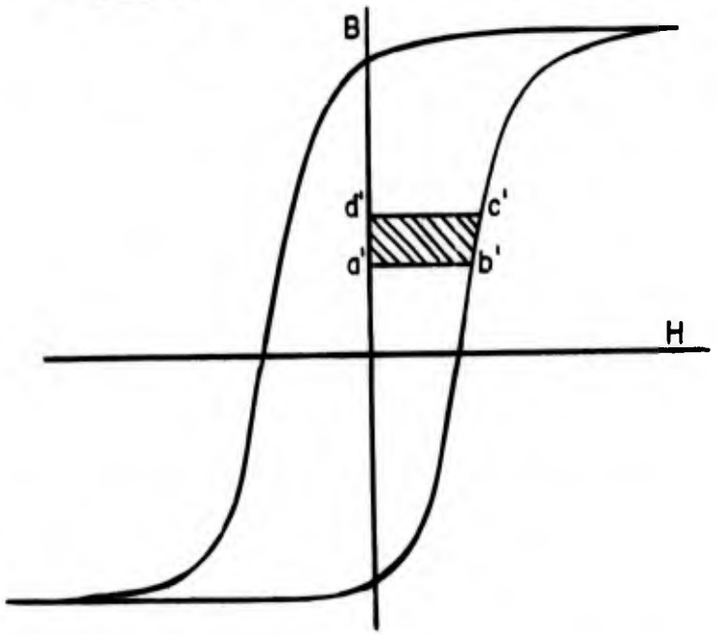

Figure 11. Hysteresis Loop of Ferrite Core

to the latter problem, we must keep in mind that as a rule flux can be observed only by its rate of change: so somehow we must effect a reversible change in the flux vector. In digital computers the problem is sometimes bypassed by conserving the value of the "bit" during read-out in an auxiliary register, and then restoring the value in the memory by a re-write pulse. While this approach is fairly foolproof (a prime requirement in digital computers) it is much too uneconomical for the analogue integrator.

The most widely accepted approach to the non-destructive read-out problem makes use of quadrature fields. A weak "strobe" field is applied orthogonal to the "write" axis of magnetization; it causes the flux vector to rotate slightly, generating a voltage proportional to its rate of change (and hence its magnitude) in the read coil (which may be the same as the write coil). At the end of the strobe pulse, the flux vector springs back to its original preferred orientation by virtue of "domain elasticity."

An extensive development program at the Aeronutronic Division of the Ford Motor Company has resulted in a working integrator based on the principles outlined above. This integrator was developed especially for perceptron type machines. A very adequate analysis of its potential with regard to perceptron applications may be found in reference 25, while the design of a pilot model employing such integrators is followed through in detail in references 26 and 27. To permit comparison with other types of integrators, the main operating characteristics of the Aeronutronic integrator, culled from references 28, 29 and 30, will now be summarized.

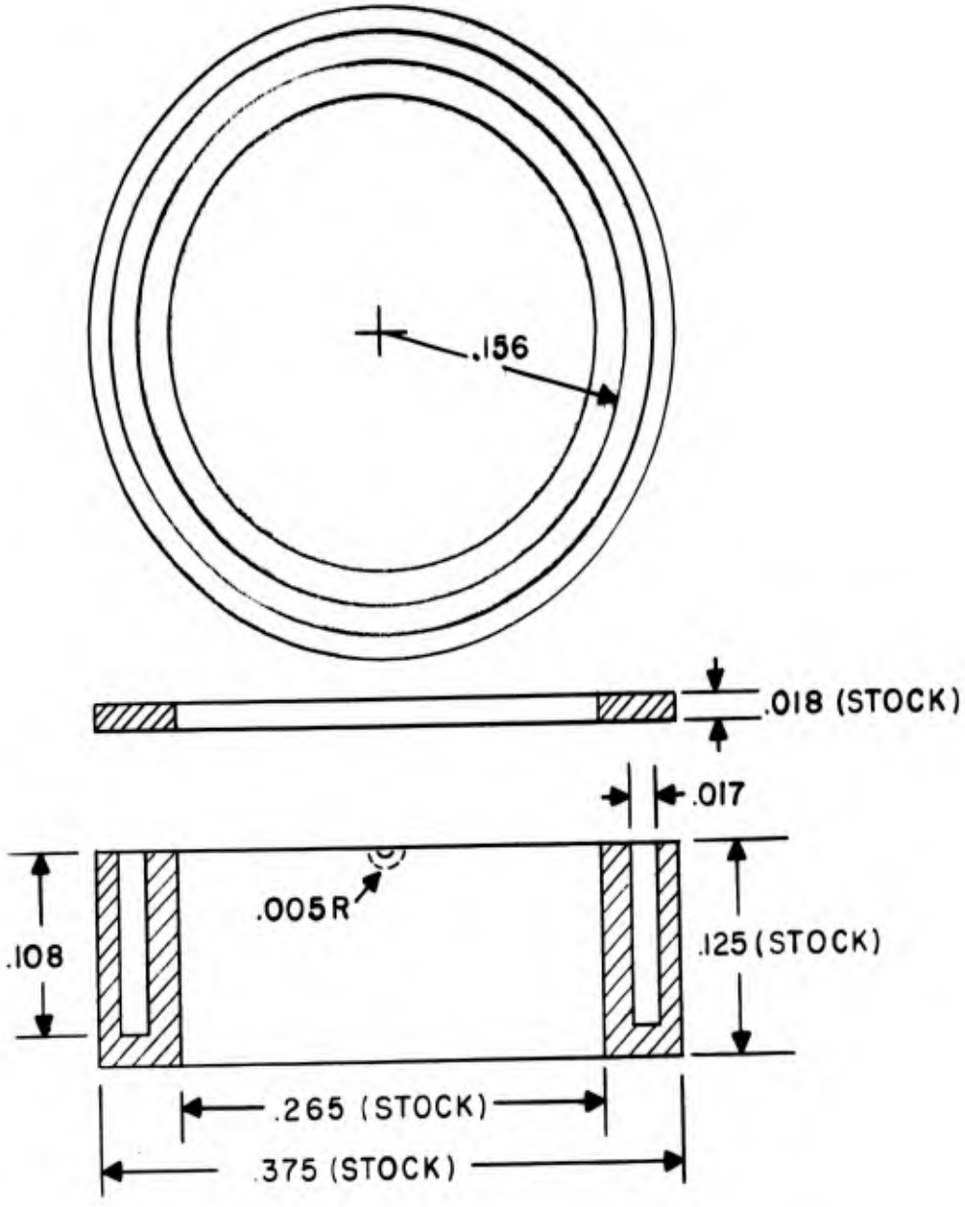

Figure 12. Aeronutronic Integrator Core and Steel Cover

The magnetic element itself is the hollow ferrite core with steel cover shown in Figure 12. The read-write winding consists of 200 turns of no. 38 enamelled wire toroidally wound on the taped core, and the strobe winding of 30 turns of the same size wire in the annular slot. Typical incrementing pulses are of the order of five volts amplitude and five microseconds duration. The strobe signal is a series of 50 ma., one microsecond pulses. Stored flux is partially destroyed by the first strobes applied after a change in value, so it is necessary to wait until equilibrium (corresponding to a reversible minor loop) is reached before the stored value is read. Nine strobe pulses are sufficient to reach this state. With a 50 ma. strobe the output at saturation is a triangular pulse of about 4 volts peak amplitude. The basic machine cycle is 240 microseconds. Return to zero is accomplished by a single oversized strobe pulse.

It can be shown theoretically,[27] and has been verified experimentally, that the stored flux in the integrator and consequently the read-out voltage is given approximately by an equation of the form:

$$e = E\ 1 - \exp\left(-\frac{n}{N}\right)$$

Where e = Output voltage
E = Maximum Output Voltage
n = Number of applied increments (from demagnetization)
N = Number of increments which would be required to produce E if all the increments were equally effective.

Differentiating with respect to n, we obtain:

$$\Delta e = \frac{E}{N} - \frac{e}{N}$$

This equation yields a measure of the linearity of the integrator. With current values as above, E/N is 0.27 and N is approximately 25. A typical growth curve, with these parameters, is shown in Figure 13.

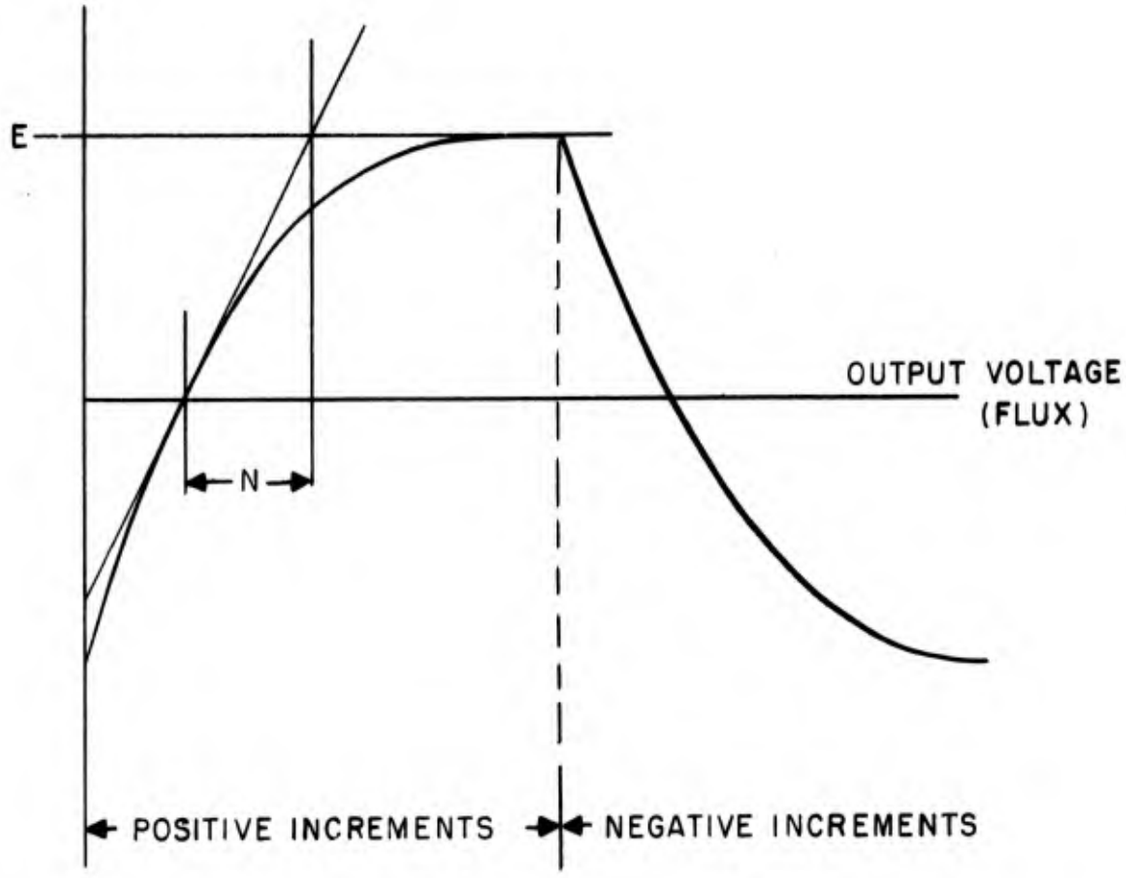

Figure 13. Aeronutronic Integrator Growth Curve

In the machine built to date, each core requires a separate, bi-directional transistor gate to control incrementation, but further research is expected to result in the development of coincidence mode switching. In this scheme the output of an active A-unit maintains a direct current bias through the write windings of all the integrators associated with it, and the reinforcement pulse is of sufficiently small amplitude to allow incrementation to take place only in biased cores. This mode of operation requires extremely good square loop characteristics, which in a toroidal core also means an I.D.-O.D. ratio very close to one. Further versatility is provided by the possibility of biassing the strobe winding; with a bias of suitable magnitude, the output signal is proportional to the product of the stored flux and the sign of the stobe current. Thus very complete and direct control of the A-units over the associated weights may be achieved at minimum expense.

Another working integrator has been developed at the Stanford Research Institute by A. Brain,[31] using the multiaperature devices (MAD) derived earlier from the transfluxor configuration by H. D. Crane.[32] A schematic of the MAD ferrite, as used for analogue storage, is shown on Figure 14. The current through the bias winding holds the core material inside the dotted line in a saturated condition, thus "trapping" any flux which may be present around the small aperture. Pulses through the set winding vary the total amount of flux in the core. A high frequency carrier in the drive winding generates a voltage in the read winding which is proportional to the flux linking the two coils; this flux will not be degraded unless the drive signal is powerful enough to switch flux all the way around the large aperture.

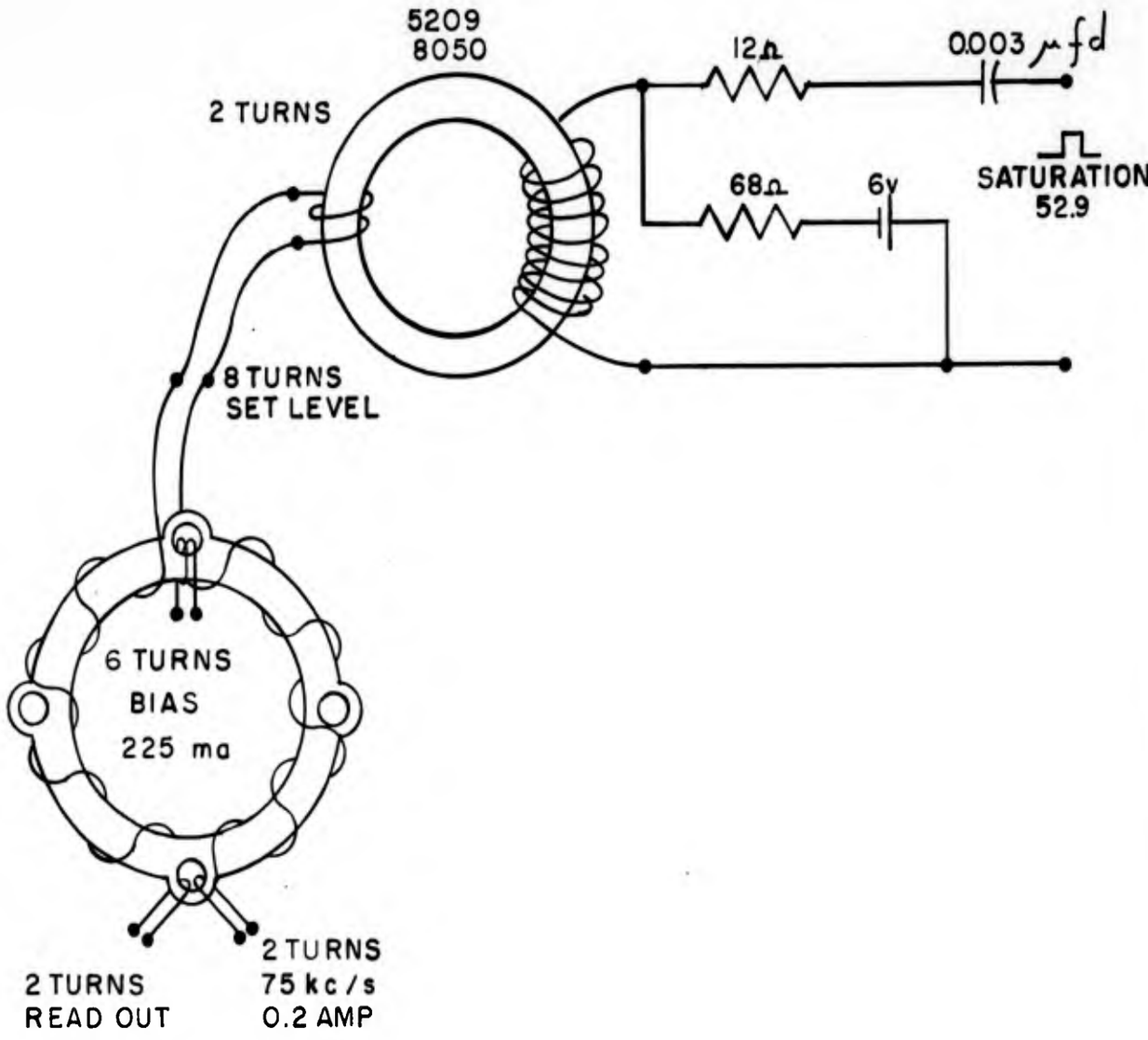

Figure 14. MAD Integrator

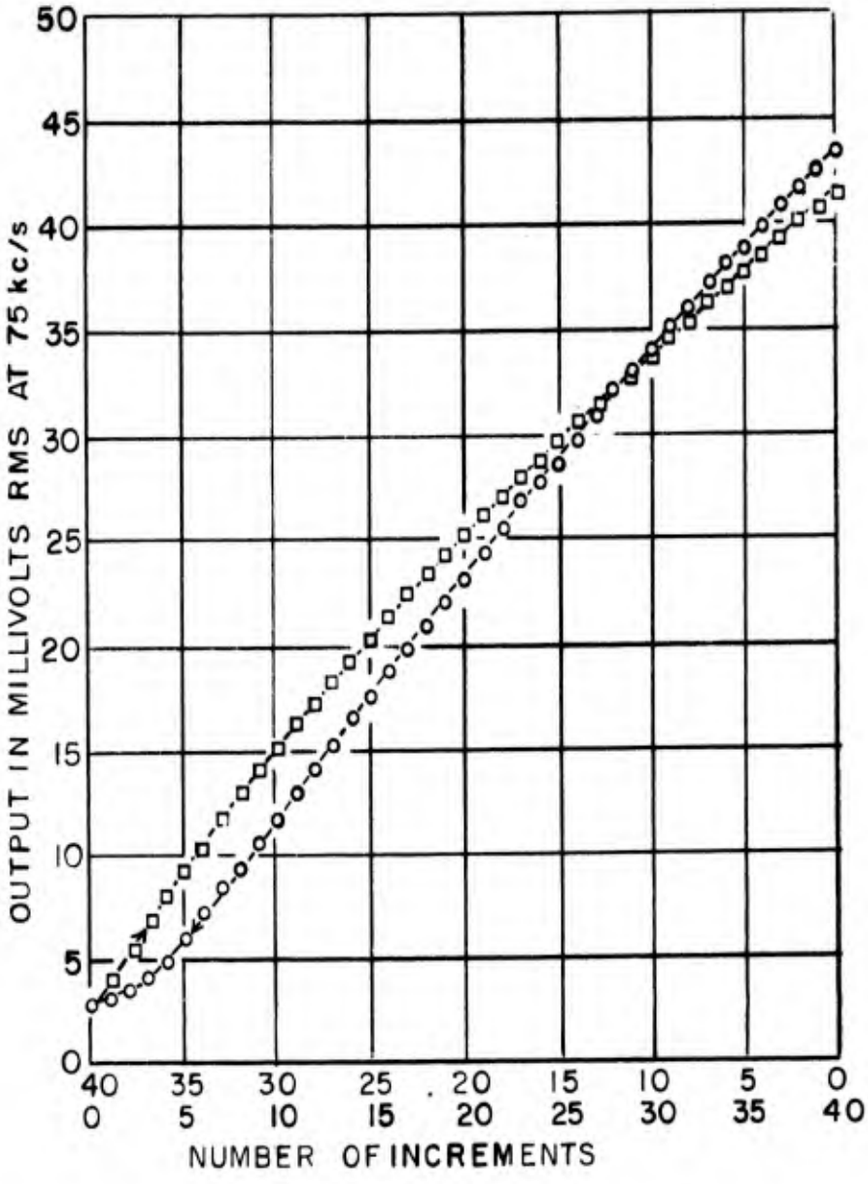

Figure 15. Storage Characteristics for MAD Integrator

The amount of flux switched at each increment is controlled by means of a "bucket" coil. The resulting linearity is indeed excellent, as shown in Figure 15. The MAD elements also afford a great deal of flexibility in the logical design: the two unused apertures may be employed to perform various gating functions. The complete logic necessary for an elementary perceptron may in fact be synthesized using only such magnetic elements.[31] The description of a pilot model incorporating several dozen MAD cores may be found in reference 33.

The Cornell Aeronautical Laboratory has also investigated the possibility of using magnetic cores for perceptron memory elements.[34,35] Theirs was largely a theoretical analysis, with a limited number of experiments to check the validity of the simplifying assumptions found necessary.

The chief source of trouble encountered by the CAL investigators seems to have been the difficulty of generating a uniform, orthogonal "read" field. It is to this obstacle that the marked assymetry and non-linearity of their test integrator, as illustrated in Figure 16, is attributed. The data in this figure relates to one microsecond, 70 volt write pulses with symmetrical, plus or minus 100 volt read drive.

A slightly different version of the toroidal flux integrator is now being patented by J. Devilbiss[36] of the University of Illinois. His device is shown in Figure 17. The novel feature here is the short-circuited loop, which controls the field available for flux switching. Unfortunately, no data is available to show the linearity of integration when both positive and negative pulses are applied.

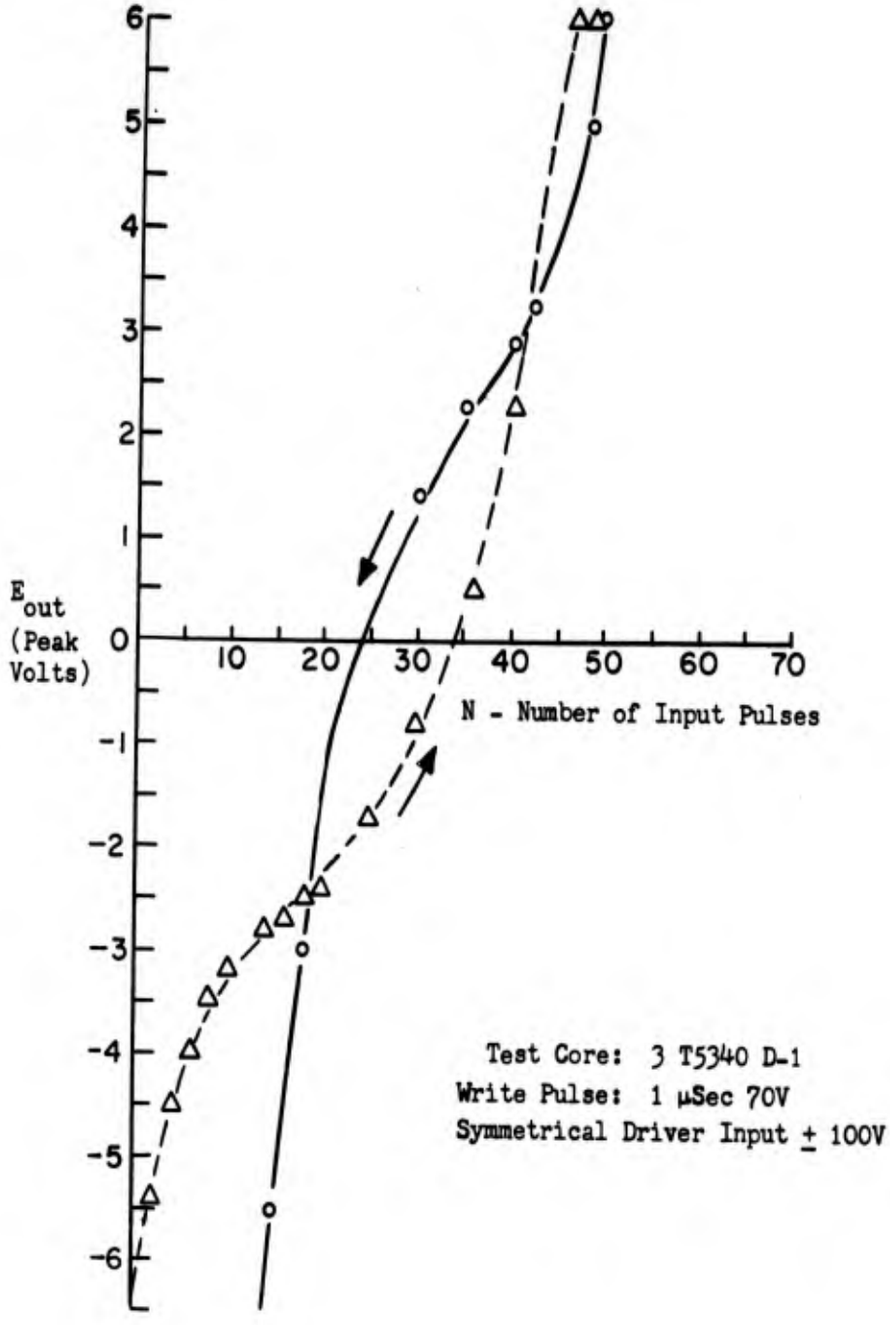

Figure 16. Storage Characteristics of CAL Integrator

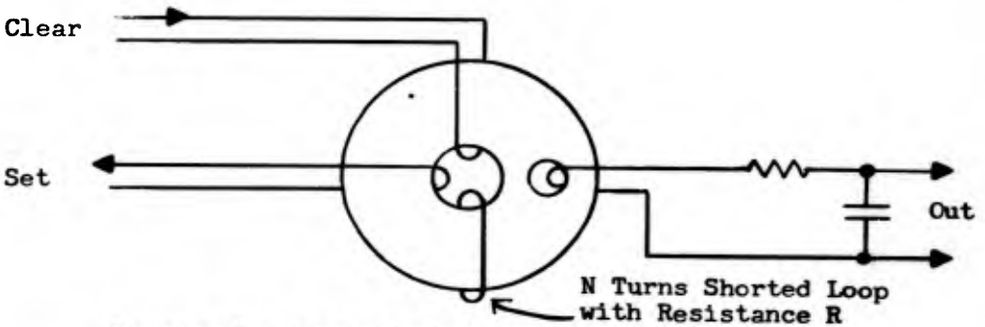

Figure 17. Devilbiss' Modified Transfluxor

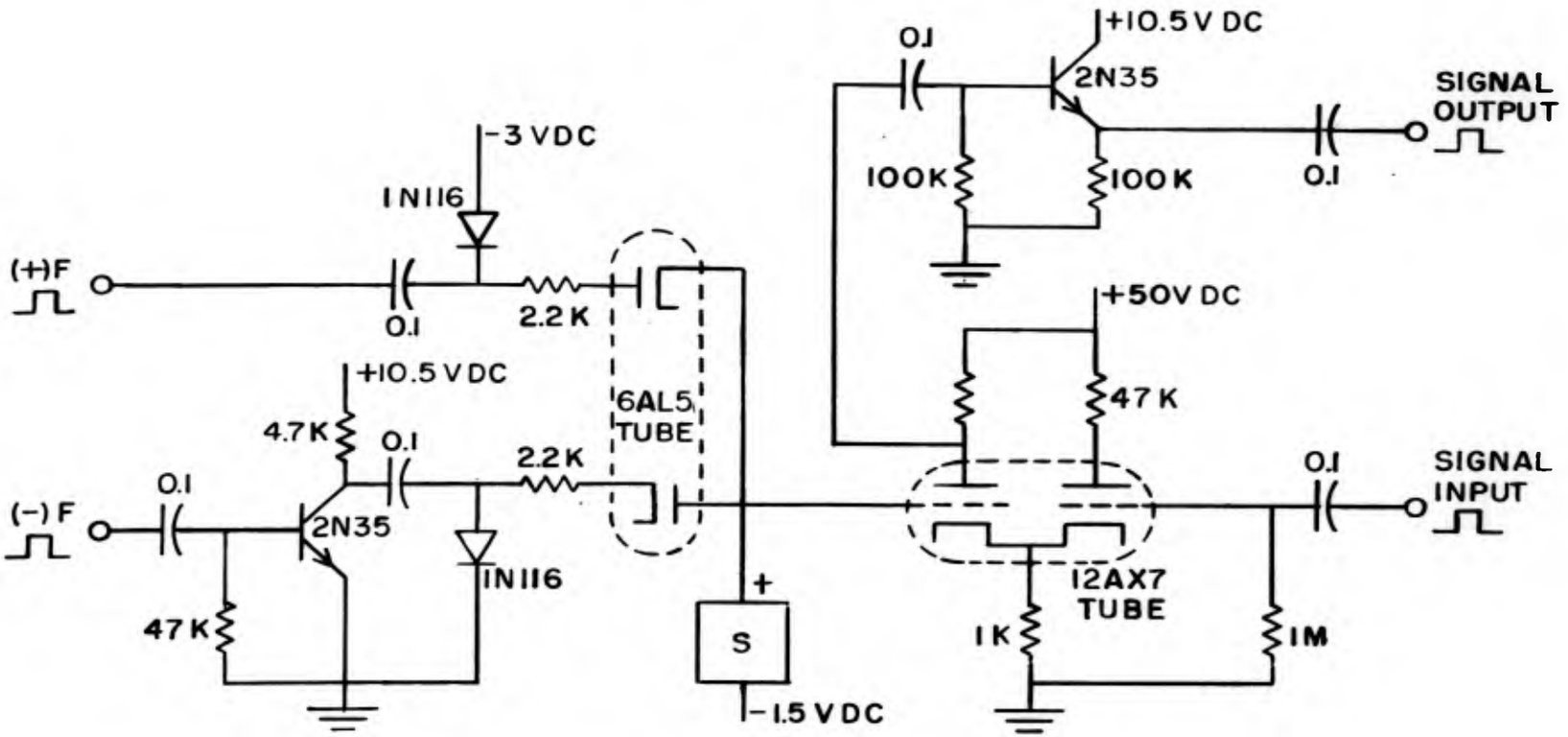

Figure 18. Babcock's "Refined Facilitator"

In summary, it has been demonstrated that a satisfactory integrator may be constructed using ferrite cores. Advantages of magnetic flux integrators include compactness, versatility of function, adequate linearity over a fairly extended range, and long term stability under quiescent conditions. Their chief disadvantage is the complexity of the required auxiliary circuitry. If a large number of such integrators is to be reinforced at once, the total current required is very large. Sequential operation is rendered extremely cumbersome, at least with pulsed strobe read-out devices, by the complicated timing scheme. From this point of view, the carrier scheme developed at Stanford seems preferable, but the configuration of the core, and the number of windings and connections required, keep the total cost rather high.

2.6. Charge Integration

The engineer's concept of a circuit with a memory generally involves one or more charged capacitors, so it is reasonable to investigate whether these hold any promise for present perceptron applications. A brief calculation is sufficient to convince one that they do not.

In order that a 1000 mfd. (taken as an upper bound to practicable values) capacitor may have a time constant of the order of 12 hours, its leakage resistance should be over 40 megohms. While this is not too outrageous a figure, a voltage sensing device of similar input impedance is also required. If the voltages of all the capacitors in the associative layer are to be added through a resistive network, each of the coupling resistors would have to be of the same order of magnitude to avoid discharging the capacitors through one another. With resistors of this size, masking of the signal by noise would present a serious problem.

Yet a time constant of 12 hours would insure a working period of only a few hours.

An additional difficulty stems from the necessity of adding just enough charge to a partially charged capacitor to increase its voltage by a more or less constant amount. This would require a close approximation to an ideal current generator, and the large series resistor necessarily associated with it would render the charging of the capacitors by the reinforcement pulses painfully slow.

It should perhaps be mentioned that the effective value of a capacitor may be increased by feedback through an operational amplifier. While in analogue computers this scheme is often employed to overcome the problems described above, it is evidently impracticable for perceptron purposes.

Nevertheless, capacitors may eventually be used in cross-coupled perceptrons with a built-in decay. Such systems may operate at a more rapid rate than present open loop configurations, if stimuli are presented automatically, and the time constants associated with the reinforcement and the decay are generally in neighboring orders of magnitude.

A recent derivative of the capacitive integration is the nickel-cadmium battery integrator proposed by Babcock.[37] The circuit is illustrated in Figure 18. The use of a vacuum tube to sample the voltage level adds to the cost, but Babcock estimates that in large quantities the complete unit could be produced at under $1.00 apiece.

2.7. Solions

Solions[38,39] is the generic name of a family of amplifying devices which function by controlling and monitoring a reversible electro-chemical reaction.

The reaction utilized in solions is a so-called "redox" reaction, in which oxidation and reduction take place in turn. In the solion tetrode four inert electrodes are immersed in an electrolyte containing both the oxidized and the reduced species of an ion, and by controlling the charge transferred between two input electrodes, a change in conductivity proportional to the integral of the input current may be obtained between the output electrodes.

A common electrolyte for the solion redox system is an aqueous solution containing a small amount of iodine and a comparatively larger amount of potassium iodide. The reactions which take place in the system are as follows:

The potassium iodide dissolves in water to yield potassium and iodide ions:

$$KI \rightarrow K^+ + I^-$$

In the presence of the iodide ion, the iodine exists predominantly as the tri-iodide ion:

$$I_2 + I^- \rightleftharpoons I_3^-$$

If a current is passed through the solution, the tri-iodide ion dissociates at the cathode:

$$I_3^- + 2e^- \rightarrow 3I^- \ ,$$

while at the anode the reverse reaction takes place:

$$3I^- \rightarrow I_3^- + 2e^- \ .$$

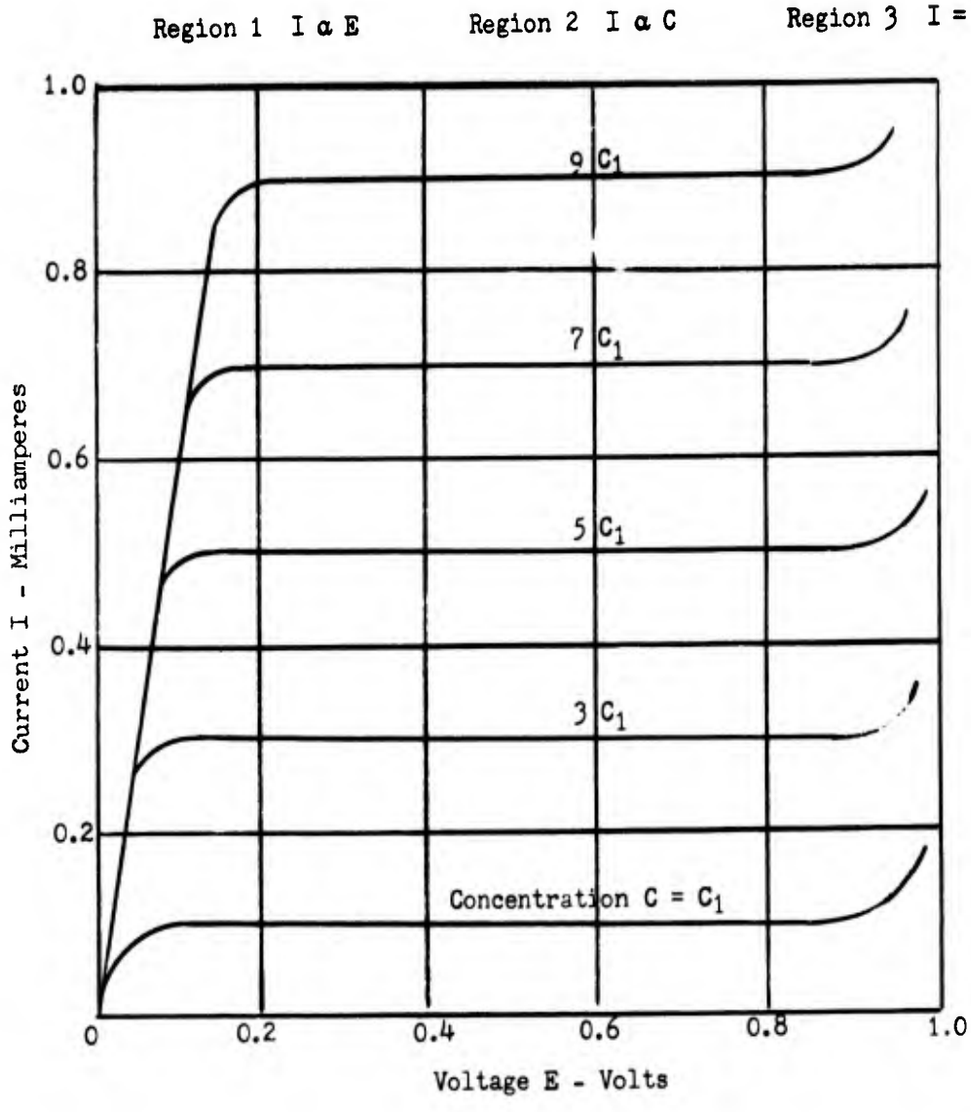

Figure 19. Typical Polarization Curves for the Solion Redox System for Various Concentrations of Iodine

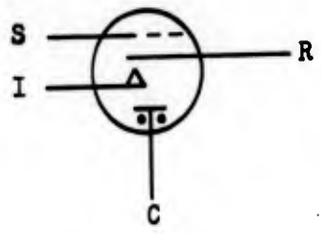

Circuit Symbol

Electrodes

I Input
S Shield
R Readout
C Common

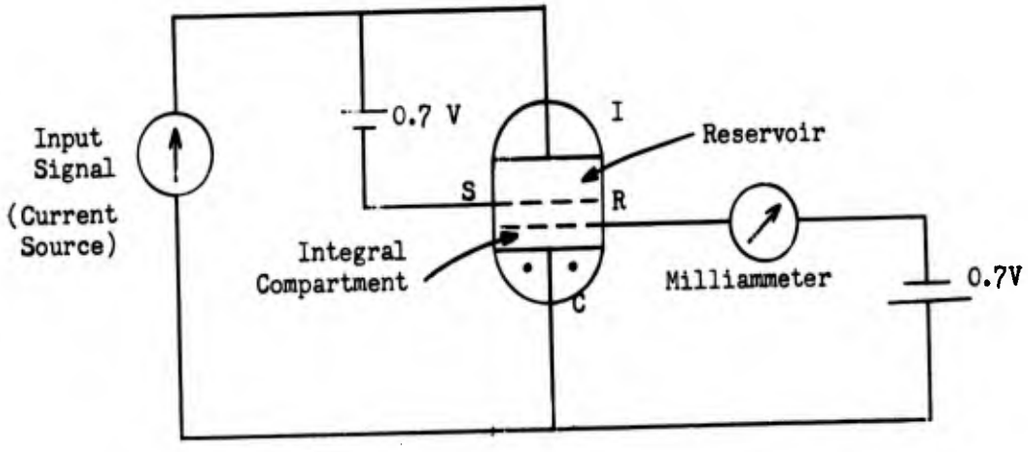

Figure 20. Solion Tetrode Connected as an Integrator

The last two reactions proceed at the same rate, so the components remain at equilibrium concentration.

In Figure 19, the current through the solution is plotted as a function of the e.m.f. applied between two electrodes. In region I the slope of the curve is determined by the conductivity of the electrolyte: in this region Ohm's Law prevails. In region II, the current is limited only by the amount of tri-iodide reaching the cathode by diffusion, hence it is proportional to the concentration of tri-iodide rather than the applied voltage. In region III hydrogen gas is liberated in an irreversible reaction.

Whenever the concentration of tri-iodide is different at one of the electrodes than at the other, (suppose, for example, that they are separated by a diffusion barrier) a concentration potential will be set up between the two electrodes. This potential is given by the equation:

$$E_c = -E_a \log_{10} \frac{C_2}{C_1}$$

where E_c - concentration potential

E_a - a constant (approximately 30 millivolts at 25°C)

C_1 - tri-iodide concentration at electrode no. 1

C_2 - tri-iodide concentration at electrode no. 2

A simplified diagram of the solion tetrode, connected as a current integrator, is shown in Figure 20. The amount of tri-iodide transferred from the Reservoir to the Integral Compartment by the input current is, by Faraday's Law, proportional to its integral with respect to time. The output current is proportional to the concentration of tri-iodide in the Integral Compartment (operating in region II), hence to the integral of the input current. The polarized shield merely serves to reduce the

tri-iodide concentration near it to the point where diffusion through the small perforations of the electrode is negligible.

To achieve small time constants, the Integrator Compartment is made very small. This allows the distribution of tri-iodide to come to equilibrium rapidly. Even with precision machined electrodes, however, 1 cps. seems to be the upper cut-off frequency.

Because of the concentration potential, the input impedance of the solion tetrode varies from about 300 ohms to 1500 ohms. A very high impedance signal source is required to avoid errors due to this effect. A more serious drawback as far as perceptron applications are concerned stems from the low output impedance of the device, which causes units connected in parallel to discharge through one another. These difficulties are similar to those encountered with capacitors, though the time constant is greatly magnified in solions by the use of a liquid medium.

At constant temperature, the stability of isolated solions is reported to be excellent, with drifts of only a fraction of 1% over periods of several days. Reasonably high packing densities may already be achieved--the volume of a tetrode now on the market is approximately 0.2 cu. in.--but prices range around $15 per unit. If solions were ever to be seriously considered for embodiment in large perceptrons, considerable redesign would be required, with the emphasis shifted from precision to ease of mass production.

2.8. Electrolytic Integrators

Yet another form of charge integration is exhibited in an electrolytic device tested by the author in 1960-61. The electrolytic integrator consists in principle of two electrodes immersed in an electrolyte

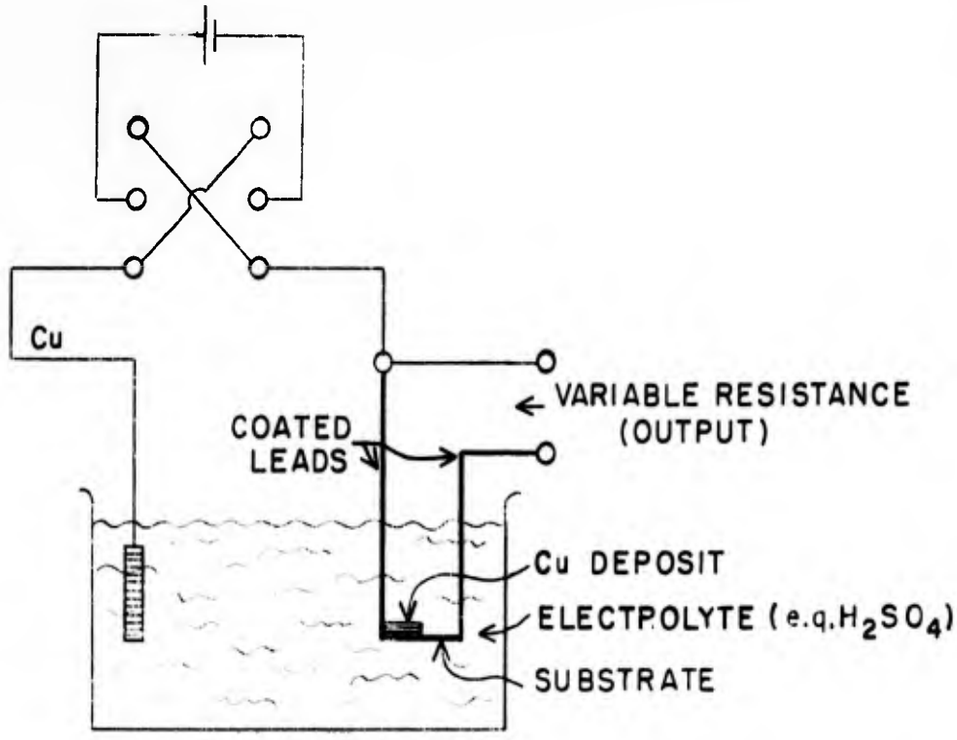

Figure 21. Schematic of Electrolytic Integrator

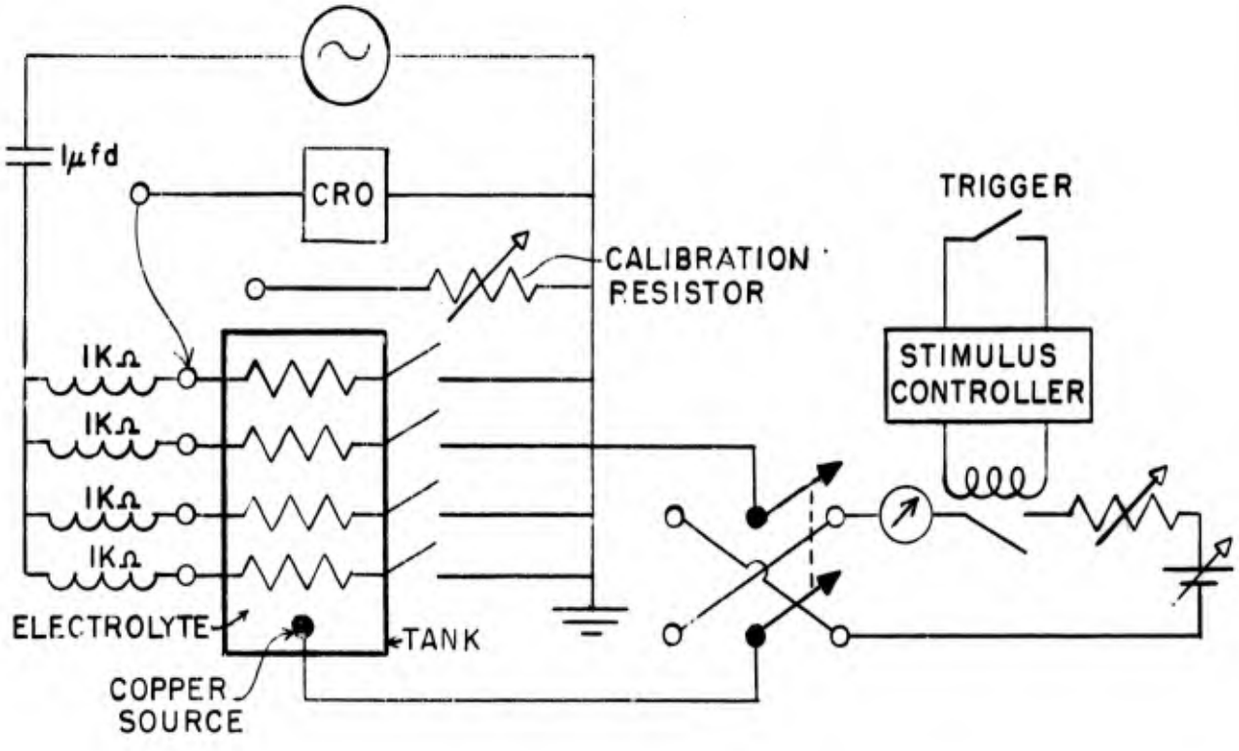

Figure 22. Test Circuit for Electrolytic Integrator

(see Figure 21) in such a way that it is possible to vary their resistance relative to one another by transferring metal in ionized form through the solution. In practice, one of the electrodes, the variable element, is a fairly high resistance conductor with two terminals accessible in order to detect resistance changes. The other electrode, the source, is simply a bar of metal.

The basic resistance of the variable element must lie in a relatively narrow range. If the basic resistance is too low compared to the resistance of the source metal, then in order to produce a detectable resistance change, very large amounts of the source metal must be deposited on the surface of the variable element. Since the maximum plating current is, as subsequently shown, limited, low basic resistance entails inadmissably slow integrating action. If, on the other hand, the basic resistance is high compared to that of the solution, then the resistance change measured at the terminals of the variable element will again be small, due to the constant low resistance of the solution which is essentially in parallel with it.

In general, the metal least difficult to plate is copper, and most of the experiments described below were conducted with copper as the source metal and copper sulphate as the electrolyte. The considerations discussed in the previous paragraph dictate that with this combination the basic resistance of the variable element be between 5 and 100 ohms for an acceptable geometry.

Three schemes which satisfy the resistance requirement are: 1) Very small diameter wire, 2) Ground down carbon composition resistors and 3) Thin metallic films.

To measure the resistance of the variable element it is necessary to use alternating current, since a direct current flowing through the element will establish a potential gradient which will in turn cause transfer of metal from the high to the low end with possible attendant changes of resistance.

A schematic of the circuit used for testing is shown in Figure 27. Provisions are made for pulsing up to four integrators simultaneously, in order to detect possible interaction among the elements. The timing relay was set for all tests at 0.4 seconds.

Tests on single integrators were run in open plastic containers 15 centimeters long by 8 centimeters wide. The wire is held at a slight tension and either pressure or soldered contacts used. The source consists of a number 12 wire parallel to the integrator and 4 cms. away from it. Both electrodes are covered to a depth of about 1 cm. by the solution.

For the simultaneous tests, 5 cm. lengths of integrator wire are placed parallel to each other and 1 cm. apart in a sealed plastic box holding 12 to 25 wires. (See Figure 23.) Here the source wire runs perpendicular to the integrator wires.

Carbon composition integrators were prepared by grinding down half watt 5% resistors to the point where the end connections show. This surface is then polished and the lead wires are coated with rubber cement in order to limit the electrolytic activity to the carbon surface. Two or three such integrators may be placed in a single test tube and copper (or nickel) plated from one onto another.

Metallic film integrators may be simply painted on a microscope slide (Figure 24). Silver paint, suitably protected by a coat of lacquer,

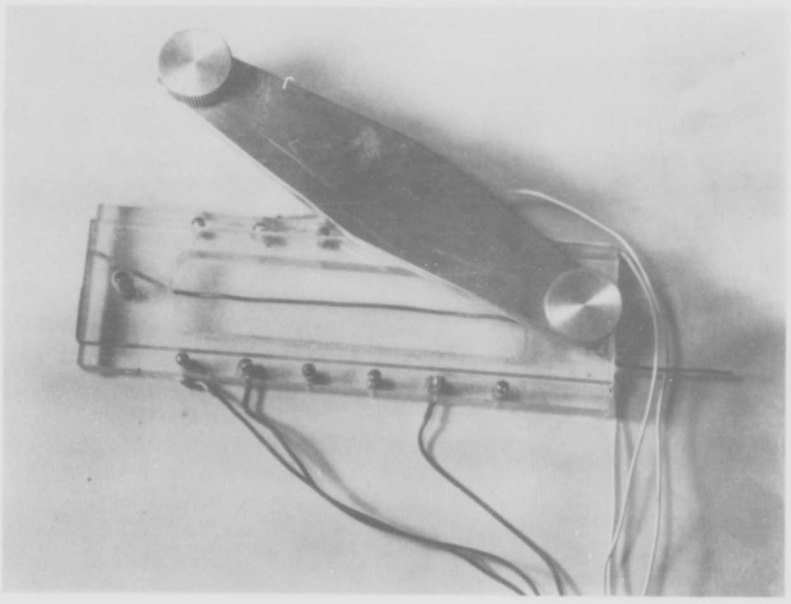

Figure 23. Plastic Tank for Multiple Integrator

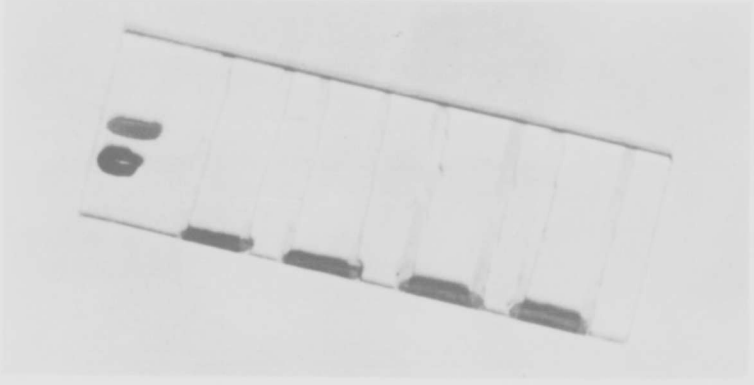

Figure 24. Thin Film Integrator

forms a satisfactory connection to miniature alligator clips gripping the edge of the slide. If reasonably linear performance is desired, a film of uniform thickness is imperative, and more refined techniques must be adopted.

The effects of the composition of the electrolyte will be reviewed briefly before proceeding with a more systematic examination of the properties of specific types of electrolytic integrators.

The simplest commercially used plating formulae[40,41] consist of an almost saturated copper sulphate solution, with acid added to regulate the pH factor, and a "brightener" to provide a more lustrous surface film.

In the application under consideration, the addition of acid to the basic electrolyte, even in minute quantities, presents two serious drawbacks. First, an acidic copper sulphate solution dissolves copper. In commercial plating this is not a disadvantage, since the rate of solution is slow compared to the rate of deposition, and in industrial practice the plating current is never interrupted. At maximum current, and recommended acid content, the ratio of the rates is about 6:1, resulting in very high "forgetfulness." Second, the presence of acid lowers the solution resistance, thus imposing a severe limitation on the resistance of the integrator element.

By way of brighteners, dacolyte and sodium lauryl sulphate were tried. Since neither led to observable improvement in performance, and dacolyte, in fact, tends to dissolve copper, a solution of copper sulphate in tap water (evidently a possible source of impurities) was adopted for all further tests.

The maximum allowable current depends on the concentration of the copper sulphate solution. With low ion densities, extensive polarization occurs at the electrodes,[40] decreasing the "limiting" current value. If the plating current exceeds this density, "arboreal" or spongy deposits are formed; these usually include hydroxides or basic salts. Accordingly, a solution of 240 grams of $CuSO_4$ per liter of water was used. Although this is an almost saturated solution, its resistance is not excessively low with respect to most of the integrators tested.

Table I lists the relevant properties of the various integrator wires. Advance, Chromel A, Chromel C, and Copel all contain some copper, and consequently erode more or less rapidly if reverse plating current is maintained after all the copper has been deplated from the wire. Hence none of these materials would be suitable for the projected application.

Nickel and Molybdenum form a granular and unstable deposit. Due to the unevenness of the deposited copper film, resistance cycles could not be obtained with a satisfactory degree of reproducibility. Tantalum, Zirconium, Platinum, and Tungsten all display to some extent the phenomenon of "anodization." Anodization is the name given to the formation of a thin insoluble film of oxide on the bared surface of the integrator electrode upon reversal of the plating current (i.e. when the integrator becomes the anode). On the other hand, to remove the film it is not sufficient to simply reverse the current again and more cumbersome methods must be employed.

Zirconium and tantalum do not form films of the required degree of smoothness and the limiting current characteristic of these metals is too low to achieve the required sensitivity with commercially available sizes of wire. With platinum, relatively high current densities are

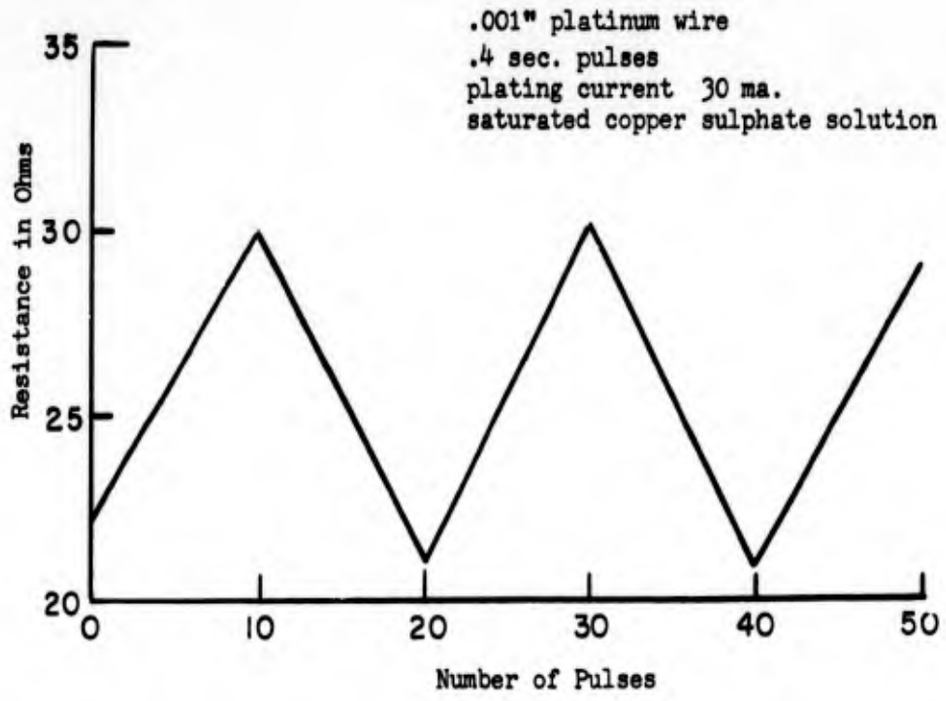

Figure 25. Sensitivity of Platinum Wire Integrator

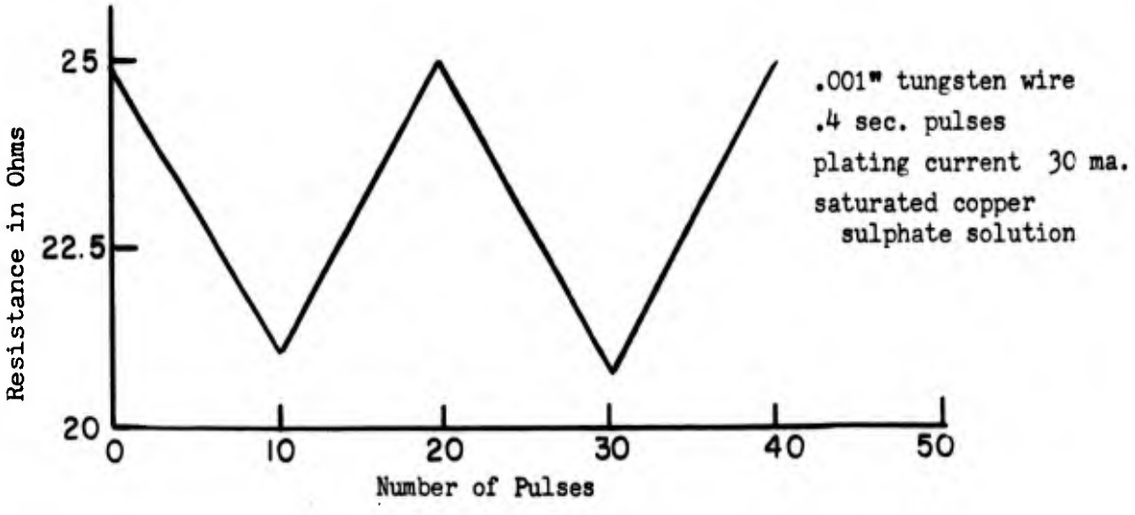

Figure 26. Sensitivity of Tungsten Wire Integrator

practicable: the sensitivity in shown in Figure 25. However, the film formed on anodization has only moderately high back resistance; with constant voltage the current drops only by 25 to 50 percent, depending on the geometry. All the copper is not removed before the current starts to drop, hence initial conditions cannot always be easily re-established. If this difficulty could somehow be circumvented, the excellent plating properties, chemical inactivity, and high resistivity of platinum would certainly render it very attractive for integrator applications.

Tungsten also exhibits sensitive and predictable resistance variation as shown in Figure 26. Here the salient feature is the extremely high back resistance (of the order of megohms) of the anodic oxide film. Common solvents, such as phosphoric, hydrochloric, sulphuric, and nitric acid, acetone, alcohol, or carbon tetrachloride do not dissolve this film. Sodium hydroxide will attack it slowly. By far the easiest way to decompose the oxide is to establish a 30 volt potential difference across the film (tungsten negative) for a few seconds. If this process were to take place in the plating bath, the large resulting current would deposit a considerable amount of granular copper on the wire, thus defeating the purpose of "initializing" the resistance. If however, the overvoltage is applied in a saline or acidic solution of more or less arbitrary concentration, near perfect cleaning action ensues. (See Figure 27.)

Reproducibility is demonstrated in Figure 28, where the performance of four different specimens of tungsten wire is displayed. Also, experiments were run to see if there was any interaction between integrators in close proximity (one cm. apart). No such interaction was observed. The "retentivity" of such integrators is not so impressive since at any given setting the copper dissolves with a time constant of

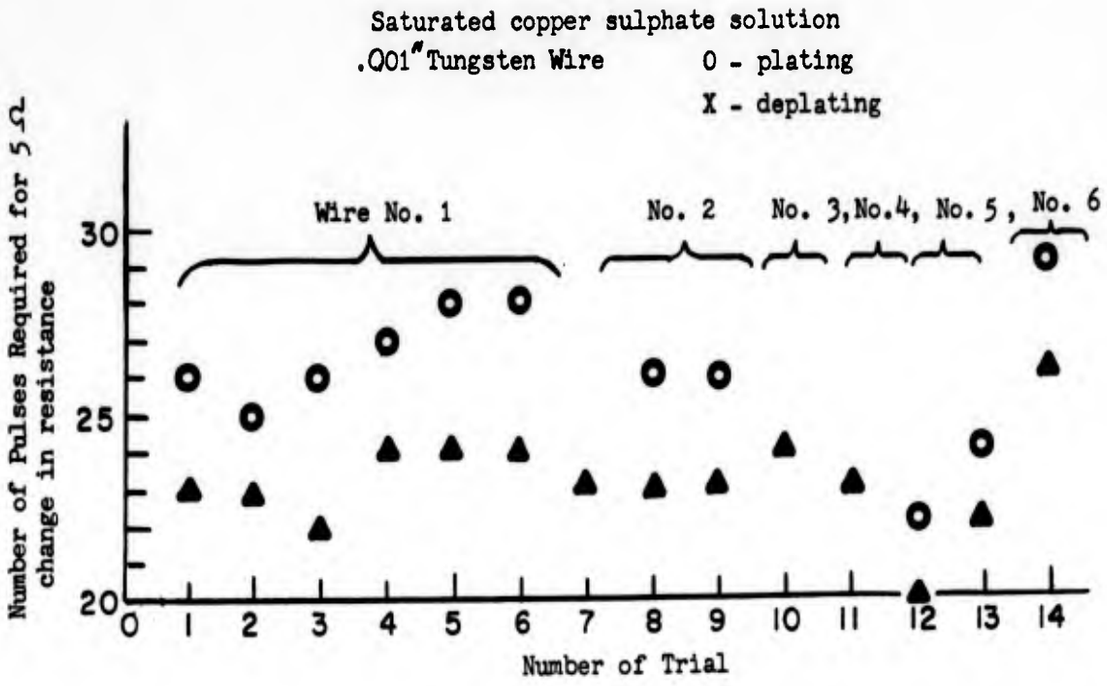

Figure 27. Cleansing of Tungsten Wire

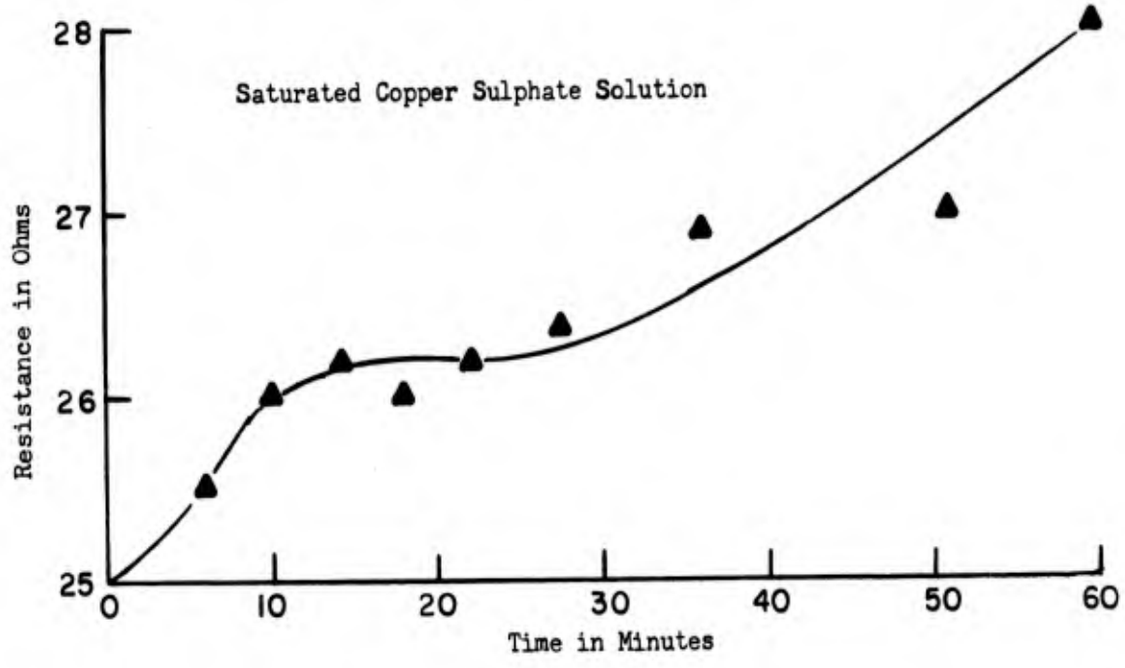

Figure 29. Dissolution of Copper from Tantalum Wire

two or three hours (Figure 29). This is likely due to the presence of both impurities and free oxygen in the solution, since chemists maintain that copper is insoluble in $CuSO_4$.

The range of the integrator described depends of course on the length of the resistor wire outside the solution (and connections) and the amount of non-linearity which may be tolerated. As a first approximation, the useful range may be taken to equal one-half of the basic resistance. In perceptron applications a twenty percent variation in resistance would probably prove adequate.

The deposition of nickel was also attempted. The following is the recipe of the nickel bath used:

$NiSO_4 \cdot 6H_2O$	218g/ℓ
NaCl	9.7g/ℓ
H_2BO_3	25g/ℓ
Sodium Lauryl Sulfate	.42g/ℓ
(Na) Saccharin	6.0g/ℓ

Although this solution was not tested under a sufficient variety of conditions to permit comparison with the copper bath, in no case was a satisfactory resistance cycle obtained. In most cases a rough uneven film was deposited, and upon reversal of the plating current, an unsoluble oxide of rather low back resistance was formed. The process was accompanied by considerable gassing of the electrodes, even at very low current densities.

In general, the limiting current of nickel is less than that of copper, and the same amount of charge will deposit less nickel. Furthermore, since the resistivity of nickel is five times that of copper, approximately five times as much nickel must be deposited on a given wire

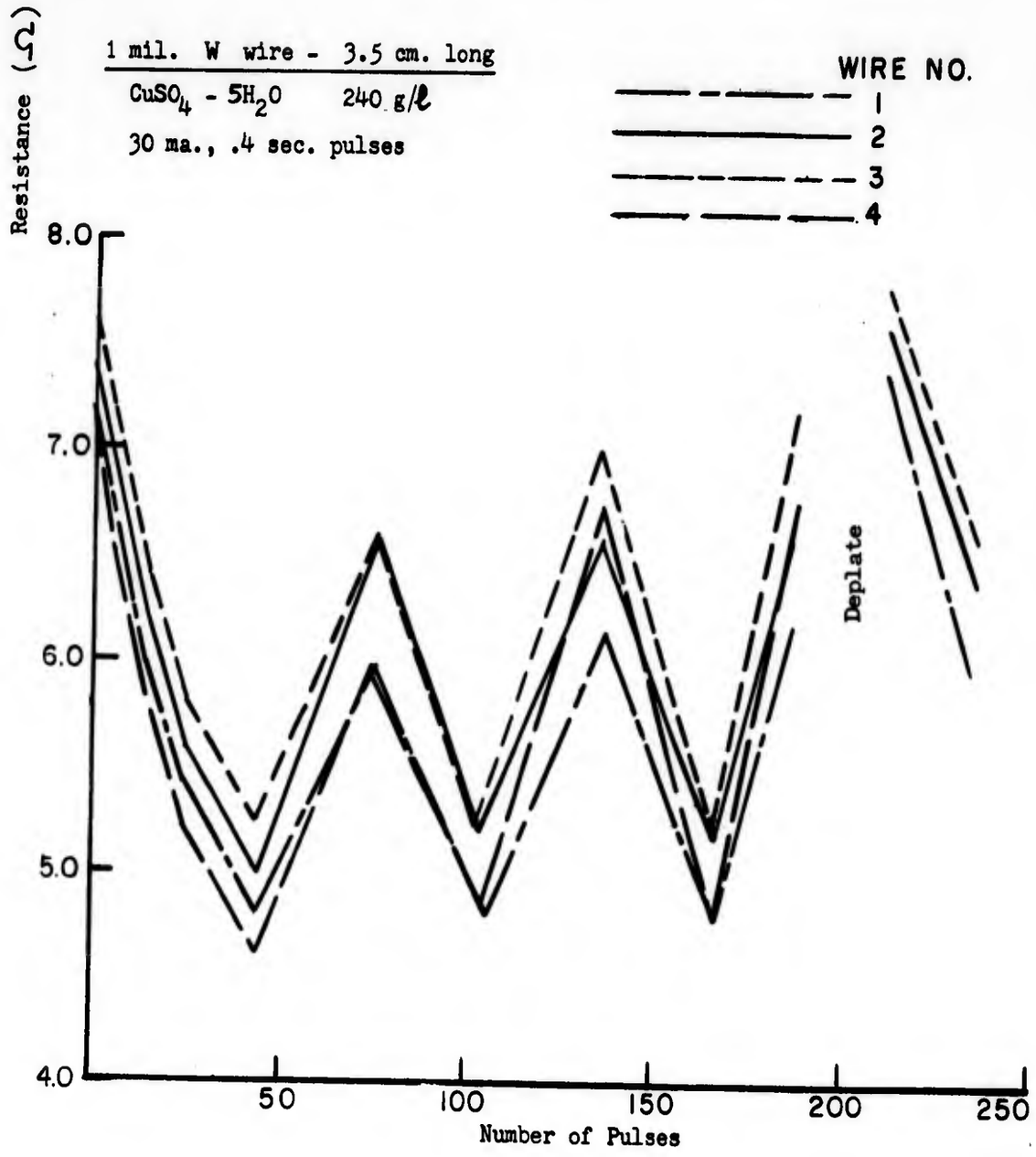

Figure 28. Behaviour of Four Tungsten Wire Integrators in a Common Tank

to effect the same resistance change as a similar layer of copper. These considerations impose very serious restrictions on the sensitivity attainable with nickel solutions, and the tests were consequently discontinued.

The few survey experiments undertaken with carbon composition resistors were prompted by the admirable results achieved by Widrow.[42] It soon became clear, however, that the low inherent sensitivity of ground down resistors (due to the large surface area) would render this type of integrator unsatisfactory for a high speed audio perceptron.

When properly prepared, carbon resistors plate smoothly, but the slightest imperfection in the surface will give rise to flagrant non-linearities in performance. Anodization presents no problem here. The only precaution necessary is to coat the end connections with some chemically inert material such as wax. In a concentrated solution of either copper sulphate or nickel sulphate (or in a dilute but slightly acidic solution) the resistor tends to swell and increase its resistance by an order of magnitude within a few days. In a dilute solution, a six percent change in the basic resistance was observed over a period of twenty-five days. Carbon resistors in coated condition are more stable than wire resistors--perhaps because more copper would have to dissolve or oxidize in order to give rise to the same resistance change.

An experiment was conducted to determine whether carbon resistors would be suitable for a perceptron operating under gamma system reinforcement rules.[15] In this experiment copper was transferred back and forth between two resistors, after the initial source had been removed. This process is very difficult to control adequately and at present offers little hope for a large scale system.

A few experiments were also performed on platinum films prepared on glass by baking on commercially available 5X Liquid Bright. The films typically have a resistivity of 20 to 50 ohms per square, depending on the thickness, and of course one may vary the geometry to obtain any desired resistance value. Connections are easily made with lacquer covered silver paint. The integrator properties appear to be limited mainly by the unevenness of the films obtained by painting--no doubt this mode of deposition could be improved upon.

Widrow reports excellent results (so far unpublished) with industrially manufactured tin oxide film on glass. This substrate lends itself readily to mass fabrication techniques, although extremely strict control is apparently required over the purity of all the components. Even a very slight contamination of the cell results in egregious degradation in performance; it is necessary, for example, to use rhodium plated leads.

Initial experiments on thin films conducted by the Cornell Aeronautical Laboratories[43] have yielded results somewhat less favorable than those reported by Widrow. Plating currents run consistently higher than deplating currents, and long term stability (over a period of days) is poor.

So far none of the electrolytic integrators described have been implemented on a large scale, and it is very difficult to make an estimate of eventual production costs. Presumably the cells would be moulded onto printed circuit boards, so as to avoid the necessity of extra leads. Widrow has each of his integrators hermetically sealed in a separate compartment, but it may be possible to house a number of integrators together. The resistance changes could be sensed most easily with a bridge arrangement. Since precision elements are not of the essence, resistance paints may be used to advantage on the ratio and balance arms.

TABLE I

Characteristics of Electrolytic Substrates

Material	Resistivity	Diameter	Resistance per meter	Remarks
	microohm cm.	mils	ohms	
Advance	48	3.1	98	Dissolves in $CuSO_4$
Chromel A	90	2.0	440	"
Chromel C	112	5.0	85	"
Copel	49	5.0	38	"
Copper	1.72			
Molybdenum	5.1	4.0	7.0	Does not anodize
Nickel	8.6	2.5	27	Poor sensitivity
Platinum	10	5.0	7.8	Partial anodization
Tantalum	14	3.0	30	Anodizes
Tungsten	5.5	1.0	108	Irreversible anodization
		0.7	218	
		0.5	432	
Zirconium	4.1	3.0	8.9	Anodizes

A slight variation on the electrode resistance integrator, proposed by H. Y. Chiu[44], deserves mention. Chiu advocates the use of cells where the resistance between the electrodes, rather than that of one of the electrodes, is changed as the result of copper transfer. For example, the cathode of such a cell may be a cylinder of copper foil, while the anode would consist of a thin gold wire concentric with the cathode. Chiu analyzed a number of different geometries, but discontinued experimental investigations after he found his process to be irreversible and of very limited dynamic range.

III. MAGNETOSTRICTIVE READOUT STORAGE

An appraisal of the contents of the previous chapter reveals that not one of the devices listed therein meets, at its present state of development, the criteria specified in section 1.4. It is seen that most of the non-magnetic devices fail to meet the necessary performance standards, while the magnetic storage elements require elaborate and expensive readout arrangements.

In 1961, Dr. C. Rosen of the Stanford Research Institute, suggested a novel, and, it appears, fructuous approach to the magnetic readout problem. When a magnetostrictive element is acoustically excited, an alternating flux wave is generated whose magnitude is proportional to the initial magnetization of the element. Would it be possible to use the voltage induced by this alternating flux for readout in a suitably designed magnetic integrator? It did not take long to demonstrate that this was indeed a practicable method for non-destructive sampling of flux levels. From then on, the Stanford group concentrated on improving the square loop characteristics of magnetostrictive materials by the application of various stress modes and electrolytic deposition in a magnetic field with a view to eventual "coincidence" switching in very large systems, while at Cornell University the author undertook to develop a somewhat less elegant system specifically designed for Tobermory.

Once the operation of the system was sufficiently understood to put bounds on the range of parameters to be considered, the next step was to run a series of experiments designed to systematically optimize these parameters. In particular, decisions were required concerning the transducer, the storage material, the driving frequency, the reinforcement

pulse width and amplitude, and coil design. Two further problems also arose at this point: the necessity of counteracting the magnetic bias due to the earth's field, and the need for a simple erase mechanism which would leave all the memory elements at "zero".

This chapter begins with a qualitative description of the modus operandi of the magnetostrictive readout integrator, followed by a quantitative discussion of magnetostriction and flux storage. Some analytical results, incorporating numerous arbitrary constants, are forced out of the theory; then theoretical considerations and experimental data, pertaining to the optimization referred to above, are presented. Some space is also given to the purely technical difficulties, such as the attachment of transducers and the fabrication of 10 mil diameter self supporting coils, which were encountered in the course of the investigation. The solutions proposed to the shielding and erasure problems are evaluated, and the chapter closed with a description of the operating characteristics of prototype integrators.

3.1. Principles of Operation

When a ferromagnetic material is heated above the Curie Temperature, all domain structure disappears. If the individual domains formed as the material cools are anisotropic in shape, the material is said to be magnetostrictive: most iron-nickel alloys, for example, display this phenomenon. A positive coefficient of magnetostriction denotes that the longitudinal axis of the domain is essentially parallel to the axis of magnetization, while a negative coefficient means that the axes are perpendicular.

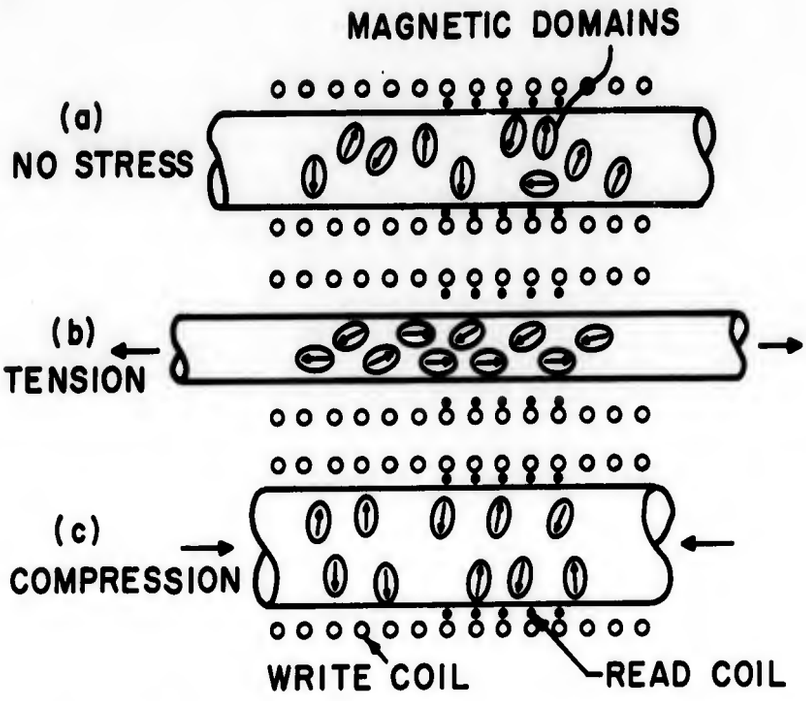

Figure 30. Permalloy Wire under Stress, No Residual Magnetization

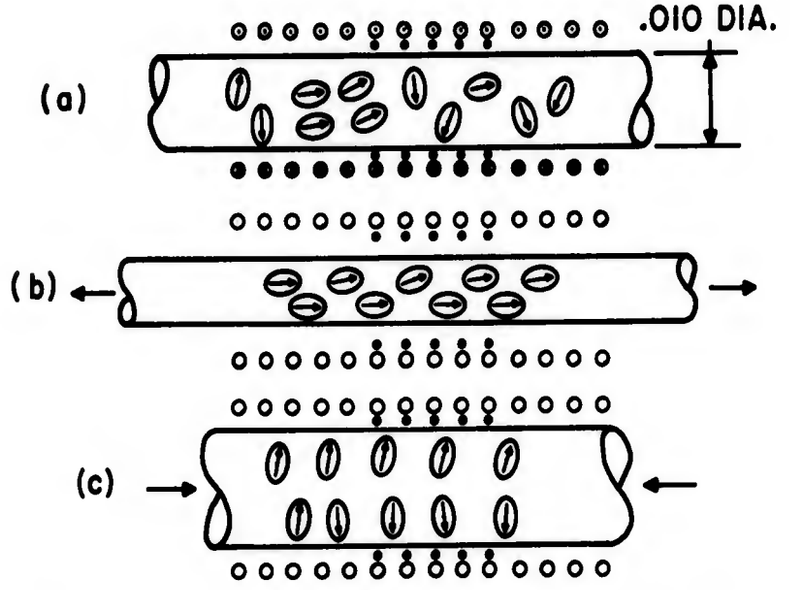

Figure 31. Permalloy Wire under Stress. Residual Magnetization B_r.

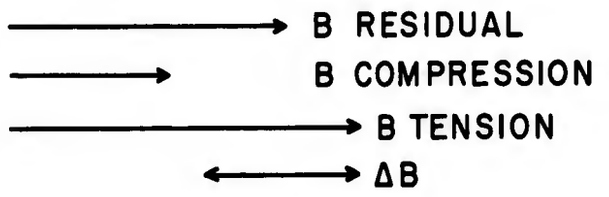

Figure 32. Origin of Flux Change

Figure 30 shows a material with a positive coefficient, such as iron, in the demagnetized state: the domains are completely randomly oriented. Under tensile stress (Figure 30b), the domains line up parallel to the axis of stress in order to minimize the strain energy, but there is no resultant flux, since there are just as many domains "pointing" in one direction as in the other. Compression causes a corresponding alignment perpendicular to the stress axis (Figure 30c).

If, however, the material is originally in a magnetized state (Figure 31a), with some alignment of the domains in a direction parallel to the stress axis, then tensile stress tends to increase the net flux (Figure 31b), and compression decreases it (Figure 31c). The resultant change in flux, depicted in the vector diagram of Figure 32, provides a measure of the initial magnetization of the sample.

Thus, if we can find a material with reasonable square loop characteristics, which has magnetostrictive properties as well, then we may store information by means of the mechanism described in section 2.5, and retrieve it by observing the flux change produced by alternating tension and compression.

This scheme may be realized with the arrangement shown on Figure 33. The magnetic medium is a thin permalloy wire attached at one end to a piezo-electric crystal. Current applied to the crystal at ultrasonic frequencies sends an alternating stress wave down the wire. "Writing" is accomplished by narrow width pulses through the "write" coil, and the level of magnetization is continuously monitored by a "read" coil wound concentrically with the "write" coil. If the frequency and the root mean square amplitude of the stress wave is maintained at a constant value, then the open circuit output of the "read" coil is approximately proportional to the flux stored in the portion of wire directly under it.

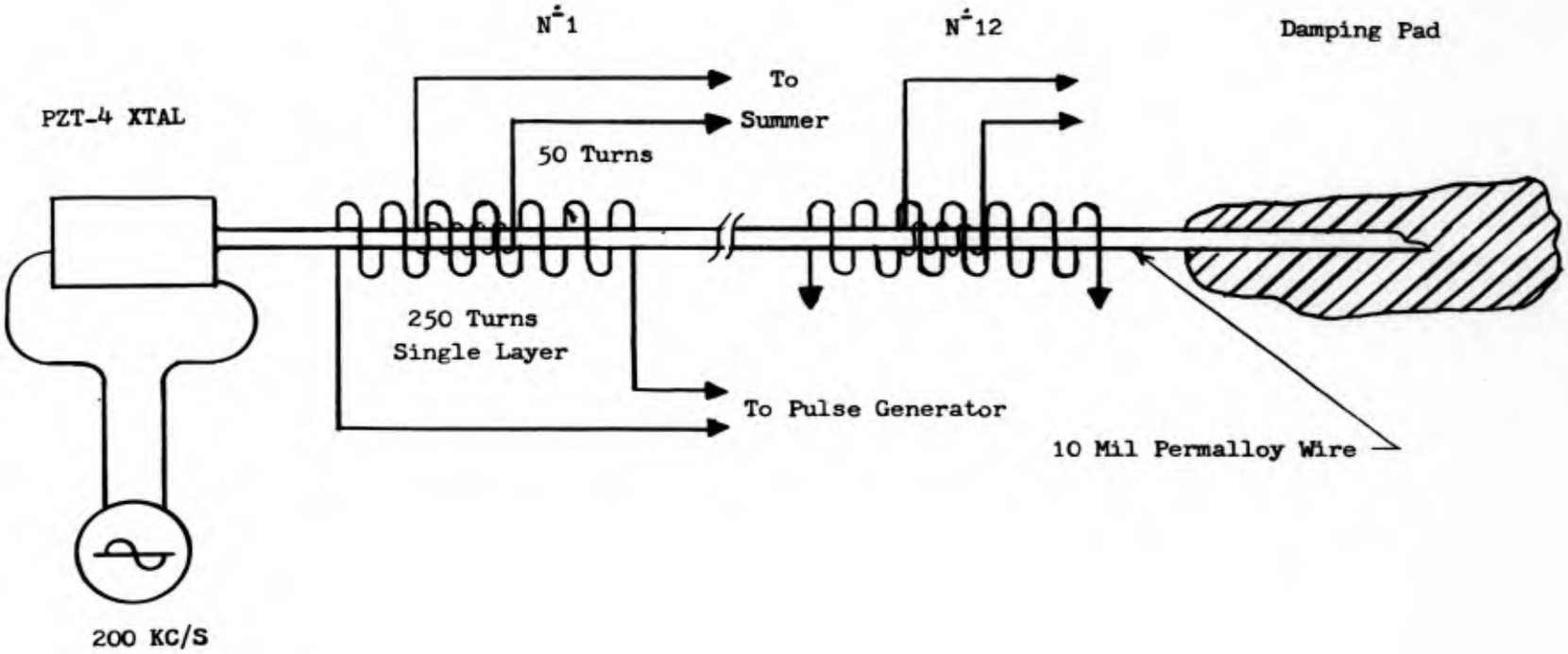

Figure 33. Schematic Diagram of Magnetostrictive Readout Integrator

3.2. Magnetostriction

The relation between the applied stress and the change in domain orientation will first be derived along the lines suggested by Becker and Doring.[45]

Consider a small spherical globule of magnetostrictive material, of diameter d, above the Curie point. If, on cooling, it is spontaneously magnetized into a single domain, there will be a change of shape which may be represented to a first approximation by the equation

$$r = A + B\cos^2\theta \ ,$$

where r is the length of a diameter measured in a direction at an angle θ to the direction of magnetization.

In the ensemble of such domains, oriented at random, the average length of a domain, measured in any one direction in the ensemble, would be

$$r_o = E\left\{A + B\cos^2\theta\right\} = A + 1/2\ B.$$

At saturation, when all the domains are aligned in the $\theta = 0$ direction, the length of each domain in the direction of magnetization of the ensemble is

$$r_s = A + B \ .$$

Let

$$\lambda = \frac{r-r_o}{r_o} \ ,$$

$$\lambda_s = \frac{r_s-r_o}{r_o} \ ,$$

then

$$\frac{\lambda}{\lambda_s} = \cos 2\theta \ .$$

The strain energy per unit volume of material can now be evaluated by letting the domains rotate from their original direction at strain λ to perfect alignment under the influence of a constant external tension σ. Thus,

$$E_s = \int_{\lambda}^{\lambda_s} d(\sigma\lambda) = 2\lambda_s \sigma \sin^2\theta ,$$

where zero strain energy is arbitrarily assigned to the saturated material. It is seen that when λ is positive, the strain energy is a minimum for $\theta = 0$, and when λ is negative, it is a minimum for $\theta = \frac{\pi}{2}$. This justifies the assertion implicit in Figure 30 of the previous section.

When a small stress is applied to a magnetostrictive material subjected to a steady "polarizing" field, the change in induction so produced is proportional to the stress.[46] In the application under consideration the assumption of a "small" stress is justified by the very small output voltage, which is indicative of a change of flux of only about 30 gauss. Bozorth and Williams[47] have calculated the incremental change in induction due to stress Λ at small stress values to be:

$$\Lambda = \left.\frac{\partial B}{\partial \sigma}\right|_{\sigma = 0} = 2.2 \left(\frac{\lambda_s B_s}{K}\right)\left(\frac{B_o}{B_s}\right)\left(1 - \frac{B_o^2}{B_s^2}\right)$$

where λ_s = magnetostrictive expansion (contraction) at saturation
B_s = saturation flux density in gauss
B = polarizing flux density in gauss
K = crystal anysotropy constant in ergs/cm^3

This relation, which has been thoroughly verified experimentally, is almost linear for polarizing flux densities less than about a third of the saturation flux density; in practice, the integrator is always operated in this condition.

The actual value of Λ obtained from the Bozorth-Williams equation cannot be readily checked with the apparatus used, since the effect of the loading of the permalloy wire on the crystal is not known. Necessary information could perhaps be obtained by Q measurements on the loaded crystal, but the check was not considered to be of sufficient interest to compensate for the labor involved.

3.3. Flux Storage

The mechanism of flux storage in toroidal cores has been amply investigated both theoretically,[48,49,50] and experimentally,[51,52] and the concensus of opinion seems to be that there is no accounting for the peculiarities of domain behaviour. The following effects are, however, deemed important:

1. The reduction of the effective magnetic field inside the material by induced eddy currents.

2. The damping of domain rotation due to "spin relaxation."

3. Hysteresis, which is the name given to losses arising from imperfections, inclusions, and inhomogeneities in the material.

4. Inertial terms affecting the acceleration of domain walls.

5. The influence of "wall energy" on wall motion.

The various mathematical treatments of the problem all reduce to the principle that the "free energy" of the system must remain a minimum throughout the switching process. Then classical eddy current theory[49] demands that the velocity of wall motion be proportional to the difference between the applied magnetic field and a somewhat nebulous entity called the coercive force of the material. The volume distribution of the eddy currents is to be such that the value of the field at the boundary of

magnetization is this same coercive force. Because of the non-linear nature of the ferromagnetic B-H loop (whether static or dynamic) none of the approaches yield numerical results which check with experiment, though several of the models are quite descriptive of particular aspects of the process.

With toroidal cores where the ratio of outer diameter to inner diameter is not too close to unity, it is reasonable to assume that flux will be switched first around the inner perimeter, where the magnetic path is shortest. As the inner regions become saturated, more and more domains would have to be switched by each pulse in order to advance the wall boundary by a constant amount; in effect, pulses at this stage of the proceedings will produce a smaller change in output.

If an infinite, axially magnetized cylinder is considered instead of a toroid, no such simple principle can be applied to explain the reduced effectiveness of cumulative pulsing. The eddy current considerations merely suggest that the boundary of flux switching moves from the outside in. Of course, one may equate the volt-time integral (energy) of the input pulse to the $\int HdB$ integral, and note that with a non-rectangular hysteresis loop less energy is required for a unit increment in flux density at the lower flux level than at the higher one, but this is a heuristic explanation at best. Quantitative predictions based on hysteresigrams obtained at 60 cps or at 400 cps, check only roughly with the nearly exponential flattening of the counting curves shown in section 3.7.

The low frequency, or static, hysteresigrams are, however, sufficient to show that the sides of the loop are steepest at the low flux densities.

It is therefore desirable to operate at the low levels, even apart from the magnetostrictive requirements of the system. In order to subdivide the range of flux available into as many levels as possible, it is necessary to write by means of very narrow width pulses. Limitations on pulse forming equipment led to the adoption of a standard .1 microsecond pulse in all experiments, while the pulse amplitude was dictated in each case by the width of the B-H loop at the level of the maximum flux.

The inadequacy of the present analysis of flux storage is keenly felt by the author, and further developments in the field are eagerly awaited.

3.4. Transducers and Operating Frequency

Transducers used to impart vibrational energy to solids at ultrasonic frequencies may be either piezoelectric or magnetrostrictive in nature. Both kinds of transducers have been used to drive the integrator described in the previous sections, and the advantages and disadvantages of the two types are rather evenly balanced.

Among piezoelectric materials, Rochelle Salt, Quartz, and Barium Titanate are typical of the crystals available. Rochelle Salt[53] is highly unstable above temperatures of about 40°C., hence the soldering of leads to the crystal is difficult. Quartz has excellent mechanical properties, but in order to obtain a sizeable longitudinal strain a driving voltage of several thousand volts is required. Barium Titanate seems in all respects the best choice; the particular ceramic tested is Clevite's PZT-4.[54]

Relevant properties of PZT-4 are listed in Table 2. This crystal can be submitted safely to temperatures of up to 200°C., and its aging

TABLE II

Characteristics of PZT-4 Crystal

Piezoelectric Coupling Coefficient	$k_p = .52$
Dielectric Constant	$K_3 = 1200$
Frequency Constant	$N_1 = 1650$ $\frac{\text{cyclemeters}}{\text{second}}$
Poisson's Ratio	$\sigma = .30$
Density	$d = 7.5$ g/cc
Resistivity	$\rho = 10^{13}$ ohm cm.
Mechanical Figure of Merit	$Q = 600$
Dielectric Dissipation Factor	$D \leq .005$
Maximum Non-resonant Driving Field	10 KV/cm.
Maximum Safe Operating Temperature	$150^{\circ}C$
Maximum Safe Tensile Stress	10^8 newtons/m^2
Maximum Strain for Linear Operation	3×10^{-4}

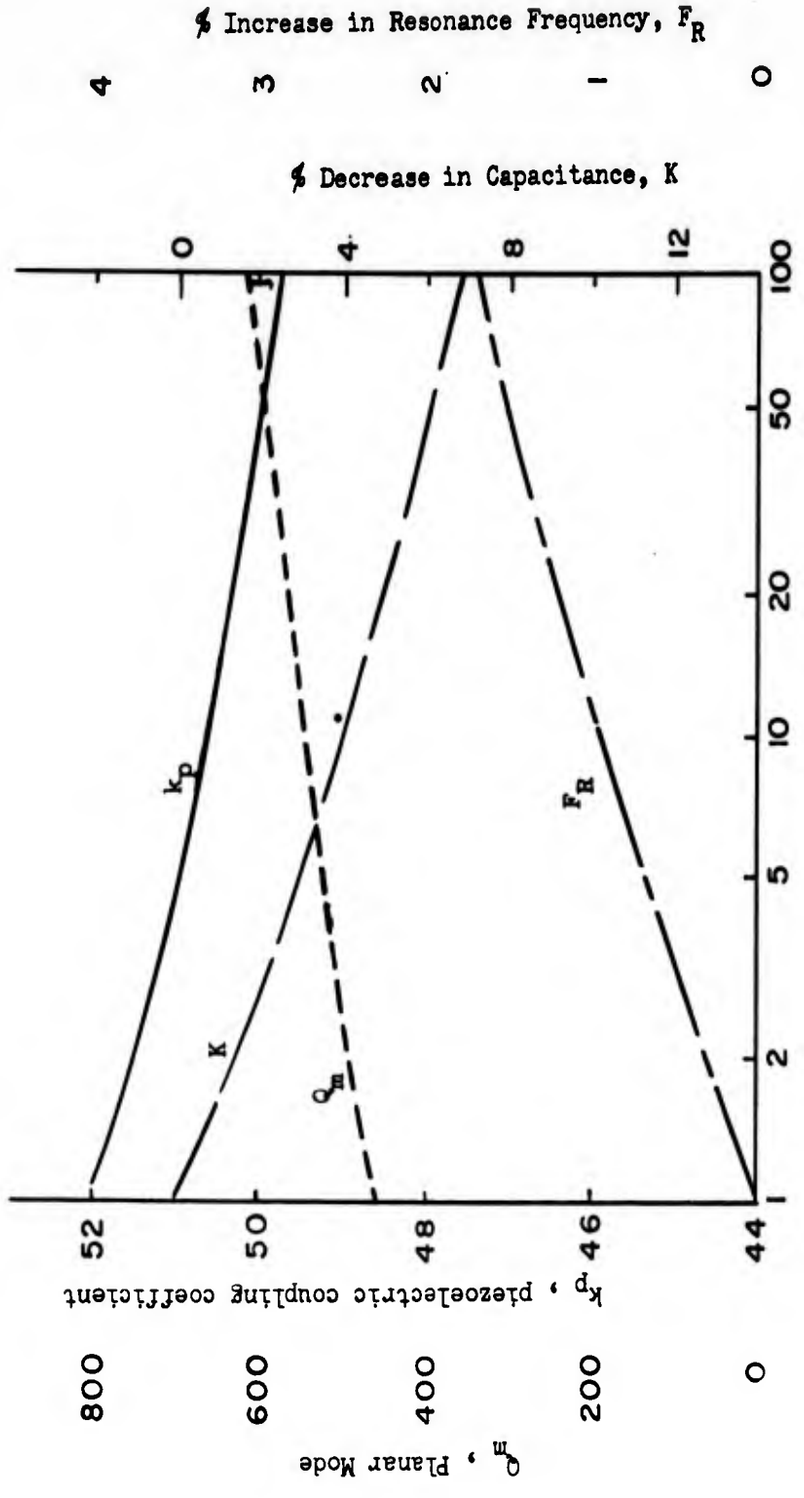

Figure 34. Typical Aging for PZT-4

characteristics, as shown in Figure 34, are also satisfactory. For many of the tests, the crystals were driven at the resonant frequency (130, 200, 250 Kcps) by a Hewlett Packard signal generator supplying about 30 volts r.m.s. This drive is sufficient to produce an output voltage of about 100 microvolts peak-to-peak per turn with a remanent flux of about 2,000 gauss. At non-resonant frequencies, much more driving voltage is of course required to produce a detectable output.

The crystal may be either a rectangular prism or a cylinder; spurious resonances were less bothersome in cylindrical crystals. In any case, the largest diameter of the crystal should be less than .29 λ,[55] where λ is the wave length of the crystal at the resonant frequency. If this caution is not observed, transverse vibrations will be set up within the crystal, greatly reducing the output. For optimum coupling, a mechanical impedance matching device, such as an exponential horn,[56] should be used, but the slight gain in energy transmission did not seem worth the additional expense.

The magnetostrictive wire was butt-soldered to the face of the crystal with Divco. Rosin Core Silver Solder (Figure 35). Ordinary solder tends to remove the thin film electrodes from the face of the crystal. The importance of a good joint can hardly be overemphasized; many of the initial experiments came to grief before the right technique was mastered; in particular, care must be exercised not to damage the crystal by the application of too much heat. Contacts to the electrodes were much more easily attached, since the No. 38 wire used here did not have to be butt-soldered--also, it took solder much more readily than the various perm-alloy and nickel wires.

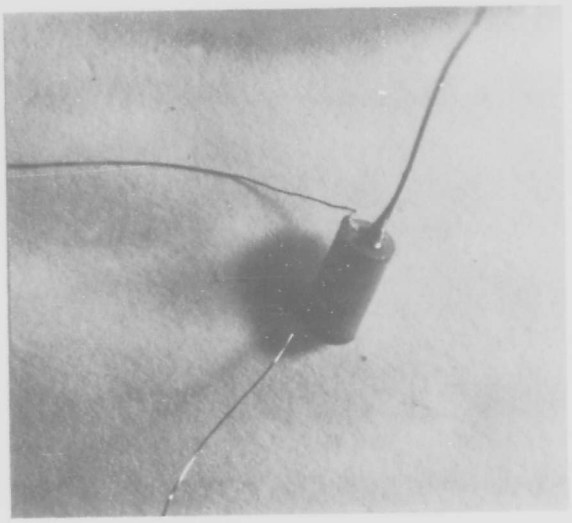

Figure 35. ¼" Crystal Transducer

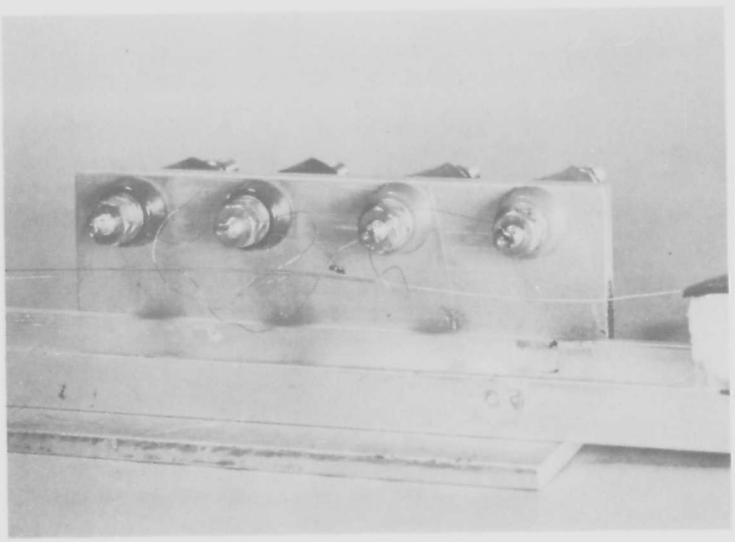

Figure 41. Coil - Assembly

Several glues, such as Carter's Epoxy Cement, Vinyl Cement, and Eastman 910 Adhesive, were also tried, but without success.

Two simple crystal holders[57] were constructed. One held the crystal at its node of vibration by means of three pointed plastic screws; this is a satisfactory mounting for resonant operations. The other consisted of a depression in a small piece of stiff plastic foam, with enough clearance to allow the sonic line to pass through. This mounting permits rapid interchange of crystals.

The magnetostrictive transducer consists simply of a coil wrapped around the sonic line; the magnetostrictive properties of the line itself are used to generate the stress wave. This configuration is very similar to the widely used ultrasonic delay line; the difference is that a continuous wave rather than pulses are applied at the drive end, and the bias at the receiving end is varied by storing flux in the line. The optimum value of the bias at the drive end may be calculated by maximizing Λ with respect to B_o in the last equation of section 3.2. If the coil is driven to saturation, the bias should be $\frac{\sqrt{3}}{3}$ of the saturation flux density. The coil may be biased by circulating a direct current through it, or by placing a permanent magnet in its proximity. In practice the optimum value is easily attained by varying the current or the position of the magnet until the output is largest.

In delay lines of this type an attenuation of 20 db. or more between input and output is typical.[58,59] Most of the loss is due to poor coupling between the coils and the line; the attenuation of the line itself is only of the order of 1/2 db. per meter.[60] In order to obtain a measurable signal in the read coils, it is necessary to drive the input transducer very hard.

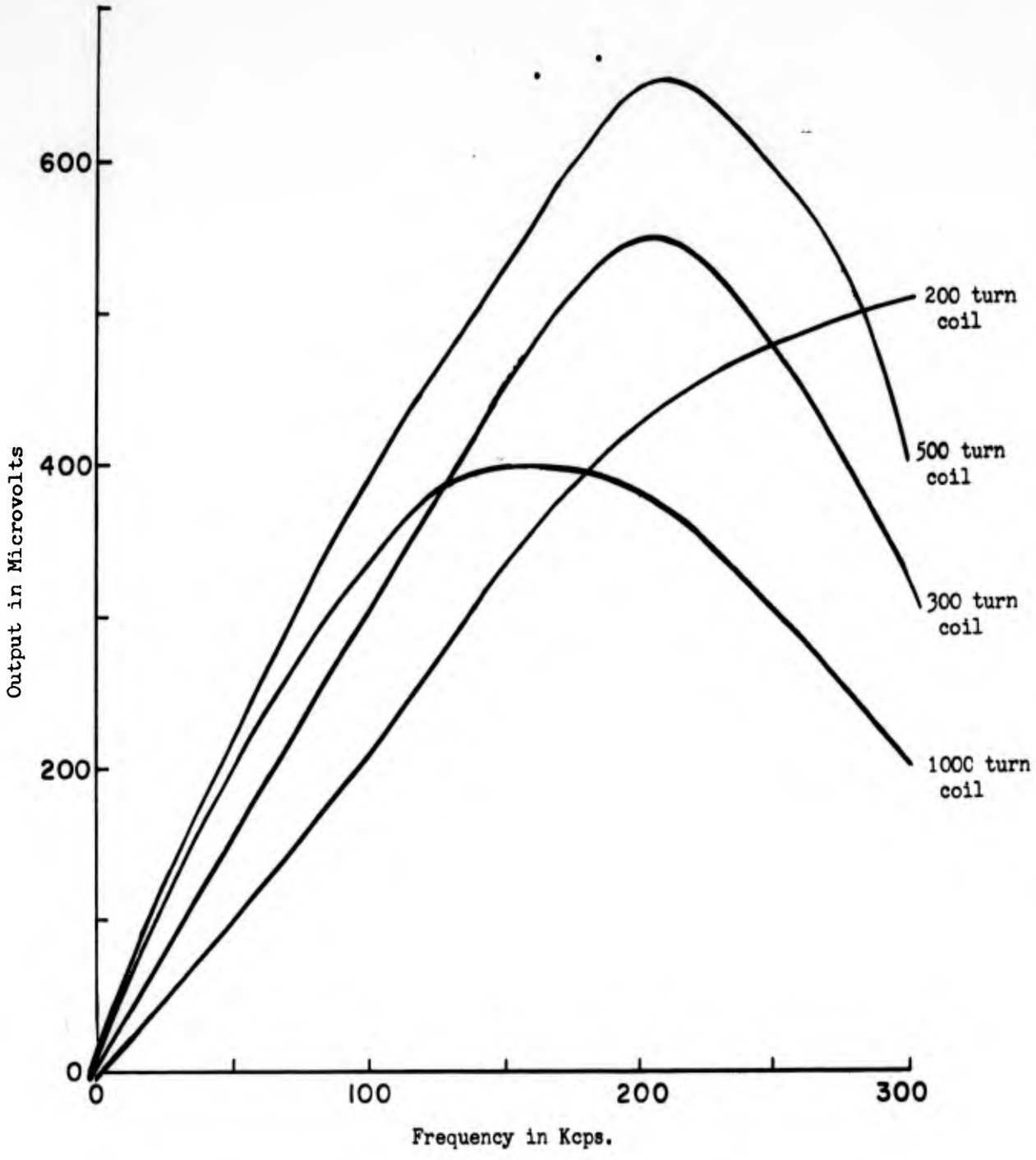

Figure 36. Frequency Response of Coil Transducers

The length of the coil must be kept under half a wave length at the driving frequency: for nickel at 250 Kcps, this is about 1 cm. The coil cannot be too thick either, lest the leakage flux spread out beyond the half wave length limit, and cause cancellation. Thus, the physical dimension, and consequently the allowable power dissipation, is severely limited, and one may not be able to obtain a sufficient number of ampere-turns to cause an appropriate strain in the delay line.

Figure 36 exhibits the variation in output voltage with frequency for input transducers of the same length but different number of turns. In each case, the output is small at the lower frequencies because the voltage generated in the read coil is proportional to the rate of change of flux. At very high frequencies the gain due to the increased rate of change of flux is swamped by the eddy current effects, which are proportional to the square of the frequency, and by the decreased input due to the increase in the impedance of the driving coil. The maximum in the curves occurs at different frequencies for the different coils because of the variation in impedance. In thicker wires (wires up to 20 mils. in diameter were tested) the eddy current losses are even more pronounced.

Even if piezoelectric input transducers are used, it is necessary to keep the amplitude of the stress wave small in order that the flux change at the output may remain proportional to the stress. In some instances, when a crystal was driven hard at resonance, distortion of the wave shape was noticeable. This occurred in the linear operating region of the crystal, so the distortion was doubtless due to the non-linear magnetostrictive effect.

The desirability of using a single layer read winding requires that the operating frequency of the device be above 50 Kcps., while the eddy current losses[61] would make it impractical to operate above 500 Kcps. In addition, at frequencies at the lower edge of the broadcast band there is appreciable radiation even with leads of a few meters in length, and the size of Tobermory would make it difficult to avoid such leads altogether.

Since both the piezoelectric and the magnetostrictive drivers adequately cover this frequency range, the choice between them must be based on cost. Crystals of suitable size are quoted at $1.60 in lots of a thousand, while coils cost about 52¢ apiece in the same quantity. The coils are somewhat easier to mount, because a pad is not needed, and they obviate the necessity of handling and transporting three foot lengths of delay line with a crystal attached to one end, but these advantages may not be sufficient to offset the additional driving circuitry required.

Crystals may be operated in either a resonant or a nonresonant mode. At the fundamental resonant frequency a 50 volt r.m.s. source is ample, but if several crystals are to be operated from the same source, precautions must be taken to ensure that the resonant frequencies, under loaded conditions, are exactly the same. Even a slight deviation in frequency will cause a significant reduction in the energy transmitted to the delay line, and hence in the output voltage induced in the read coils. The Q of the loaded crystal is about 50, and its input impedance is 2,000 ohms capacitive. Under nonresonant conditions, an r.m.s. input of several thousand volts is required for a similar output, but the currents involved are of course small, so that it may not be necessary to provide a repeater for every crystal.

The coils have a much lower impedance than the crystals, typically a few hundred ohms inductive. Because of the indirect coupling, a driving current of several hundred milliamperes is needed. Furthermore, the coils have to be spaced exactly the same distance from the driving end of the delay line, otherwise reflections will cause variation in the amplitude of the stress waves in the different lines. An alternative to the accurate spacing is to put damping pads on both ends of the line.

While standing waves on the line are economical from the energy point of view, when several integrators share the same wire a flat line is desirable in order to conserve magnitude and phase relationships among the output voltages. These phase relationships are indicative of the "sign" of the stored flux. Damping pads used on conventional delay lines include neoprene pads,[62] synthetic sponge pads,[63] and p.v.c. in the form of Welvic Paste,[64] which forms a soft rubbery solid after oven curing at 150°C. Gum rubber, Faber plastic cleaner, art eraser, and plastic tape were also tested for attenuation; the most effective among these is the plastic type cleaner. If care is taken to mould the pad into a conical shape, just barely touching the delay line at the narrow end, a standing wave ratio as low as 1.05 may be attained. A quicker method is to put kinks of increasing sharpness at the end of the line. The wave is reflected back and forth between the kinks until it is finally dissipated by the inherent scattering in the wire.

3.5. Ferromagnetic Magnetostrictive Materials

The application of stress affects the magnetic properties of most ferromagnetic materials to such an extent that stress may be ranked with field strength as one of the primary factors affecting magnetic behaviour.[46]

TABLE III

Properties of Magnetostrictive Materials

Material	Initial Permeability	Maximum Permeability	Saturation Flux Density	Coercive Force	Maximum Strain Sensitivity
			gauss	oersteds	gauss per $\frac{kg}{mm^2}$
Iron	200	5,000	21,500	1.0	--
Nickel	250	2,000	6,000	0.7	500
Cobalt	70	245	16,000	8.9	--
Permalloy *20%	200	1,000	20,500	11	--
30%	800	5,000	3,000	.8	0
40%	2,500	15,000	15,000	.4	1300
50%	3,000	17,000	16,000	.25	2600
60%	3,500	17,000	14,500	.13	3500
80%	6,000	80,000	10,000	.06	500

* Figures refer to air-quenched permalloy.

In discussing the effect of unidirectional stress it is customary to speak of materials whose magnetization increases with tension and which expand when magnetized as having positive magnetostriction, and of materials whose magnetization decreases with tension and which contract when magnetized as having negative magnetostriction. These definitions agree with the ones proposed in section 3.1.

The ideal material for the integrator would have a high magnetostrictive coefficient, a dynamic B-H loop with very steep sides, high saturation flux density, and a coercive force which is large compared to the earth's field, yet small enough not to require excessive magnetizing currents. Unfortunately, square loop materials display very little magnetostriction (because the domains seldom lie in an intermediate orientation), so a compromise must be expected.

Among ferromagnetic metals, cobalt yields alloys which are brittle and generally unsuitable for drawing in wire form. One exception, Vicalloy, has a coercive force of several hundred oersteds, and need not be considered here. Iron and most steels have a very low magnetostrictive coefficient. Nickel has a high magnetostrictive coefficient, but its hysteresis loop is very far from square. Thus one is led to the iron-nickel (permalloy) alloys. The hysteresigrams of several of these materials, in wire form, are exhibited in Figure 37. The slight assymetry is due to the earth's magnetic field; the coercive force is in each case rather low. Figure 38 shows that the loop may be "squared up" by the application of various modes of stress. It is, however, difficult to maintain a wire soldered to a crystal, or smothered in damping pads, under tension and/or torsion, and consequently this line of experimentation was abandoned.

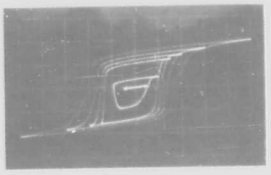

Figure 37. Hysteresigram of 152 permalloy - No Strain

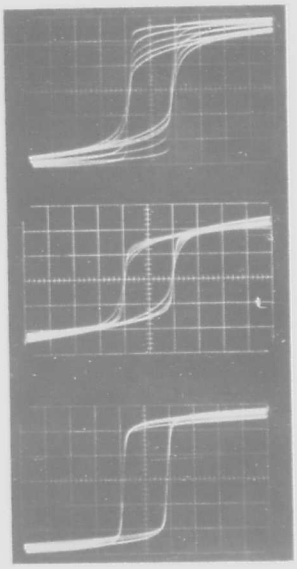

Figure 38. Hysteresigram of 152 permalloy under tension, twist, and tension and twist.

Initial experiments showed, in any case, only a slight improvement in the linearity of the counting curves over the non-stressed case.

Properties of interest of the various materials tested are tabulated in Table 3. The best initial linearity was shown by the 72 percent Nickel-28 percent Iron alloy, but the .1 microsecond write pulses are too long to take advantage of the square loop properties of this material. On the basis of overall performance, Driver Harris 152 wire (52°/o Ni, balance Fe) was selected; with this wire up to 70 observable flux levels may be obtained under optimum conditions.

The 60 cps hysteresigram shows that the B-H loop of a material becomes more and more square as thinner and thinner wire is used; this may be due either to the additional stretching during the drawing of the wire, or to behaviour approaching thin film single domain switching as the diameter becomes very small. The output voltage, however, also decreases in direct proportion to the cross-sectional area, and although the output impedance of the read coil is very low, noise perturbs the system due to radiation from the input transducer. With wire diameter above about 10 mils, driving frequency eddy currents introduce additional coherent noise.

3.6. Coil Design

The aspect ratio (length to diameter) of the write coil has considerable bearing on the overall linearity of the integrator. The magnetic poles induced in the wire at the ends of the coil reduce the field inside in proportion to the flux density (B is, of course, continuous throughout). The field at the center of the coil is given by:[46]

$$H = H_o - \frac{N}{4\pi} (B-H)$$

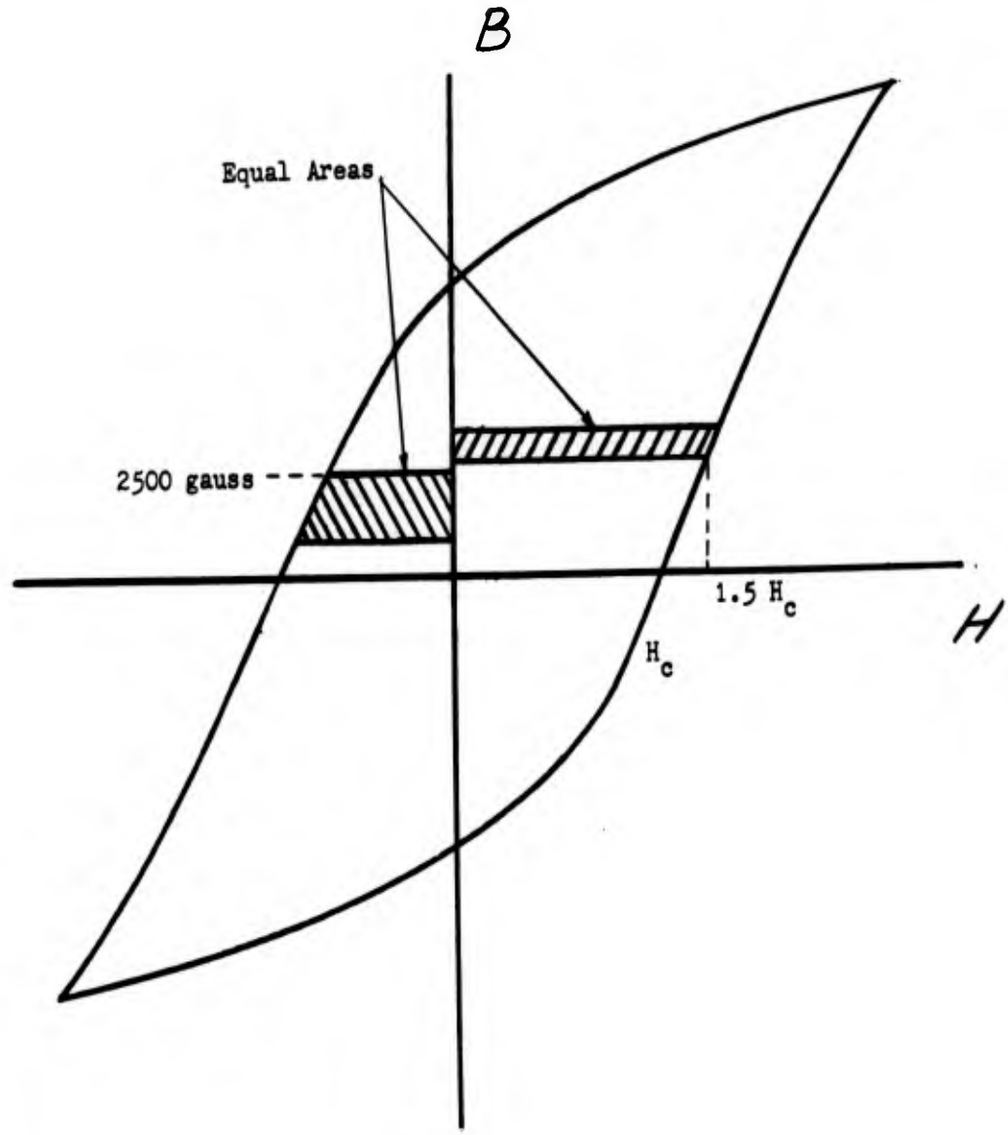

Figure 39. Integrator Nonlinearity Due to "Tilt" of Hysteresis Curve

where H_o is the field due to an infinite solenoid carrying the same current,

B is the flux density in the wire,

and N is the demagnetizing factor, which depends on the aspect ratio of the coil as well as the permeability of the wire.

Now suppose that the coercive force of the wire material is H_c, that the maximum level to which the wire would be magnetized is 2,500 gauss, and that the field required to reach this level of flux is 1.5 H_c. This situation is depicted in Figure 39--the numbers are appropriate for 42 permalloy. On the basis of the simple calculation outlined in section 3.3, we would expect a magnetizing pulse to be about 3 times less effective than a demagnetizing pulse in changing the flux level at either the upper or the lower extremity of the flux range. The corresponding areas of the B-H loop are shaded to emphasize the difference. Thus, in order to avoid additional non-linearity in a counting curve, one would like the change due to the demagnetizing effect of the coil ends at the maximum flux level to be small compared to H_c.

Arbitrarily selecting .1 H_c as the maximum tolerable change, and solving the demagnetization equation for N with H = 7 oersteds, and B = 2500 gauss, a figure of 120 is obtained from Figure 40 for the aspect ratio. With permalloy wire .010 inches in diameter, a minimum I.D. of 12 mils is required for the coil; if number 38 enamelled wire is used for the winding, the mean diameter is 15 mils, and the length of the coil should be at least 1.8". In the initial experiments, the coils were wound on .035" to .050" diameter sleeving, but this construction was abandoned in favour of self-supporting bonded coils.

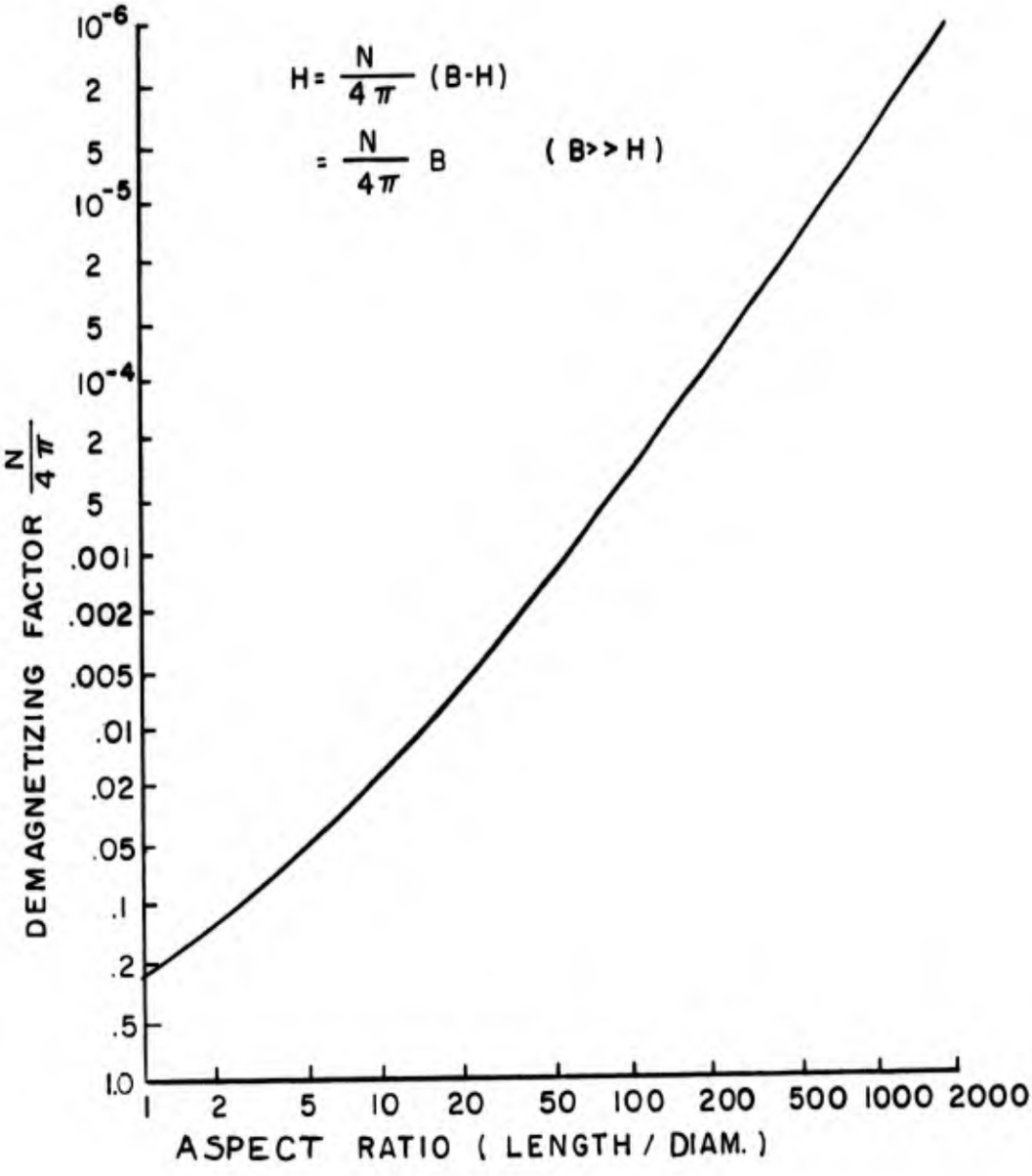

Figure 40. Demagnetizing Factor for Round Rod

The design of the read coil is less critical; here the only important consideration is that the length of the coil be less than half an acoustic wave length at the operating frequency of the line. Fifty turns arranged in a single layer were found to yield a sufficient output voltage at all but the lowest drives. While in order to enclose as many flux lines as possible it is desirable to have the search coil wound next to the delay wire, in the interest of a uniform magnetizing field the read coil was wound outside the write coil. A photograph of a complete coil assembly is shown in Figure 41.

3.7. Magnetic Erasure

In order to remove all traces of previous learning from a perceptron and have it start on a new problem with an unbiased outlook it is necessary to reset the integrators from time to time. With toroidal flux integrators of the type described in section 2.5 this is easily done by passing an extra large pulse through the strobe winding, thus orienting all the domains in a direction perpendicular to the normal direction of magnetization. With the delay line configuration it is, however, difficult to generate an orthogonal erase field, and other means of erasure must be sought.

One possibility is to heat the delay wire momentarily above the Curie point; on cooling, the distribution of the domains will be completely random. Unfortunately, the Curie Temperature of 42 permalloy is of the order of 600°C, which is above the safe operating temperature of even the best enamel insulation.

In the experimental setup a commercial portable recording tape demagnetizer, known as Jiffy-rase, was often used to advantage. This device

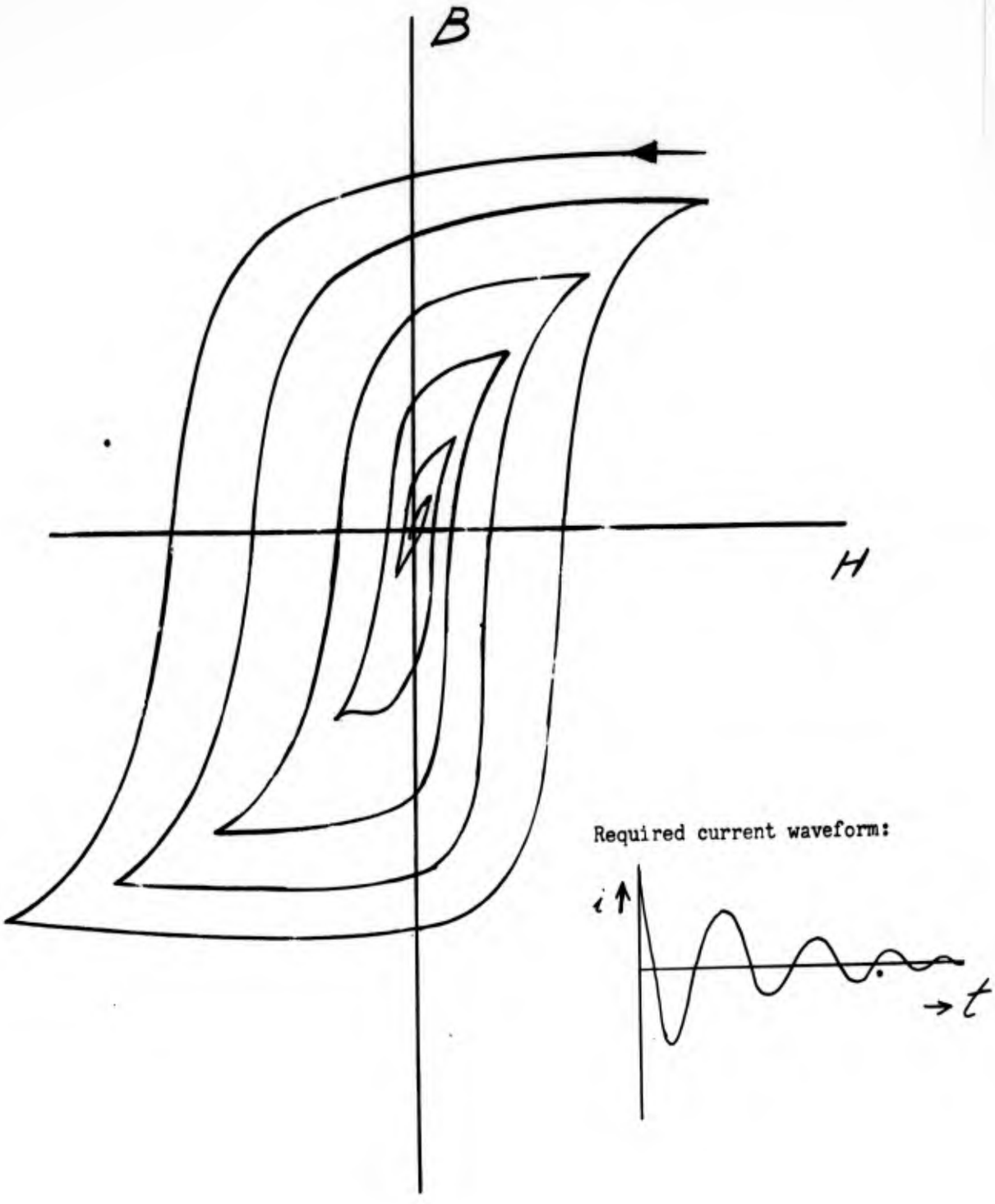

Figure 42. Demagnetization

consists of a very powerful 60 cps electromagnet, and erasure is accomplished simply by approaching and retreating the magnet in the vicinity of the wire.

The solution actually adopted makes use of the write coil itself to effect demagnetization. A 400 cps current, of initial amplitude about three times that of the write pulses, and gradually decreasing to zero over a period of several seconds, is circulated in the winding. What presumably happens to the B-H relationship in the wire is illustrated in Figure 42. The variation in the magnetizing field with time is shown in Figure 43, and a schematic of an electromechanical arrangement used to generate this wave form in Figure 44a. A ten-turn helipot was used instead of an ordinary composition rheostat in order to obtain a finer current gradation. An even smoother wave form is generated by the voltage controlled, variable gain amplifier, illustrated in Figure 44b. The exponential decay of a step input in an R-C circuit controls the amplification; the decay constant may be varied continuously from .2 seconds to 4 seconds, and the compression ratio is better than 200:1.

Demagnetization is most thorough when sections of the wire adjacent to the main write coil are also demagnetized. This was accomplished by connecting three coils in series. It is also of paramount importance to cancel out the earth's field during demagnetization, otherwise the remanent flux after demagnetization will be a considerable fraction (as much as 50 $^{o}/_{o}$) of the maximum flux level induced by the write pulses. Methods of neutralizing the earth's field will be discussed in the next section.

In some applications a much cruder sort of zeroing, requiring neither demagnetization nor cancellation of the earth's field, may be acceptable. It would be sufficient to saturate all the integrators in a given direction,

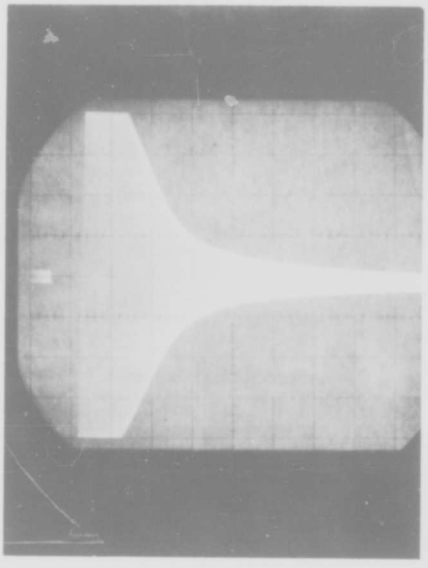

Figure 43. Demagnetizing Current Waveform
(Horizontal scale: 1 cm. = .5 sec.)
(Vertical scale: 1 cm. = 50 ma.)

and then pulsing all of them at the same rate until the total output, as monitored at the R-units, is zero. Because of local variations, however, this will in no way guarantee that the individual integrators are anywhere near the zero setting. Furthermore, if some of the integrators were once biased beyond their normal range by a stray magnetic field or a switching transient, their counting curve would remain thereafter highly assymetrical.

3.8. Shielding

Provisions have to be made to guard the coils against interference at the driving fequency, incoherent noise from fast pulses elsewhere in the system, cross-talk from adjacent coils, and the steady bias of the earth's magnetic field. Among all of these, the earth's field alone offers a significant problem.

Radiation emitted by the input transducer at 200 Kcps is about 10 times as large with a magnetostrictive coil as with a crystal, but if coaxial leads are used right up to the transducer, and if the read coil is at least 5 cms away from it, then the signal radiated by the transducer constitutes only about 2 $^{o}/o$ of the output signal.

The output impedance of the read coil is below 5 ohms, so that 60 cps. noise, and interference from other low frequency sources are negligible. The sharp spikes picked up by transformer action from the write coil are too short to affect the normal operation of the sense amplifiers and threshold devices.

Cross talk from adjacent coils, which would be significant if the read winding sampled the flux level under the whole write coil, is eliminated by the 1.5 cm guard band extending on either side of the central "active" area. It is thus permissible to leave no spacing whatever between adjacent coil assemblies.

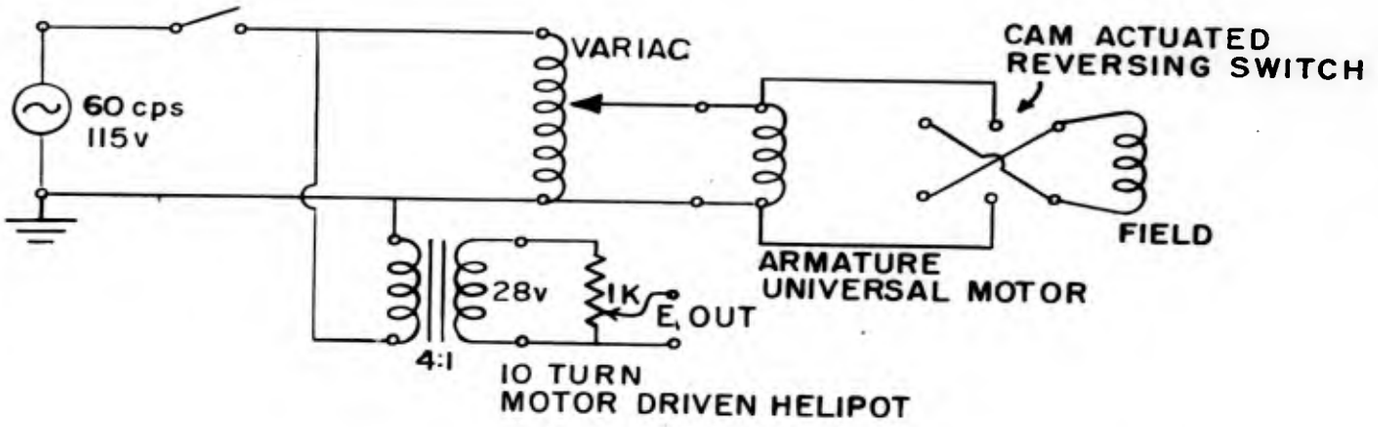

Figure 44a. Demagnetizing Current Generator (Electromechanical)

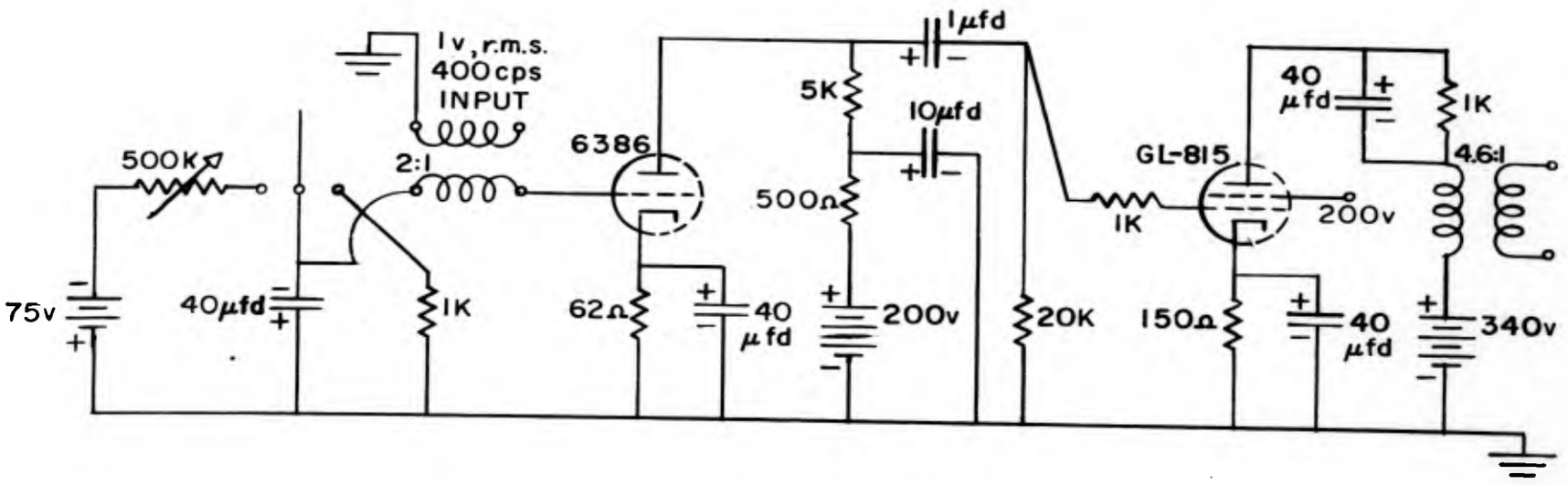

Figure 44b. Demagnetizing Current Generator (Electronic)

Customary expedients to neutralize the earth's field include Helmholtz coils and metallic shielding. Helmholtz coils are evidently impractical in the present application, while shielding is prohibitively expensive. In any case, a single layer of .014" Conetic AA foil ($6.30 per ft.^{2}) reduces the 80% assymetry due to the earth's field on demagnetization only to about 75%, while three layers of .005" Conetic ($3.50 per ft.^{2}) reduce it to 60%. These figures refer to a coil orientation at about 45 degrees to magnetic north. Orienting all the coils at right angles to the earth's field is not easily feasible either, because structural steel and heavy steel equipment in the building distort the field, as shown by the map of Figure 45.

In this instance, too, recourse was finally had to the write coil. A direct current of the order of 3 or 4 milliamps is sufficient to neutralize the earth's field. If this current is very carefully adjusted by repeated trial and error, the integrator may be demagnetized to about 3 percent of its original level. The remanent flux, expressed as a percentage of the original level, corresponds roughly to the assymetry obtained after continuous pulsing, and this in turn is proportional to the difference in effectiveness between a positive and a negative initial pulse.

The optimum neutralizing currents required by a particular integrator in different positions in the relay rack are shown in Figure 46. Depending on the excellence of performance required in particular applications, a trimming potentiometer may or may not be needed for each assembly. The unbalance resulting from various current deviations from the optimum is plotted in Figure 47.

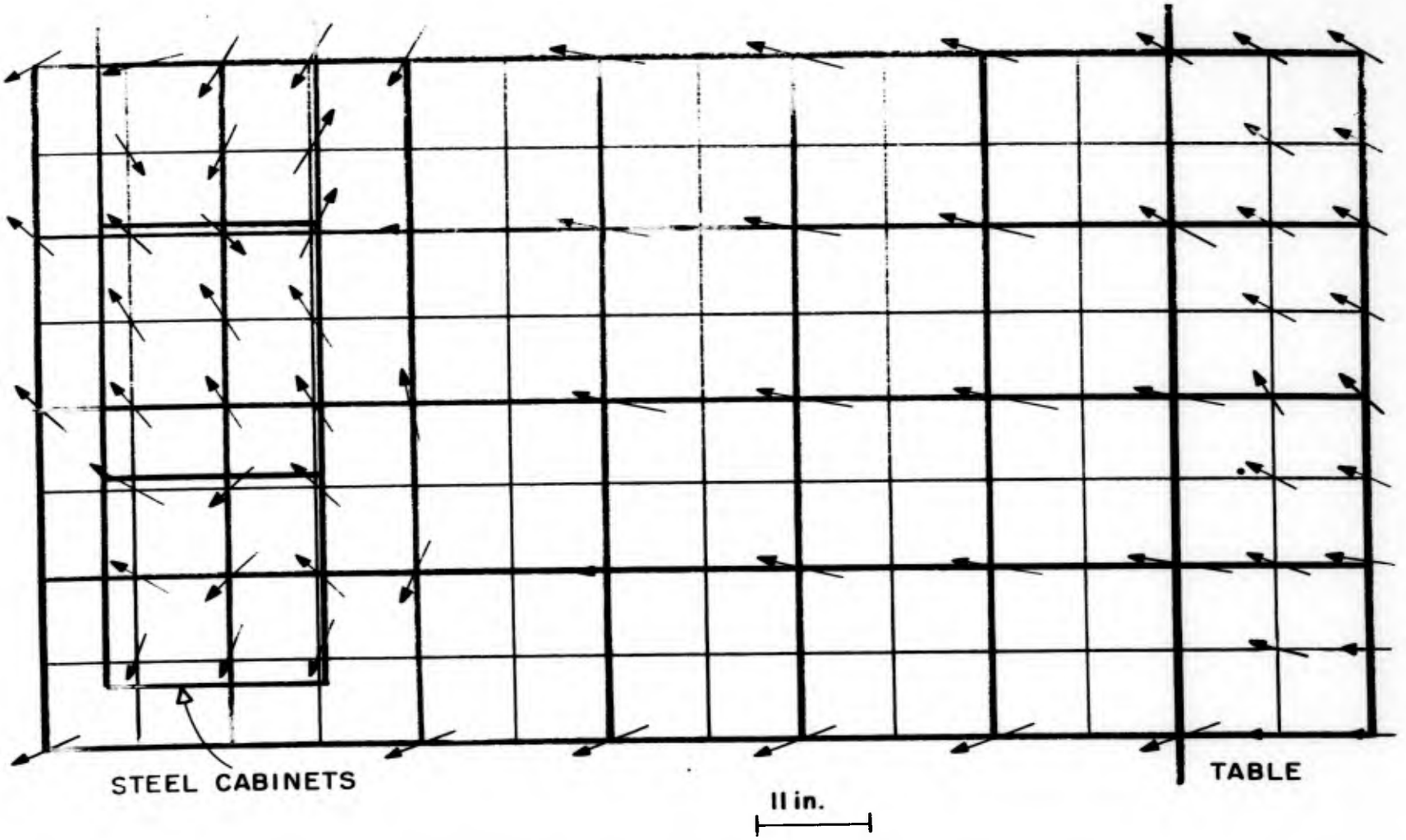

Figure 45. Direction of Magnetization in a Section of the Laboratory

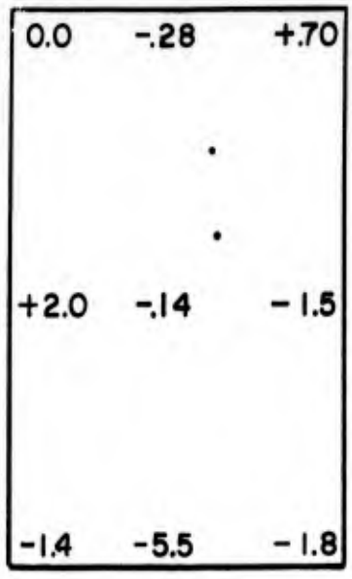

Figure 46. Neutralizing Current Required for Different Locations in ma.

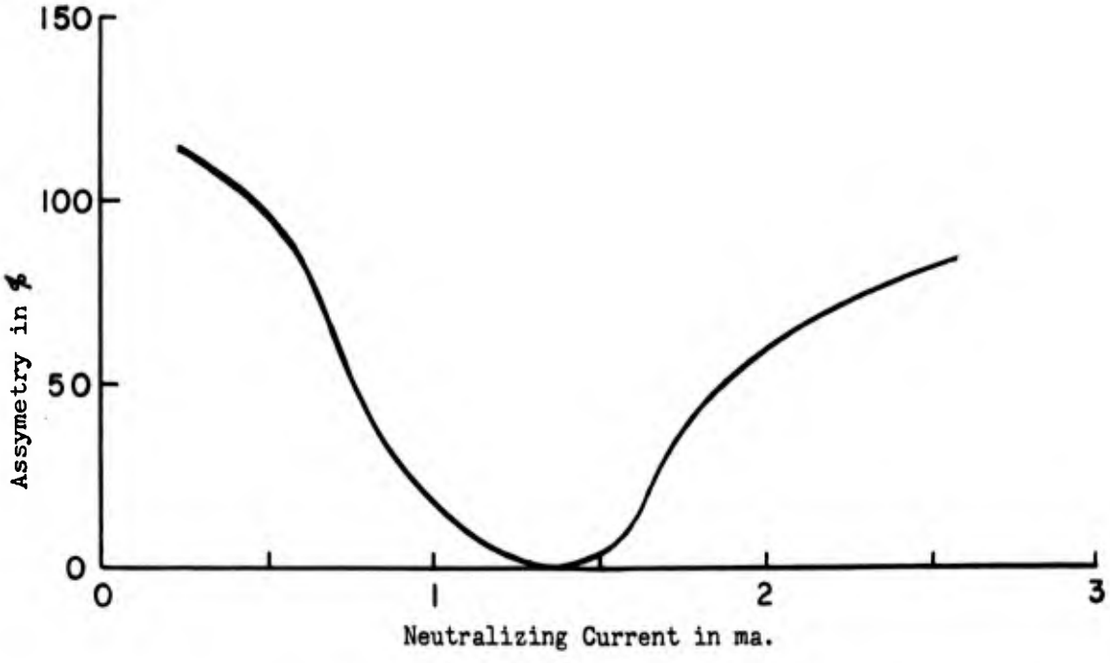

Figure 47. Assymetry Resulting from Deviations from the Optimum Neutralizing Current

TABLE IV

Output Voltage and Optimum Neutralizing Current in Twelve Integrators on the Same Line

Coil No.	Maximum Output Voltage	Neutralizing Current Required
	millivolts	milliamps
1	4.2	+ 1.5
2	4.3	+ 1.4
3	4.0	- .7
4	4.1	+ 1.4
5	4.1	+ 1.8
6	3.4	- 1.1
7	3.9	+ 1.0
8	4.0	+ .2
9	4.1	+ .5
10	4.0	+ .9
11	3.9	- 1.9
12	3.8	- 1.6

The presence of a direct current as well as of the occasional 400 cps. demagnetizing current in the write winding offers some grounding difficulties, but the different component frequencies are so far apart that they may be separated by cheap capacitors and chokes.

It is interesting to note that the effect of the earth's field is most pronounced during demagnetization; if the neutralizing current is slowly removed after demagnetization has been completed, the resulting unbalance is only 60% of the full output.

3.9. Operating Characteristics

The test circuit designed to check the performance of a single integrator is diagrammed in Figure 48. The signal from a Hewlett-Packard 200-C signal generator is amplified (amplifier schematics in Figure 49) and fed to the transducer. A 30-cm. length of the wire under test stretches from the transducer to a damping pad at the other end. A photograph of the complete apparatus is shown on Figure 50.

Pulsing is accomplished through an inverting switch by a Dumont 404B Pulse Generator with a 10 ohm resistor inserted into the circuit to monitor the current. The pulse generator is triggered by a low frequency free-running multivibrator. The circuit on Figure 51 is capable of supplying trigger pulses at the rate of one every two seconds; the slow speed facilitates direct counting of the number of steps required for complete reversal.

The output signal is observed directly on the screen of a high sensitivity Tektronix Oscilloscope. The CRO should be triggered by the drive voltage to permit observation of the phase changes in the output. If the output is to be monitored on a graphic recorder as well, it must

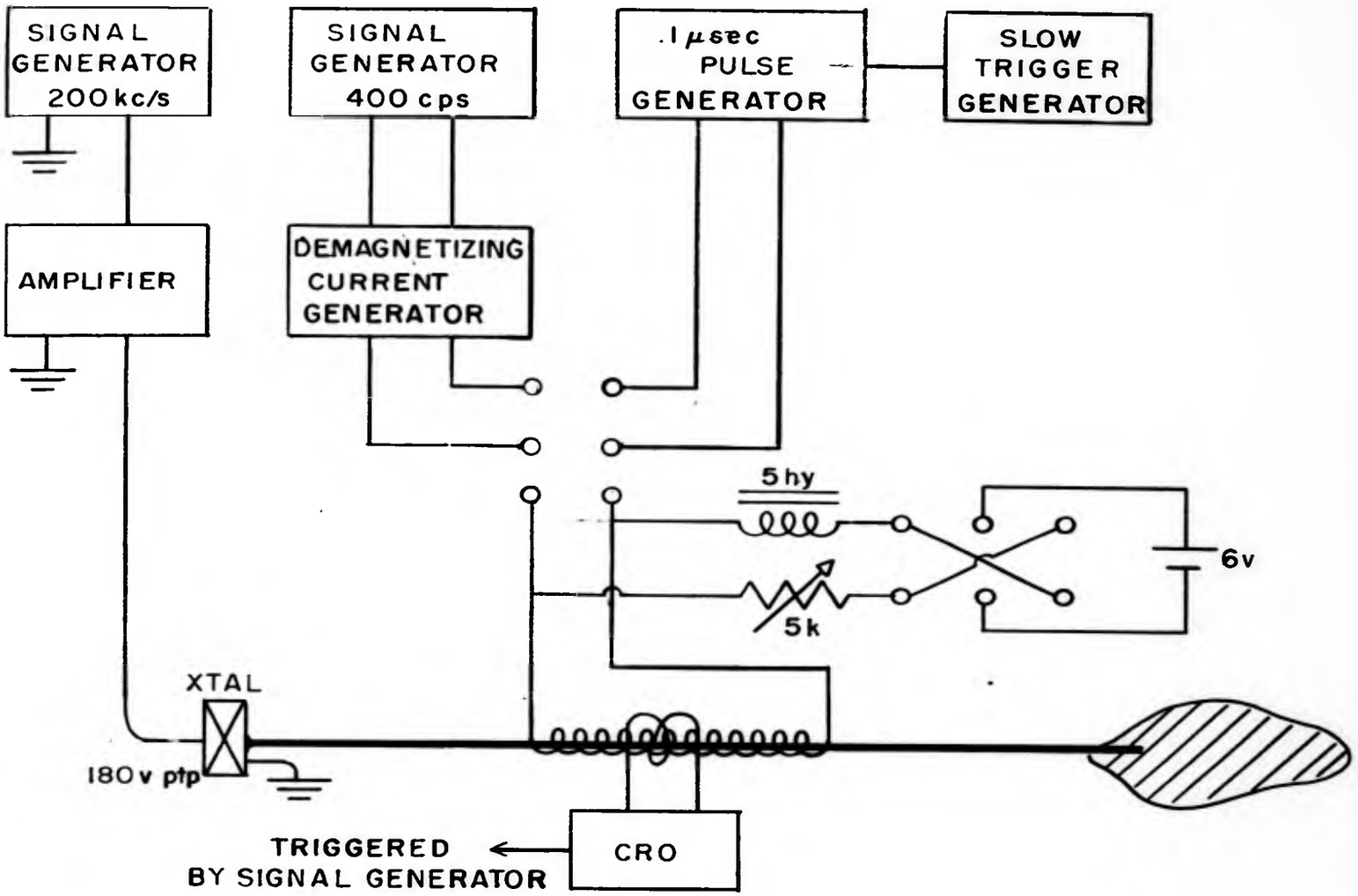

Figure 48. Integrator Test Circuit

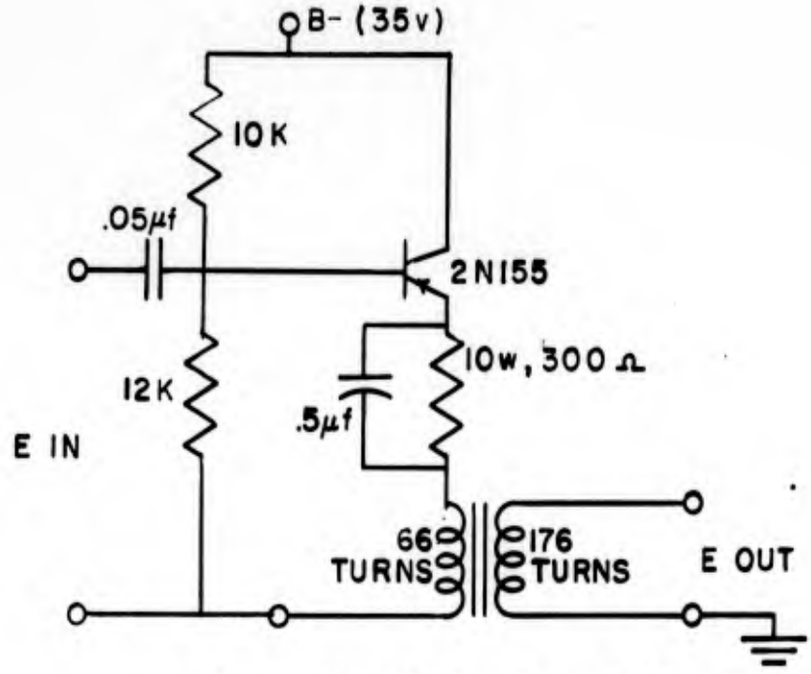

Figure 49. 200 Kcps. Power Amplifier

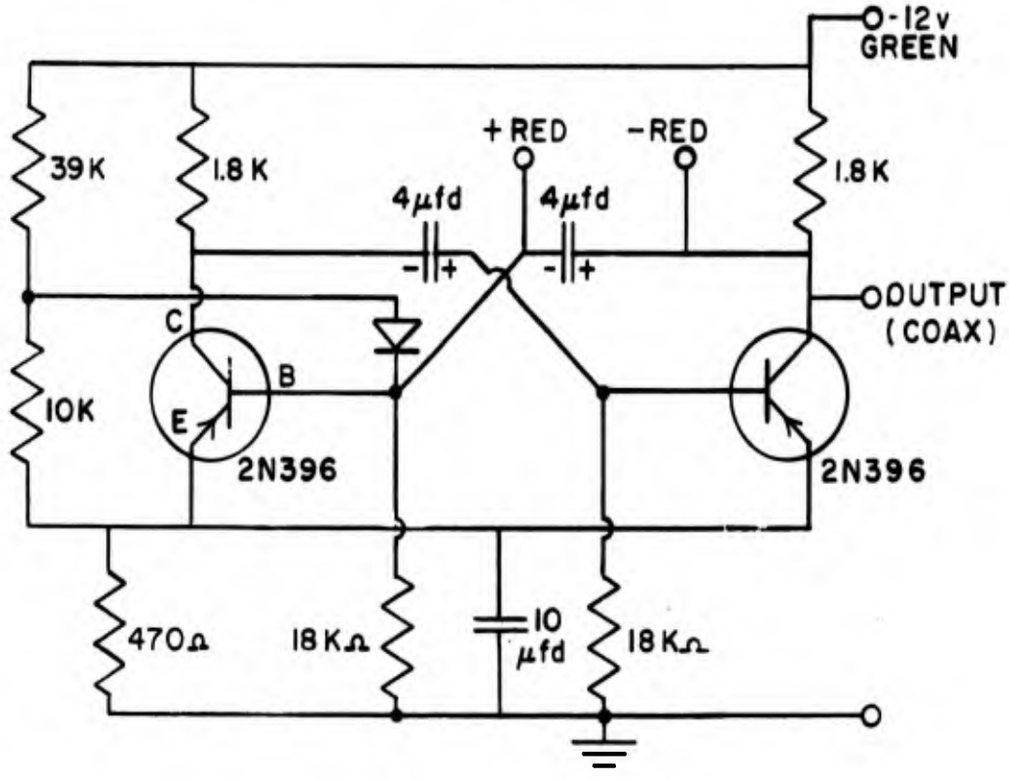

Figure 51. Slow Trigger Circuit

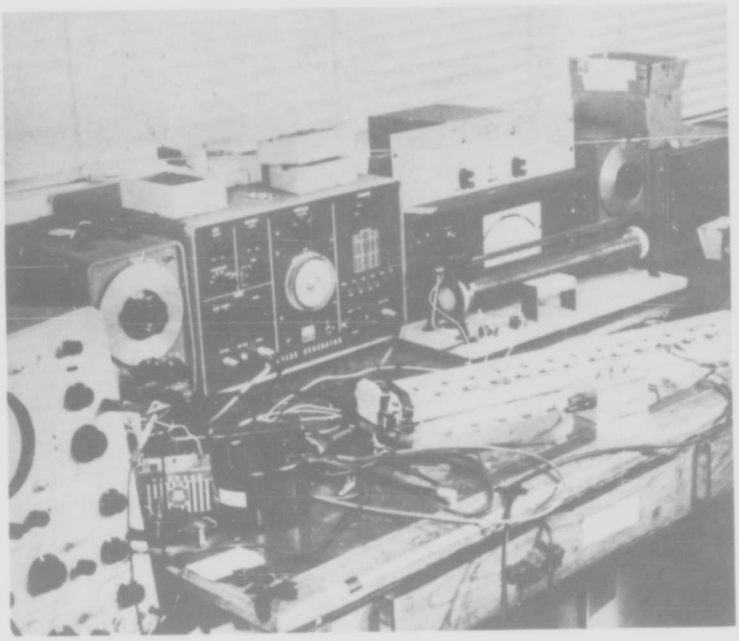

Figure 50. Test Equipment for Magnetostrictive Readout Integrator

first be rectified and filtered, but this is not as satisfactory an arrangement as demodulation with a fixed phase reference.

The envelope of the output voltage is shown in Figure 52 for different pulse amplitudes. When the output is rectified and filtered, the result is Figure 53. It is seen that it takes about three times as many pulses to reach 90 percent of "saturation" on ascending than on descending; as explained in previous sections, this is a consequence of the assymetry about the B axis of the hysteresis curve. Figure 54 is a photograph of the output sinosoid, on an expanded scale, during pulsing. This picture shows clearly the change in phase as the flux level skirts zero. The fact that the output voltage is never actually zero in amplitude, although the phase shifts close to 180 degrees, would seem to indicate that the boundary of magnetization moves along the longitudinal axis as well as from the outside in.

Photographs of the write pulse, with amplitudes set as above, are shown in Figure 55. A comparison with the current through a 47-ohm composition resistor suggests that the pulse impedance of the write coil is of the order of 50 ohms. Since this is also the output impedance of the pulse generator, very little impedance matching is required. The improvement in the pulse current wave shape resulting from the addition of a 100 picofarad parallel capacitor is illustrated in Figure 56c, but this does not affect the counting curve significantly. For completeness, a photograph of the voltage wave form, exhibiting the typical inductive peaking, is also included in Figure 57. Figure 58 is an oscillograph of the current wave form in a write coil with the permalloy core removed--evidently the permalloy wire absorbs only a small fraction of the input power.

Figure 52. Envelope of Readout Voltage

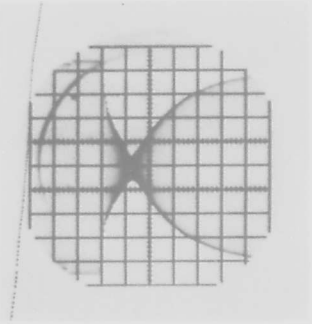

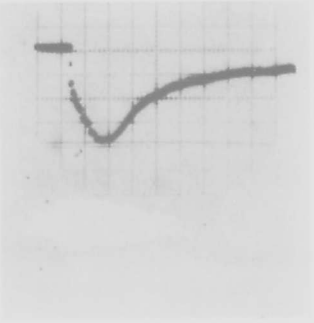

Figure 53. Rectified Envelope of Readout Voltage

Figure 54. Readout Voltage

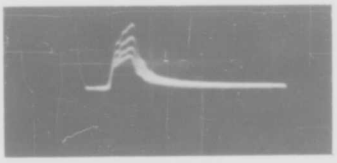

Figure 55. Current into Saturated Integrator

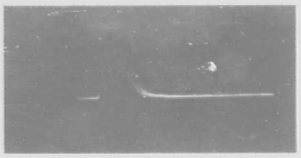

Figure 56a. Photograph of write pulses of different amplitudes

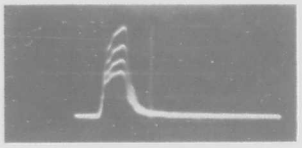

Figure 56b. Write pulse into 50 ohm resistor

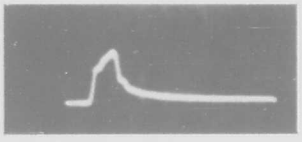

Figure 56c. Waveform improved by addition of 100 microfared capacitor

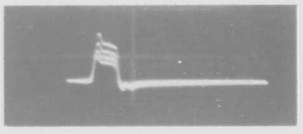

Figure 57. Voltage developed across write coil

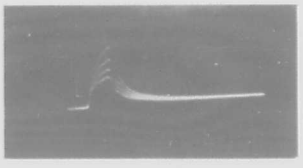

Figure 58. Write pulse with permalloy wire removed from coil

The relation between drive voltage and output in the case of a crystal transducer, and drive current and output in case of a magnetostrictive transducer, is quite linear, as seen in Figure 59.

Several prototypes for Tobermory, consisting of 12 coil assemblies strung on 50 cms. of wire, were also prepared. A photograph of one of these lines, with the associated control box, is shown in Figure 60. A schematic diagram of the control box is shown in Figure 61. The box selects which read coil is observed, which write coil is pulsed, the polarity of the pulse, the magnitude of the 400 cps. erase, and the polarity and magnitude of the neutralizing current. In addition, provisions are made to connect all the write coils in series in order that they may be demagnetized simultaneously and that the same neutralizing current may circulate in each coil.

The optimum neutralizing current and the "saturated" output voltage of the different coils on the line are tabulated in Table 4 , these numbers refer to the line oriented at 45 degrees to magnetic north. The inequalities in output voltage are the result of imperfect damping of standing waves. That the average is only slightly smaller at the far end of the line than at the drive end is proof that the coils do not materially load the line.

There is a 12 degree phase shift observable between adjacent coils: this agrees well with the shift predicted from the velocity of propagation of longitudinal sound waves in permalloy.[57]

The inherent stability of the flux level is plotted in Figure 62. The slight variation exhibits no bias, and is likely due to change in the frequency of the signal generator.

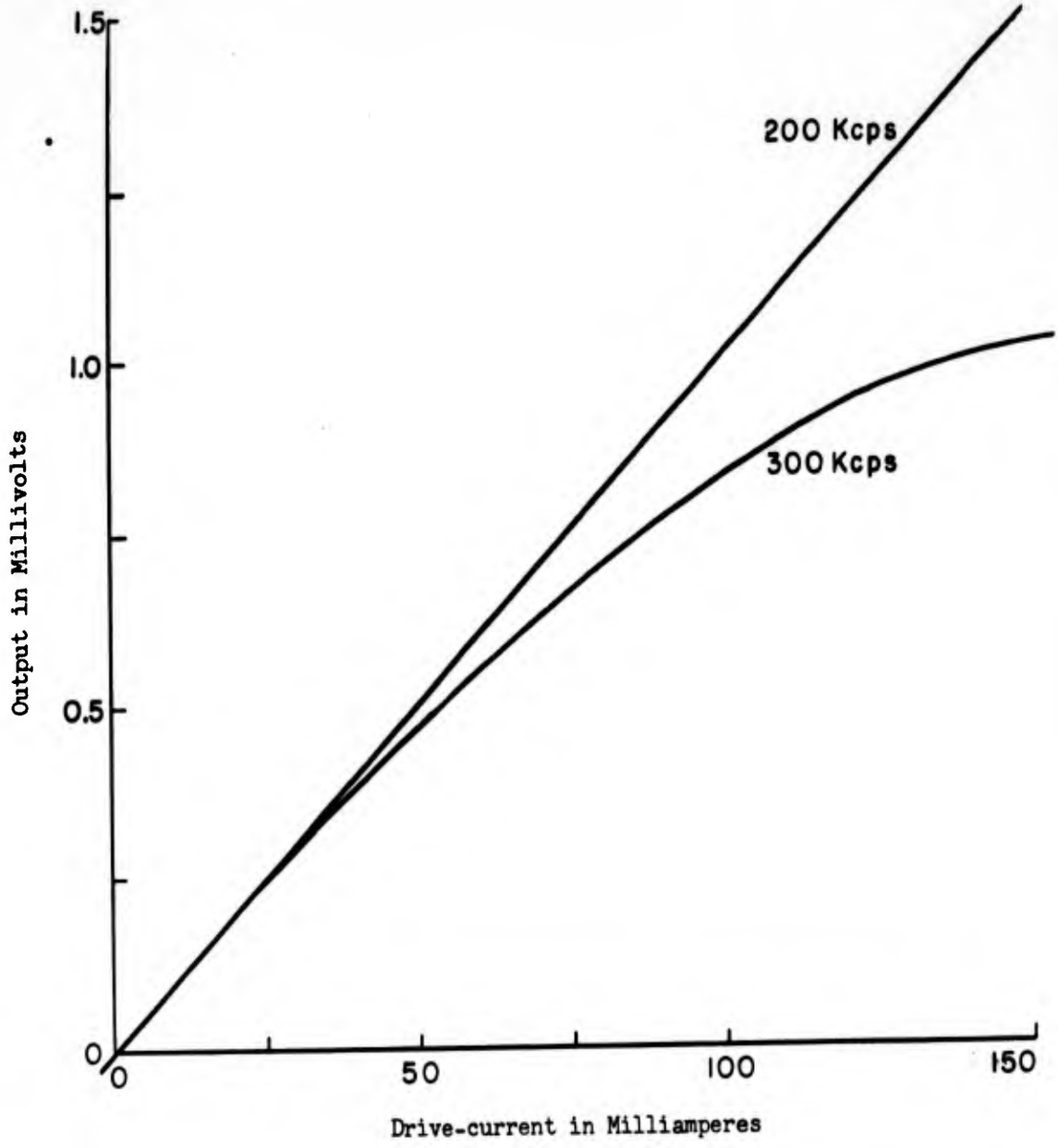

Figure 59. Plot of Output Voltage vs. Drive Current

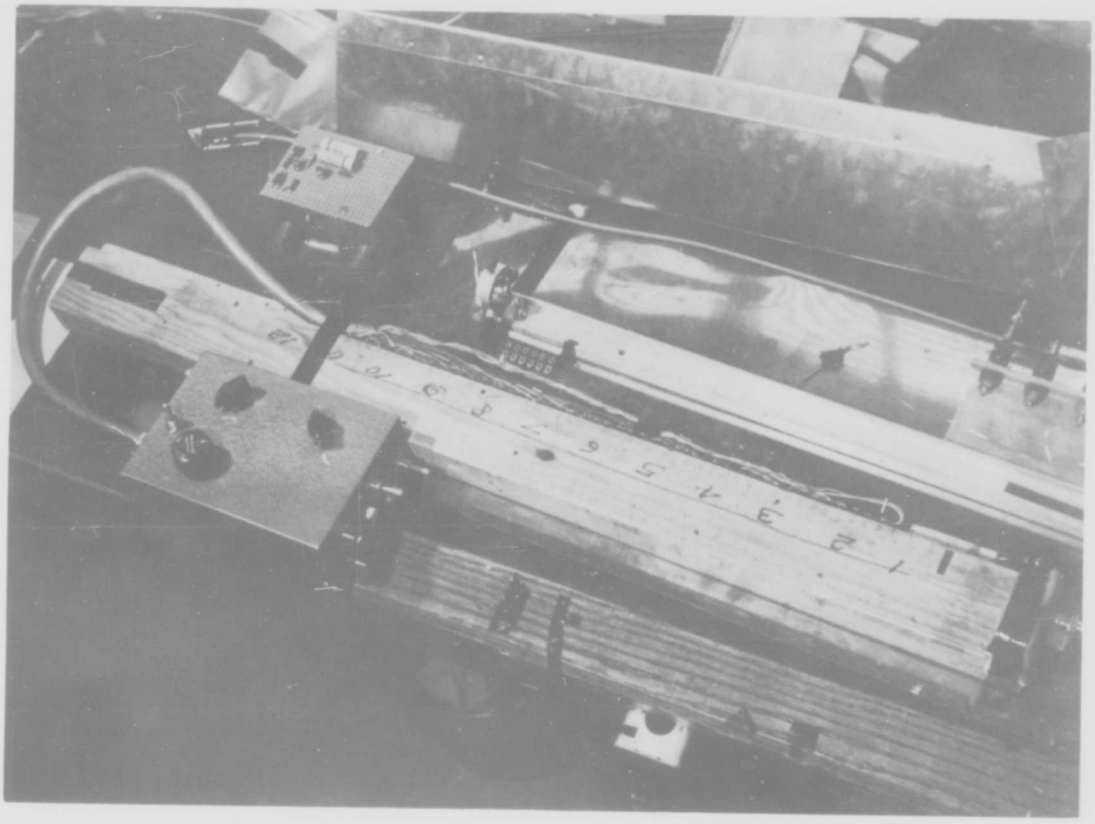

Figure 60. 12-Coil Integrator Assembly

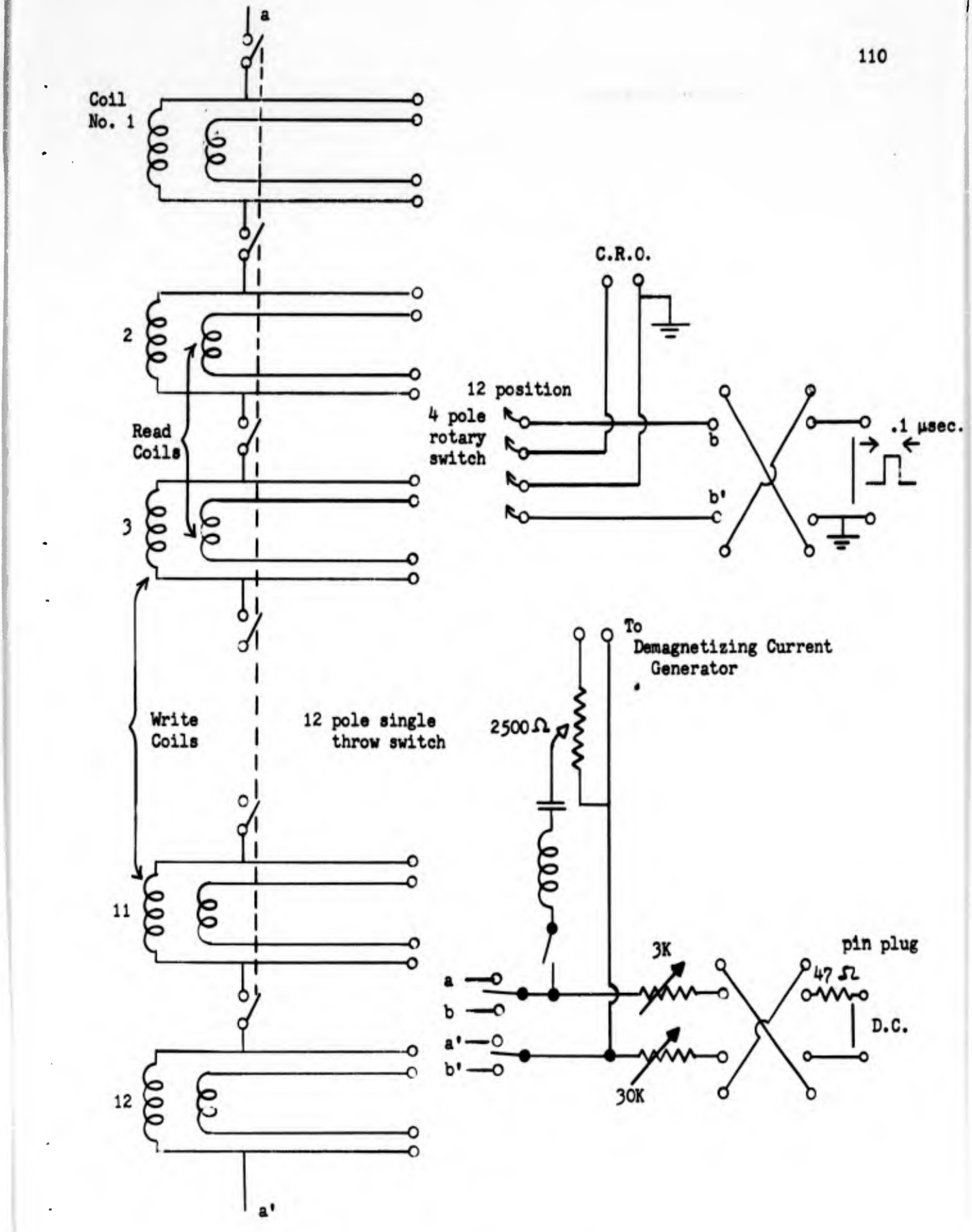

Figure 61. Schematic Diagram of Control Box

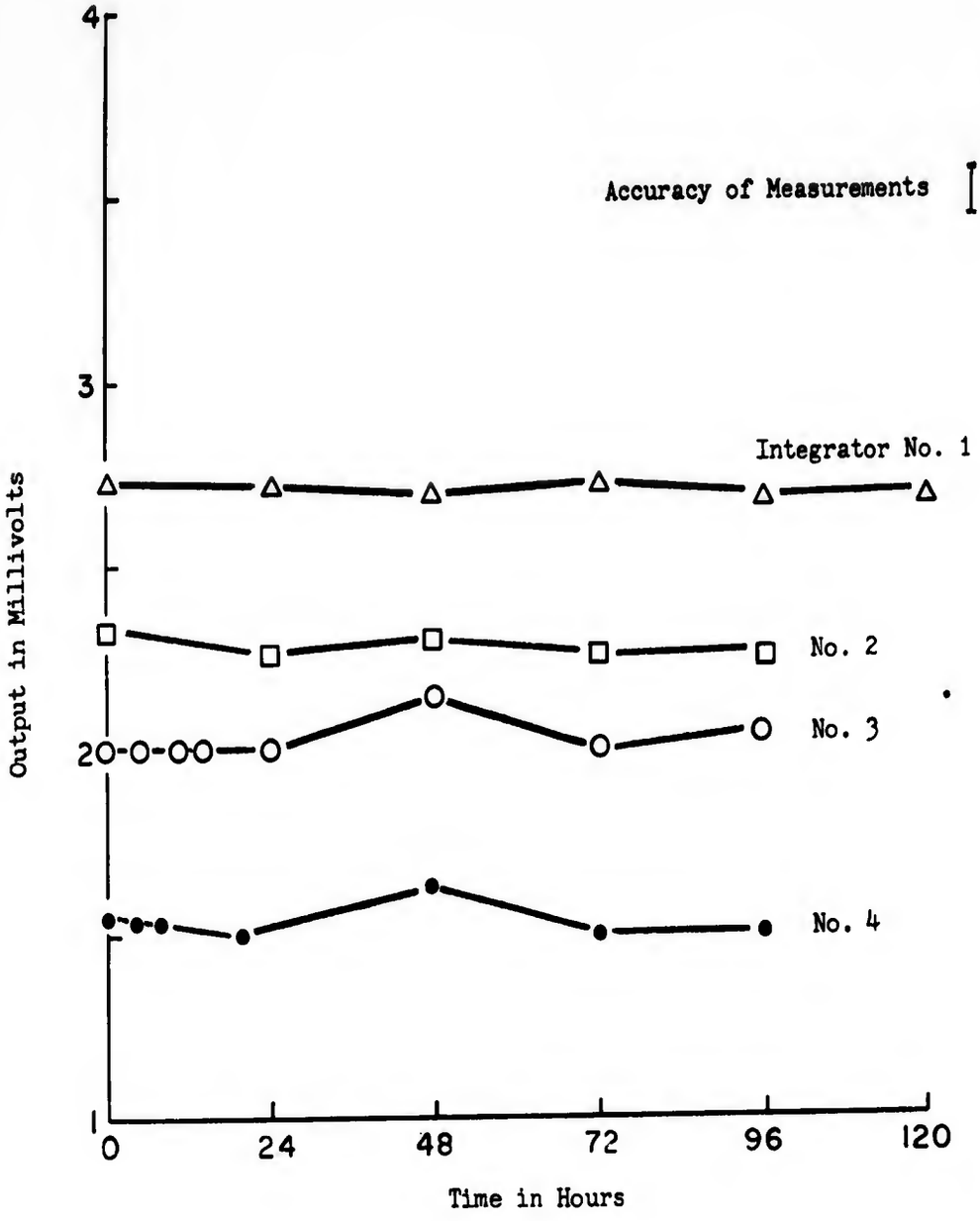

Figure 62. Stability of Integrator Storage Characteristics

IV. TOBERMORY

This chapter contains a preliminary description of the audio-perceptron, Tobermory. Although construction of some parts began over nine months ago, Tobermory is still essentially in the design stage; consequently not all aspects of the machine will be treated in equal detail.

At the time of writing, the main functional units of the sensory end have been all but completed, and prototype input channels are being tested; the wiring of the sensory to association layer plug board has absorbed approximately 500 man hours; final experiments are being conducted on the memory system "in vitro"; several implementations of the error-correction reinforcement scheme are at the breadboard stage; and the design of the R-unit sense amplifiers and threshold units is well under way. At a less advanced stage of planning are the threshold units of the associative layer, the control logic of the whole system, and the physical layout of the soundproof control booth.

A simplified block diagram of Tobermory is presented in Figure 63. A word enters through the microphone or tapehead, then it is split up into amplitude and frequency components at 10 to 100 millisecond intervals by a filter bank and associated asynchronous delay bank. The output of the delay units constitutes the sensory mosaic which serves as input to the association layer. The A-units are monostable threshold devices; once triggered, they stay "on" for a preset time interval. Each A-unit is connected by variable weight links to each of twelve R-units, which are again on-off devices.

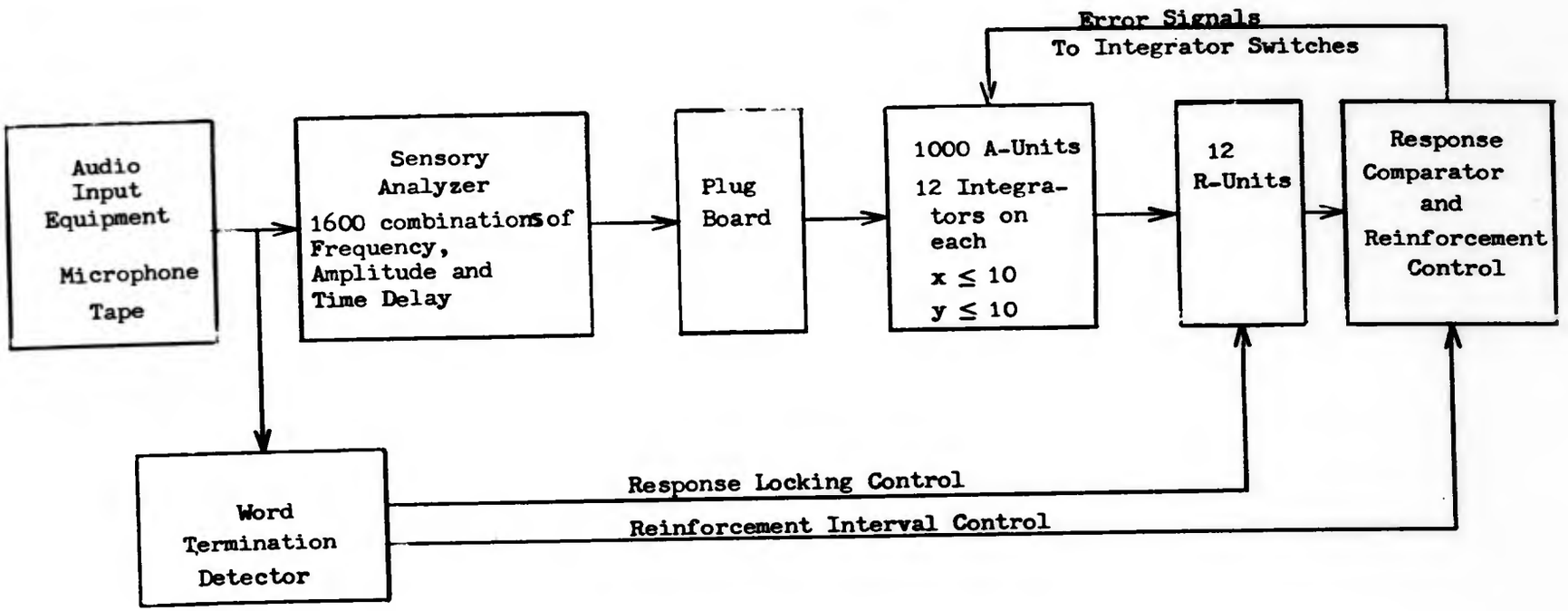

Figure 63. Block Diagram of Tobermory

The twelve-bit binary representation of the class into which a word is to be classified is fed into the machine immediately preceding the word itself. Whenever, during the passage of the word through the sensory delay lines, a particular R-unit shows a response which disagrees with the prescribed code, all the weights connecting the R-unit with active A-units are changed in the direction which would force the correct response.

Speech spectrograms (a typical speech spectrogram is shown in Figure 64) indicate that there is at least some continuity in the frequency components, as well as in the amplitude, in spoken words. This is also true of most other audio signals which Tobermory may be called upon to classify. Hence we may expect the A-unit activity pattern of a given word at successive short time intervals to be somewhat similar to that shown in Figure 65, with considerable overlap between consecutive patterns. Accordingly, the only initializing required is to ensure that reinforcement will not begin until the whole word has entered the delays, and that it will cease before the word leaves. Typically, a word may be expected to be reinforced half a dozen times during its sojourn across the "retina".

Tobermory differs from the elementary perceptron described in the first chapter in several respects. The most significant deviation is that we are no longer dealing with a synchronized system; because the sensory delay lines are free-running, a particular A-unit may go "on" at any given time, and stay "on" for an arbitrary period independent of changes in the stimulus world. The R-units are no longer "simple" either: they go "on" whenever the sum total of the input from active A-units reaches a positive threshold, and remain "on" until the signal falls below the negative threshold. Of course, these R-units may be converted to "simple" R-units by setting both thresholds identically equal to zero.

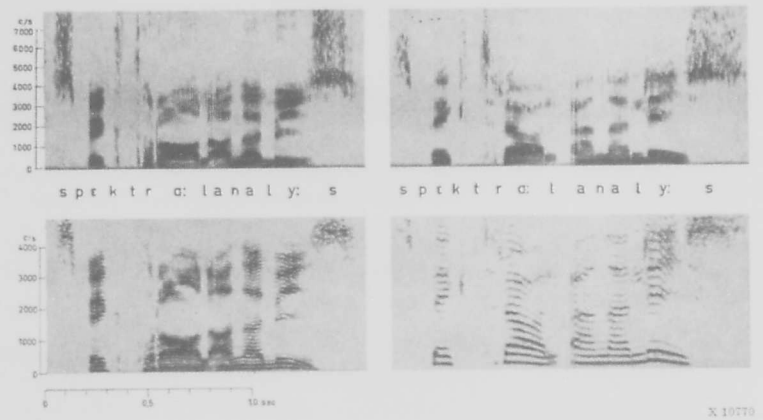

Fig. 4. Sonagraph spectrograms taken with broad-band filter, above, and with narrow-band filter, below. Male speaker to the left, female speaker to the right.

(Taken from "Acoustic Analysis and Synthesis of Speech with Applications to Swedish" by Gunnar Fant.)

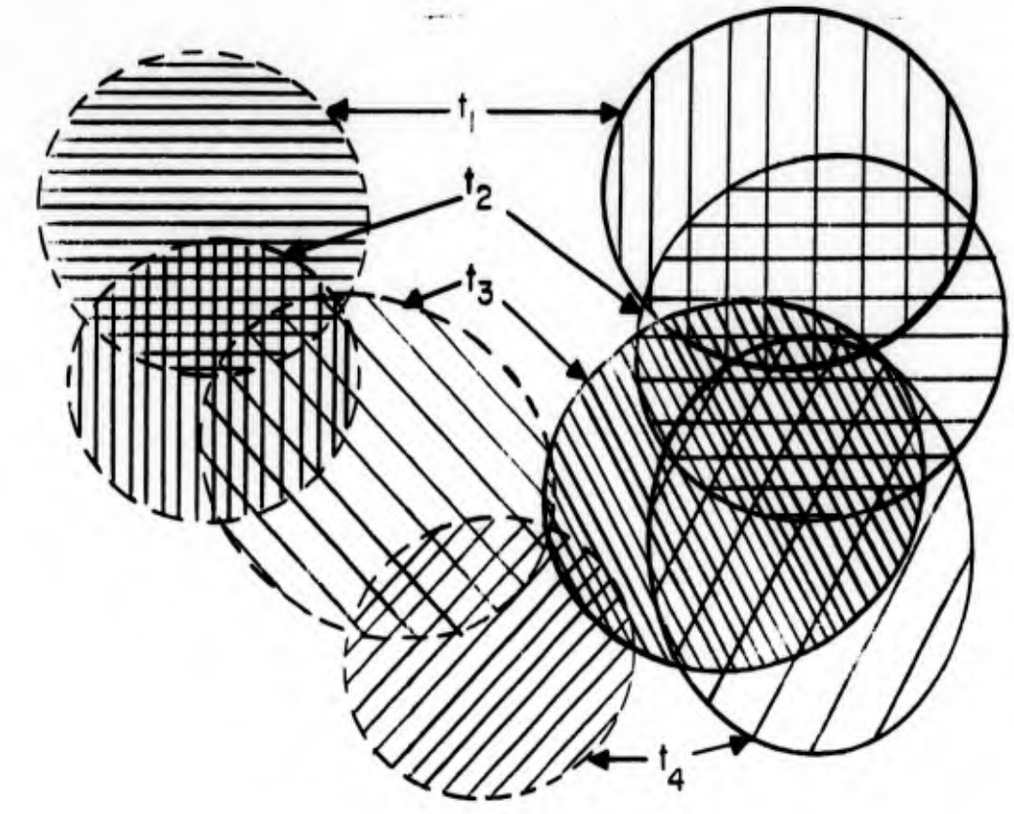

——————— Word A

- - - - - - Word B

Figure 65. Typical A-unit Activity Pattern for Two Words at Four Consecutive Time Intervals

The analysis referred to in section 1.3 is still applicable if we consider Tobermory a set of 12 elementary perceptrons with identical S to A connections, and each word a set of equivalence classes imbedded in a larger equivalence class of words which share identical symbols (one or zero) in some position of the classification code. For complete solution of a problem, modification of the weights associated with a particular R-unit should cease only if the R-unit shows the correct response on presentation of every word in the training sequence.

Tentative designs for the circuitry required to utilize the magnetostrictive read out integrator introduced in the previous chapter will be discussed under the headings "A-units", "R-units", and "Reinforcement", in sections 4.2, 4.3, and 4.4. For the sake of completeness, the S-units will also be briefly described in section 4.1, although the author was not directly involved in their design and construction.

4.1. S-units

The two alternative inputs to Tobermory consist of a low impedance dynamic microphone with a built-in blast filter, and a two channel fully metered tape recorder with automatic repeat mechanism and remote control. Normally the tape recorder will be used for training; one channel, tapped at the read head, will carry the stimulus words, while the other will be used for "start of word," "end of word," and "desired classification" signals, as well as for instructions to the operator.

The output of the tapehead is channeled to an automatic gain control amplifier and a linear amplifier in parallel. The AGC amplifier normalizes the amplitude in preparation for spectral breakdown, while the linear amplifier feeds the signal to eight unilaterally inhibited voltage comparators which retain the amplitude information lost during normalization.

The signal from the AGC serves as the input to seventy-two active filters. The center frequencies of these narrow band filters are distributed in the "useful" audio frequency range, from 80 cps. to 6,400 cps. Each filter is followed by a Schmitt trigger; the thresholds of adjacent frequency bands are set cyclically at one of four levels.

The Schmitt triggers, and also the voltage comparators used for amplitude detection, activate the first of 20 identical series-coupled delay units. These are simply monostable multivibrators, whose period may be varied from 10 to 100 milliseconds. Each delay unit drives the next one, and also serves as one of 1600 input points to the plugboard connecting the Sensory to the Association units.

On the plugboard the sensory mosaic is duplicated 25 times by means of parallel wiring. There are 20 sockets available for each A-unit, 10 for excitatory and 10 for inhibitory connections. The plugboard makes it possible to experiment with different sensory to association layer connection configurations; in addition, it provides for eventual extension to inputs in other sense modalities.

4.2. A-units

The threshold devices of the A-units are monostable multivibrators with a period adjustable down to a minimum of 10 milliseconds. The inputs from the plugboard are summed through 20 Kilo-ohm resistors. These inputs are all of the same polarity, but the excitatory inputs are connected to the base of one of the transistors of the multivibrator, while the inhibitory links are connected to its emitter. The value of the threshold may be varied with a potentiometer.

The A-unit multivibrators control the amplifiers which drive the transducer (crystal or coil) for the twelve integrators associated with each A-unit. When the A-unit is "on", the amplifiers are biased in the middle of their linear operating range, and each integrator puts out a sine wave corresponding in magnitude and in phase to its previous history in regard to reinforcement. When the A-unit is "off", the amplifiers are in the cut-off region, and all the integrators are silent.

An additional function performed by the A-unit threshold devices is the opening of a gate which permits reinforcement of integrators belonging to active A-units. This function will be treated more explicitly in section 4.4.

The four transistors, neon indicator light, and sundry passive elements which form an A-unit are to be mounted on printed circuit boards at the head of the magnetostrictive delay lines supporting the integrator coils. Tentatively a 7" by 27" board has been assigned to each A-unit and its 12 integrators, with boards spaced 1½" apart.

4.3. R-units

The 1000 inputs to the R-unit are added in a resistor network. A tentative design for the threshold device of an R-unit is shown on Figure 66. The first stage is just an intermediate frequency preamplifier, while the second stage amplifies and clips the wave form. If the input is large enough, the output of the second stage is a square wave, while for smaller inputs it is a distorted trapezoid or a pure sine wave. The output of the clipper is fed to two phase detectors, which compare the phase of the signal either to the output of the main ultrasonic frequency oscillator, or to its inverse, suitably phase shifted (possibly by a delay

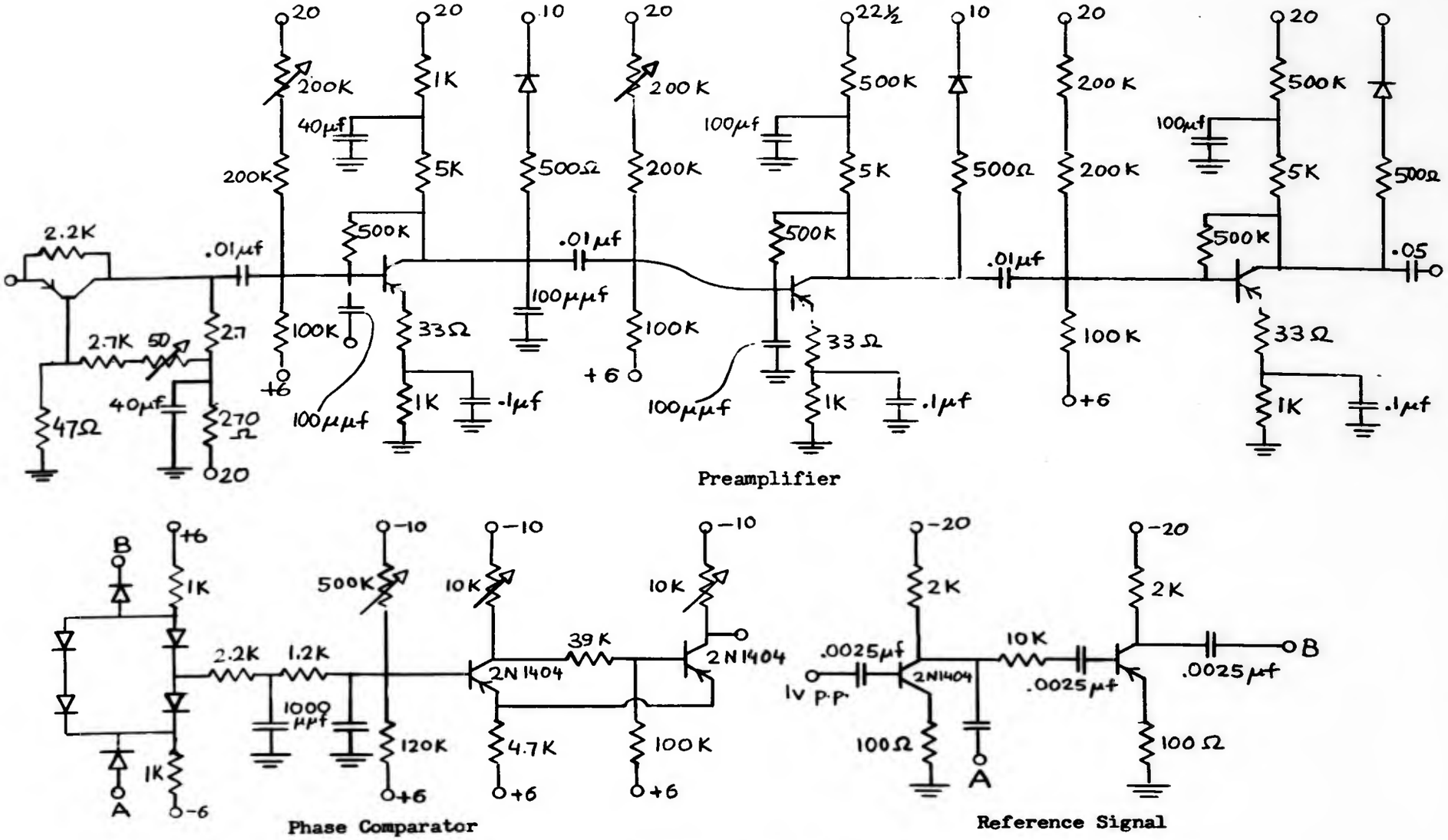

Figure 66. Schematic Diagram of R-Unit

line) to correspond to the position on the delay line of the integrators associated with that particular R-unit.

The phase comparators consist of a single transistor; the signal whose phase is to be established is fed to the base, and the reference signal to the emitter. The base is slightly back-biased, so that a pulse is emitted only if the base and the emitter are subjected to a sufficiently large voltage difference. The width of the output pulse depends on how close the output signal is to a square wave, and hence is proportional to the initial amplitude of the input to the R-units. The output of the phase shifters are filtered and serve as triggers to a bistable multivibrator (flip-flop). This multivibrator changes state only if the output of one of the phase comparators exceeds that of the other by a preset amount.

The guard-band between the two thresholds reduces the effect of noise, and prevents the R-unit from oscillating in response to small changes in the A-unit configuration.

A voltage comparator compares the actual output of the R-unit ($\pm$ 1) with the desired output. If the actual output is smaller than the desired output, then the blocking oscillator attached to the R-unit emits .1 microsecond 100 milliampere positive reinforcement pulses, while if the actual output is larger than the desired output, the blocking oscillator emits pulses of negative polarity. If the outputs are identical, the blocking oscillator puts out no pulse. The reinforcement pulses are channeled to the proper integrators by the mechanism described in the next section.

4.4. Reinforcement

The increase in flux level in the integrator is, as seen in the previous chapter, extremely sensitive to variations in the magnitude of the reinforcement pulse. It would, therefore, be desirable to have a separate pulse generator for each integrator, then we could guarantee that if a particular integrator is not to be reinforced, because the A-unit to which it belongs is inactive, it would in no way effect the incrementation of other integrators. A pulse generator capable of delivering 100 milliamps in .1 microseconds costs, however, at least $5.00, so that this arrangement is hardly practicable.

In the opinion of several manufacturers of pulse generating equipment, it is difficult to design a high speed pulse generator whose output would be unaffected by a load change of 10 to 1, or even 3 to 1. Thus any effective paralleling of integrators is precluded.

Fortunately the length of a reinforcement pulse is only .1 microseconds, while significant changes in A-unit configuration take at least 10 milliseconds; consequently we may have time to visit each integrator in turn between A-unit changes. With twelve pulse generators, one for each R-unit, we would only have to make one thousand "call", allowing 4 microseconds for each "call", the total time required would be well within schedule.

Several implementations of this scheme are now under experimental investigation. One is illustrated in Figure 67. Each R-unit blocking oscillator generates positive pulses, negative pulses, or no pulses, depending on the required reinforcement. The pulses are generated at the rate of 250 Kcps. A central clock also drives a three-decade 250 KCS counter, which has partial control over gate G_1 . G_1 is a four way coincidence gate;[64] it opens whenever the number of the A-unit to which

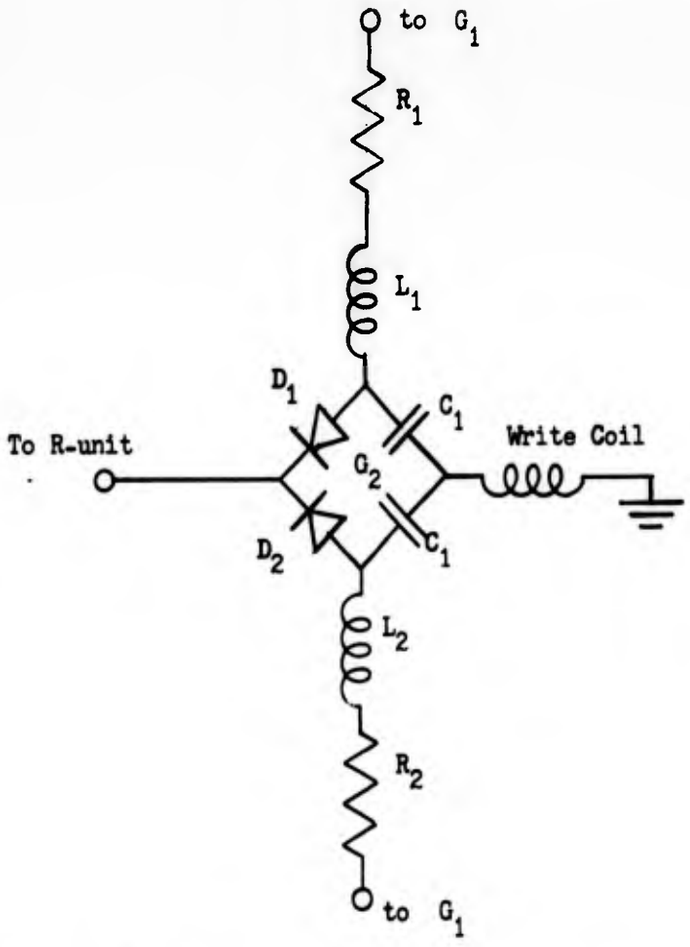

Figure 67. Bidirectional Diode Gate

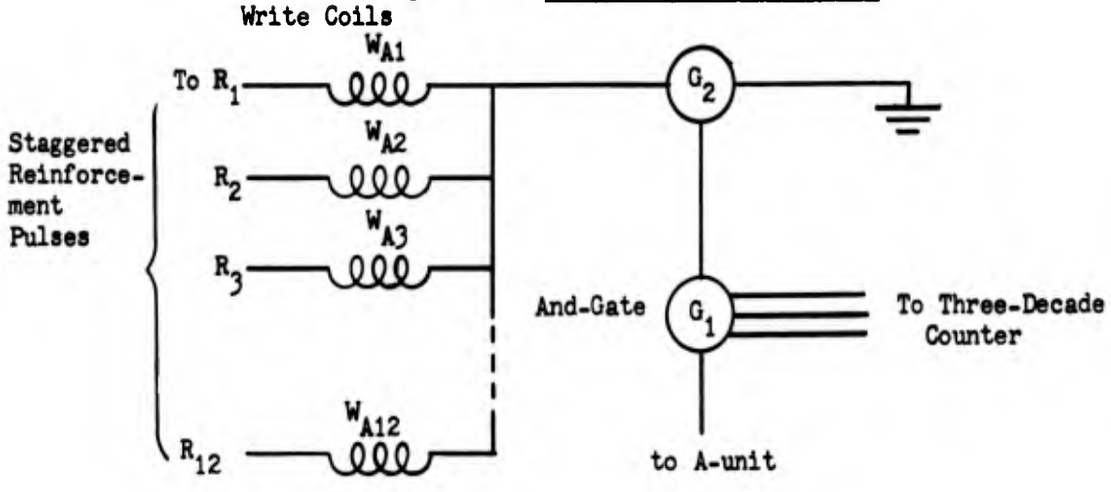

Figure 68. Reinforcement Schematic

it is attached comes up on the counter, and the A-unit threshold device is "on". The counter emits 1 microsecond pulses, thus each coincidence gate is open for at most 1 microsecond every 4 milliseconds. When G_1 is closed, both diodes D_1 and D_2 are back-biased and no pulse can get through gate G_2. Chokes L_1 and L_2 keep the oscillator from being loaded by the control circuit of G_2. When G_2 is open, L_1 and L_2 are floating and pulses of either polarity may pass through the coil. The two capacitors, which are necessary to keep the diode back-bias from flowing through the integrator coil in case of unbalance in the control voltages, must be sufficiently large so that a single pulse will not charge them up appreciably. Some external discharge path may also have to be provided. The success of this scheme depends largely on how much the open diodes and chokes of 1000 gates in parallel load down the pulse generator; this point is being investigated at present.

Another possible solution is illustrated on Figure 68. The advantage of this arrangement is that it requires only a single bi-directional gate, instead of twelve, for each A-unit. This gate could be a bi-directional transistor, or two ordinary transistors, or a conventional four or six diode bridge.[65] The gate would be opened by the selector gate and the A-unit threshold device as before. To prevent the coils from being reinforced through one another, the pulse generators would have to present an infinite output impedance between pulses, and the firing angles should be staggered.

Further modifications may be introduced. For example, instead of a three stage decade counter with four-way coincidence gates, it may be more economical to use two 32-digit counters and three-way gates, or even to dispense with the counter altogether and adapt a delay line to activate

each A gate in turn. Or, if the bi-directional gates are too expensive, two superimposed write coils, grounded at opposite ends, may be used. Another possibility is to have separate phases for positive and for negative reinforcement; the twofold loss of time is tolerable.

4.5. Auxiliary Circuits

The auxiliary circuits in Tobermory may be divided into two categories; those which facilitate training and help monitor machine performance, and those which are essential to the operation of the memory.

The former include automatic recycling of training sequences, interrogation programs, arrangements to study frequency and amplitude distribution, metering of A-unit activity, keeping track of R-unit reversals, and similar housekeeping operations. Provisions will have to be made to change the thresholds of all units. The reinforcement rate will also be variable; whether the pulse height, the pulse width, or the pulse repetition frequency is to be the "manipulated variable," is still to be decided.

The auxiliary circuits required for the smooth operation of the magnetostrictive integrators are the neutralizing circuits, and the demagnetizing circuits. Both of these are very simple. The neutralizing current is regulated by a trimpot provided for each A-unit board (Figure 69). The high resistance R_s in series with each coil serves the dual purpose of equalizing the direct current in the coil in spite of slight differences in coil resistance, and of rejecting the reinforcement pulses from the DC circuit.

The erase circuit consists of the voltage controlled amplifier shown in Figure 44b. It is not yet certain that 400 cps., rather than a somewhat higher frequency, will be used for this function. Toggle

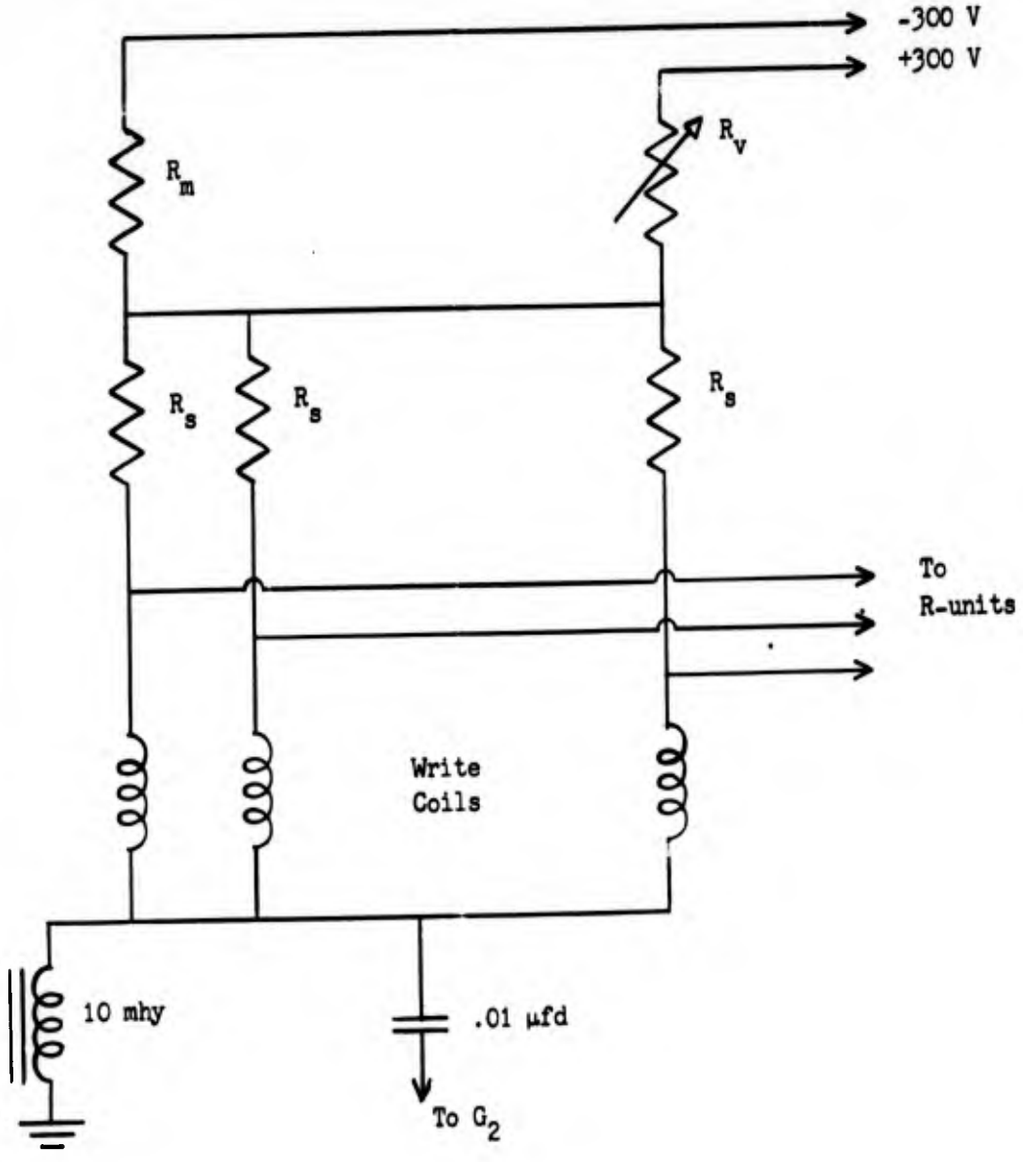

Figure 126. Magnetic Neutralizing Current

switches will render it possible to erase only the coils belonging to one particular R-unit at a time. Four 12-position rotary switches, inserted into the circuit just ahead of the R-unit summing resistors, will enable an operator to monitor the performance of any selected integrator.

V. CONCLUSIONS

By way of conclusion, the first section of Chapter V contains a comprehensive review of the integrators described in Chapter II. The second section summarizes the operating characteristics of the magnetostrictive read out integrator, and it also includes an estimate of the fabrication costs likely to be encountered in the portion of Tobermory directly involving the integrators. Section 3.3 explores possibilities of improving the magnetostrictive integrator to the point where the prospect of systems larger than Tobermory by an order of magnitude will not seem entirely impracticable.

5.1. How To Select An Integrator

This section is a commentary on Table 5, which contains numerical and other data pertinent to the various integrators. The entries in the table are reviewed in order of their appearance.

Electromechanical Integrators have done yeoman service, but for neuron memories they are about as obsolete as the Bush Differential Analyzer displayed at the Harvard Computer Museum.

Thermistors are grossly assymetrical with respect to incrementing and decrementing, and hence unsuitable for most perceptron applications.

Photochromic Integrators seem well suited to two layer processing of visual data, but there appears no way of adapting them to more complicated topologies.

The Transpolarizer is still in the initial stage of development. If accurate crystals could be formed by optical techniques and a suitable circuit worked out to control polarization, the transpolarizer might well turn out to be the answer to a large number of problems. The most

attractive feature about the transpolarizer is its high input impedance: with appropriate gates there should be no difficulty in incrementing or decrementing hundreds, or even thousands, of crystals simultaneously.

Flux Integration, in its various forms, is by far the most popular method of loosely keeping track of pulses. The linearity of these integrators, and the area of the hysteresis curve formed by the counting curve, depends on the resolution and the number of levels required. Unfortunately, the most linear region does not contain the origin. Flux integrators share the characteristic that the cost of the integrator itself is negligible compared to the associated circuitry. The object is, therefore, to make the requirements for the driving and sensing circuitry as simple as possible. In order to reduce the magnetizing current, the cross-sectional area of the toroid should be small, yet the interior diameter should be large enough to provide room for the additional turns on the read coil required to sense the decreased flux. The drive signal must in any case be fairly small, otherwise it will disturb the flux level. The complete read-write cycle of most toroidal integrators is just slightly too long (3-80 microseconds) to permit sequential operation in a machine such as Tobermory, but in other systems the logical flexibility of multiaperture cores may render them quite economical.

Charge Integration in capacitors presents the problem that the large series resistance required for linear operation renders incrementation intolerably slow. The sensing of the charge offers a further problem. These difficulties are largely overcome by Babcock's cadmium-nickel battery, but full details are not yet available.

TABLE V

Characteristics of Proposed Integrators

Integrator	Number of Available Levels	Time Req'd for Re-inforcement	Stabil-ity	Means of Reinforce-ment	Approximate Cost
Electro-mechanical	500	.1 sec.	infinite	2 amp. d.c.	$40.00
Thermistors	continu-ous	5 sec.	5 min.	40 ma. d.c.	$ 0.50
Photochromic	2	--	6 hours	high energy flash	--
Transpolarizer	40	1 μsec.	6 months	electron beam	--
Ferrite	20-200	3-80μsec.	infinite	1 micro-second 1 amp. pulse	$10.00
Capacitor	continu-ous	1-1000 milli-seconds	6 hours	1-1000 milli-second pulses	$ 1.00
Solions	continu-ous	1 second	30 days	50μamp. d.c.	$15.00
Electrolytic	100	100 milli-seconds	6 months	100 milli second 1 ma. pulse	$20.00
Magnetostrictive	50	.1μsec.	infinite	.1 μsec. pulse	$ 1.00

Solions are, at present, far too expensive to be competitive. The elaborate impedance matching required and inherent slowness renders them even less likely candidates for brain model applications.

Electrolytic Integrators are now commercially manufactured; it is claimed that in a few years they will be available at $2.00 or $3.00 apiece in large quantities. Present quotations range, however, from $15.00 to $50.00, so that in spite of their reputedly excellent performance and ease of application they must be restricted to small demonstration models.

5.2. The Magnetostrictive Integrator

The magnetostrictive read out integrator fulfills the requirements outlined in Chapter I. 20 to 80 levels of flux are available with .1 microsecond magnetizing pulses, and the ratio between incrementing steps and decrementing steps is not more than 5:1 even at the extreme limits of the useful range. The power required for reinforcement is 80-100 milliamps into a 50 Ω inductive load, and for driving 60 volts r.m.s. into 2000 Ω (crystal transducer) or 200 milliamps r.m.s. into 500 Ω (coil transducer). Erasure is accomplished by passing a 400 cps. alternating current of decreasing amplitude through the write coils of the integrator. The integrator is insensitive to environmental conditions with the exception of stray magnetic fields; in particular, the effect of the earth's magnetic field must be neutralized for optimum performance.

Because of the relatively large amplitude and short duration of the magnetizing pulses needed for setting the integrator, in a moderately large system, such as Tobermory, it is practicable to use only a small number of pulse generators and to reinforce the integrators in sequence.

TABLE VI

Cost of Components for Magnetostrictive Readout Integrator

Circuit	Component	Cost
Integrator proper	coil assembly	$ .30
	permalloy wire	negligible
Selector gate	4 diodes, 1 transistor (1 req'd. per 12 integrators)	$3.00
Bidirectional gate	2 transistors	$4.00
Pulse generator	blocking oscillator (1 req'd. per 1000 integrators)	$50.00
Drive Transducer	PZT-4 Crystal (1 req'd per 12 integrators)	$1.62
Amplifier	3 transistors, 1 transformer (1 req'd. per 12 integrators)	$10.00

A major part of the cost of the memory resides in the switching circuitry required to implement the sequential reinforcement scheme.

More explicitly, the cost of a coil assembly, in lots of 10,000, is approximately 30¢ apiece. The cost of the permalloy wire is negligible, and 200 Kc/s crystals, mounted on the magnetostrictive wire, are quoted at $1.63 each. The components required for a two-transistor bi-directional gate would come to about $4.00 (500 Kc/s transistors could be used), while the four-way coincidence gate could be built for less than $3.00. The pulse generators have to be quite powerful in order to overcome the loading imposed by 1000 closed gates, but even so $600.00 for the dozen would be ample. These figures are summarized in Table 6. It is seen that the total cost of the circuitry required for each integrator, exclusive of labor, cabling, and printed circuit boards, is about $1.30. This figure compares favorably with the other alternatives available.

5.3. Further Research

The devices used in Tobermory by no means represent the ultimate in magnetostrictive read out integrators; they should rather be regarded in the light of a project smoothing the way for larger and more sophisticated brain models.

The next important step will be the elimination of the cumbersome semiconductor gates required for each A-unit; with square loop materials, it will no doubt be possible to use the inherent threshold characteristics for coincidence mode switching in a manner analogous to the selection of the proper bit in standard computer core memory matrices. Next, to reduce the magnetizing current, and improve the speed and linearity of the response, deposited thin film techniques will be perfected; research in all these

areas is in progress at the Stanford Research Institute. It appears likely that within the next five years integrators offering superior performance will be available under 30¢ apiece.

In spite of such developments, the pair of electromechanical transducers required for each integrator is eventually bound to hinder further increases in the speed, and reduction in the size, of the magnetostrictive readout integrator. Models which will be built to study the higher centers of the brain will require considerable cross-coupling and interaction between memory elements, and the spatial requirements of the magnetostrictive integrator will prove a hindrance to the implementation of such logical complexity. By then, however, electron-optical fabrication techniques, now being developed by Dr. K. Shoulders[66] in Palo Alto, may be sufficiently advanced to allow the construction of a "cryogenic" machine.

Such a machine would be many orders of magnitude more compact than any presently built, and the power level required to operate it would also be much lower. The memory of such a system may have to operate on only two levels, but it can be shown that a perceptron logically equivalent to any conventional perceptron may be designed using a sufficient number of binary devices. The cryogenic perceptron would, in fact, be more likely to be a fairly general purpose parallel computer, with the connection scheme necessary for a given experiment established by external control, and a separate input section.

In spite of the very considerable improvements in components now within reach, it is not to be hoped that the hardware will keep apace with the desires of the brain modeller. Still, as much as ever, the investigator will have to display the utmost ingenuity in the design of both machines and experiments; only then can he expect to extract signficant information from systems so piteously limited in comparison to the biological scale.

BIBLIOGRAPHY

1. Monro, H.H., The Chronicles of Clovis, The Bodley Head Ltd., London, 1911.

2. Gardner, E., The Fundamentals of Neurology, W.B. Saunders and Co., Philadelphia, 1958.

3. McCulloch, W.S., and Pitts, W., "A Logical Calculus of the Ideas Immanent in Nervous Activity," Bull. Math. Biophysics, 5, 115-133, 1943.

4. Turing, A.M., "On Computable Numbers, with an Application to the Entscheidungs-problem," Proceedings of the London Mathematical Society, Ser. 2, Vol. 21, 230-265, 1936-7.

5. Culbertson, J.T., A Neural Analysis of Behaviour and of Consciousness, W.C. Brown Co., Dubuque, Iowa, 1950.

6. Hayek, F.A., The Sensory Order, Routledge and Kegan Paul Ltd., London, 1952.

7. Uttley, A.M., "Conditional Probability Machines and Conditioned Reflexes," in Shannon and McCarthy, Automata Studies, Princeton University Press, Princeton, 1956.

8. Buhr, R.J.A., The Development of a Conditional Probability Computer, Report No. 2, Computer and Control Systems Laboratory, University of Saskatchewan, Saskatoon, 1961.

9. Gamba, A., "Pattern Recognition," Supplement of Nuovo Cimento, 22, 102-232, 1961.

10. Ashby, N.R., Design for a Brain, Wiley, New York, 1952.

11. Hebb, D.O., The Organization of Behaviour, Wiley, New York, 1949.

12. Rochester, N., J.H. Holland, L.H. Haibt, and W.L. Duda, "Tests on a Cell Assembly Theory of the Action of the Brain, Using a Large Digital Computer," I.R.E. Transactions on Information Theory, IT-2, 80-93, 1956.

13. Rosenblatt, F., The Perceptron: A Theory of Statistical Separability in Cognitive Systems, Cornell Aeronautical Laboratory Report No. VG-1196-G-1, Buffalo, Jan. 1958.

14. ---------- The Principles of Neurodynamics, Cornell Aeronautical Laboratory Report No. VG-1196-G-8, Buffalo, March 1961.

15. ---------- On the Convergence of Reinforcement Procedures in Simple Perceptrons, Cornell Aeronautical Laboratory Report No. VG-1196-G-4, Buffalo, February 1960.

16. ---------- "Application of Perceptrons to Speech Recognition," Proc. Speech Communication Seminar, (awaiting publication), Stockholm, Aug. 1962.

17. ---------- Integrator Requirements for the Perceptron, Technical Memorandum No. 1, Project PARA, Cornell Aeronautical Laboratory, Buffalo, June 1958.

18. Hay, J.C., Martin, F.C. and Wightman, C.W., "The Mark I Perceptron, Design and Performance," Record of the IRE National Convention, Part 2, New York, 1960.

19. Hay, J.C., Lynch, B.E. Smith, D.R. and Murray, A.E., Mark I Perceptron Operators Manual, Cornell Aeronautical Laboratory Report No. VG-1196-G-5, Buffalo, 1960.

20. Arking, A., and Chiu, H.Y., Proposal for Construction of a Thermistor Perceptron, Laboratory of Nuclear Studies, Cornell University, Ithaca, 1959.

21. Cameron, S.H., Self Organizing Networks, Annual Report, Armour Research Foundation of Illinois Institute of Technology, Project No. E 154, Chicago, 1962.

22. Pulvari, P., "The Transpolarizer: An Electrostatically Controlled Circuit Impedance with Stored Setting," Proc. I.R.E. 47, 1117-1122, June 1959.

23. Anderson, J.R., "Ferroelectric Materials as Storage Elements of Digital Computers and Switching Systems," Trans. AIEE, Paper 52-309, 1952.

24. Chiu, H.Y., An Investigation of Transpolarizers as A-units, Laboratory of Nuclear Studies, Cornell University, Ithaca, N.Y. 1959.

25. Hawkins, J.K., Mansey, C.J. and Stafford, R.A., A Magnetic Integrator for the Perceptron Program, Summary Report, Aeronutronic Research Laboratory Publication No. U-1405, Newport Beach, California, 1961.

26. Hawkins, J.K. and Munsey, C.J., A Magnetic Integrator for the Perceptron Program, Quarterly Progress Report No. 4, Aeronutronics Research Laboratory Publication No. U-1068, Newport Beach, California, 1960.

27. ---------- A Magnetic Integrator for the Perceptron Program, Annual Summary Report, Aeronutronic Research Laboratory Publication No. U-603, Newport Beach, California, 1960.

28. ---------- A Magnetic Integrator for the Perceptron Program, Quarterly Progress Report No. 1, Aeronutronic Research Laboratory Publication No. U-591, Newport Beach, California, 1959.

29. ---------- A Magnetic Integrator for the Perceptron Program, Quarterly Progress Report No. 2, Aeronutronic Research Laboratory Publication No. U-592, Newport Beach, California, 1959.

30. ---------- A Magnetic Integrator for the Perceptron Program, Quarterly No. U-601, Newport Beach, California, 1960.

31. Brain, A.E., The Stimulation of Neural Elements by Electrical Networks Based on Multi-Aperture Cores. Stanford Research Institute, Menlo Park, California, 1960.

32. Bennion, D.R. and Crane, H.D., "Design and Analysis of MAD Transfer Circuitry," Proc. W.J.C.C., 21-36, March 1959.

33. Brain, A.E., Novikoff, A.B. and Bourne, C.P., Graphical Data Processing Research Study and Experimental Investigation, Report No. 4, Stanford Research Institute, Menlo Park, California, April 1961.

34. Guckel, H., Integration and Non-Destructive Sensing with Magnetic Cores, Cornell Aeronautical Laboratory Report No. UD-1298-P-2, Buffalo, Aug. 1959.

35. ---------- Development of Transfluxor Circuitry, Cornell Aeronautical Laboratory, Report No. UD-1298-P-2, Buffalo, August 1959.

36. Devilbiss, J., A Magnetic Pulse Integrator, Disclosure of Invention and Letter of Transmittal, University of Illinois, Urbana, Ill., 1962.

37. Babcock, M.L., Reorganization by Adaptive Automation, University of Illinois, Nonr 1834(21) Technical Report No. 1, Urbana, Illinois, January 1960.

38. An Introduction to Solions, Texas Research and Electronic Corporation, Dallas, June 1961.

39. Solion Principles of Electrochemistry and Low-Power Electrochemical Devices, U.S. Department of Commerce publication No. PB 131931, Aug. 1958.

40. Bloom, B., and Hogaboom, H., Principles of Electroplating and Electroforming, McGraw Hill, N.Y. 1949.

41. Handbook of Electroplating-Canning, W. Canning and Co., Ltd., Birmingham, 1960.

42. Widrow, B., An Adaptive "Adaline" Neuron Using Chemical "Memistors," Solid State Electronics Laboratory Technical Report No 1553-2, Stanford University, Stanford, October 1960.

43. Whitcomb, D.W. and Syverson, C., Experimental Evaluation of Thin Film Resistor Films as Electro-Chemical Integrators, Computer Research Department, Cornell Aeronautical Laboratory, Buffalo, May 1961.

44. Chiu, H.Y., An Investigation of the Possibility of Using Electrolytic Cells as A-Units in the Construction of a Perceptron, Laboratory for Nuclear Studies, Cornell University, Ithaca, 1959.

45. Becker, R., and Doring, W., Ferromagnetismus, W. Springer, Berlin 1939.

46. Bozorth, R.M., Ferromagnetism, Van Nostrand, Princeton, 1951.

47. Bozorth, R.M. and Williams, H.J., "Effect of Small Stresses on Magnetic Properties," Rev. Mod. Physics 17, 72-80, 1945.

48. Say, N.G. (editor), Magnetic Alloys and Ferrites, George Newness Ltd., London, 1954.

49. Friedlander, F.J., "Flux Reversal in Magnetic Amplifier Cores," Trans. AIEE, Paper No. 56-219, 1956.

50. Katz, H.W. (editor) Solid State Magnetic and Dielectric Devices, Wiley, New York, 1960.

51. Polydoroff, W.J., High Frequency Magnetic Materials, Wiley, N.Y., 1959.

52. Wylen, J., "Pulse Response Characteristics of Rectangular Hysteresis Loop Material," Trans. AIEE, Part 1, 72, 648-656, 1953.

53. Crawford, A.E., Ultrasonic Engineering, Butterworth Scientific Publication, London, 1955.

54. PZT-4 Specification, Clevite Corporation, Cleveland, March 1958.

55. Tehon, S., "Wire Sonic Delay Line," Research and Development, General Electric Publication, Syracuse, June 1959.

56. Hunt, F.V., Electro-Acoustics, Harvard University Press, Cambridge, May, 1954.

57. Carlin, B., Ultrasonics, McGraw Hill, New York, 1960.

58. Fairclough, J.W., "A Sonic Delay-Line Storage Unit for a Digital Computer," Proc. IEE, 103, Part B, Supplement 3, paper no. 2041M, 491-498, 1956.

59. Beurle, R.L., "Video Signal Integration Using Acoustic Delay Lines and Dynamic Magnetic Storage," in W. Jackson's Communication Theory, Academic Press, London, 1953.

60. Hueter, T.F. and Bolt, R.H., Sonics, Wiley, New York, 1955.

61. McConnell, H.M., "Eddy-current Phenomena in Ferromagnetic Materials," Trans. AIEE 73, part 1, 226-236, 1954.

62. Bradburd, E.M., "Magnetostrictive Delay Line," Electrical Communication, 28, 46-55, March 1951.

63. Scarrot, G.G., and Naylor, R., "Wire Type Acoustic Delay Line for Digital Storage," Proc. IEE, 103, Part B., Supplement No. 3, paper No. 2027M, 497-502, March 1956.

64. Millman, J., and H. Taub, Pulse and Digital Circuits, McGraw Hill, N.Y. 1956.

65. Millman, J., and Puckett, T.H., "Accurate Linear Bidirectional Diode Gates," Proc. IRE, 43, 27-37, January 1955.

66. Shoulders, K.R., Research in Microelectronics Using Electron-Beam Activated Machining Techniques, Stanford Research Institute, Menlo Park, Cal. 1960.

DISTRIBUTION LIST

Addressee	No. of Copies
Armed Services Technical Information Agency Arlington Hall Station Arlington 12, Virginia	10
Assistant Sec. of Def. for Res. and Eng. Information Office Library Branch Pentagon Building Washington 25, D. C.	2
CAMPAIGNE Howard National Security Agency Fort Geo. G. Meade, Maryland Code R4	3
Commanding Officer, Office of Naval Research Navy # 100, Fleet Post Office New York, New York	10
Chief of Naval Research Department of the Navy Washington 25, D. C. Attn: Code 437, Information Systems Branch	2
Director, Naval Research Laboratory Technical Information Officer/Code 2000/ Washington 25, D. C.	6
INSTITUTE FOR DEFENSE ANALYSES Communications Research Division Von Neumann Hall Princeton, New Jersey Attn: Director	2

Addressee
(1 copy each)

Air Force Cambridge Research Center
Laurence C. Hanscom Field
Bedford, Massachusetts
Attn: Electronic Research Directorate Library

ALEXANDER Dr. S. N.
National Bureau of Standards
Washington 25, D. C.

ABRAHAM G.
Security Systems, Code 5266
Naval Research Laboratory
Washington 25, D. C.

ALPERT D.
University of Illinois
Control Systems Laboratory
Urbana, Illinois

AMASSIAN Dr. Vahe E.
Air Force Office of Scientific Research
Washington 25, D. C.

Dr. J. G. Andreae
Standard Telecommunication Lab. Ltd.
London Road, Harlow, Essex
England

APPLIED Physics Laboratory
Johns Hopkins University
8621 Georgia Avenue
Silver Spring, Maryland
Attn: Supervisor of Tech. Reports

ARKING Albert
National Aeronautics and Space Administration
Theoretical Division
8719 Colesville Road
Silver Spring, Maryland

ASHBY Dr. W. Ross
University of Illinois
Dept. of Electrical Engineering
Urbana, Illinois

Addressee
(1 copy each)

C. H. Ball
I.T.T. Federal Laboratories
937 Commercial
Palo Alto, California

BAR-HILLEL Prof. Y.
Hebrew University
Jerusalem, Israel

BARUS Prof. Carl
Department of Electrical
Engineering
Swarthmore College
Swarthmore, Pennsylvania

BECK, Dr. Jacob
Department of Psychology
Harvard University
Cambridge 38, Mass.

BREMERMANN, Prof. H. J.
Department of Mathematics
University of California
Berkeley, California

BROOK Dean Harvey
School of Applied Science
Harvard University
Cambridge, Massachusetts

BROWNSON Helen L.
National Science Foundation
Program Director for
Documentation Research
Washington 25, D. C.

Bureau of Naval Weapons
Department of the Navy
Washington 25, D. C.
Attn: RAAV Avionics Division

BUREAU OF NAVAL WEAPONS
Department of the Navy
Washington 25, D. C.
Attn: RMWC Missile Weapons
Control Div.

Addresses
(1 copy each)

Bureau of Naval Weapons
Department of the Navy
Washington 25, D. C.
Attn: RUDC ASW Detection and Control Div.

Bureau of Ships
Department of the Navy
Washington 25, D. C.
Attn: Code 671 NTDS

Bureau of Ships
Department of the Navy
Washington 25, D. C.
Attn: Communications Branch Code 686

BURKS A. W.
Dept. Of Philosophy
University of Michigan
Ann Arbor, Michigan

BUSBY Cdr. J. C., Code W3
Bureau of Supplies and Accounts, Chief
Navy Department
Washington, D. C.

CAMERON Mr. Scott
E. E. Research Department
Armour Research Foundation
10 West 35th Street
Chicago 16, Illinois

CAMPION Miss Anna Louise
University of Pennsylvania
Moore School of Electrical Engineering
200 South 33rd Street
Philadelphia 4, Pennsylvania

CECCATO Prof. Silvio
Universita di Milano
Centro di Cibernetica
Via Festa del Perdono, 3
Milano, Italy

CHANNEL E. W., ORDTL-012
Diamond Ordnance Fuze Laboratory
Connecticut Ave. and Van Ness Street
Washington 25, D. C.

Addresses
(1 copy each)

Chief of Naval Operations
OP-L7T-12
Navy Department
Washington 25, D. C.

CHIU Dr. Hong Yee
Institute for Advanced Study
Princeton, New Jersey

Commanding Officer, ONR Branch Office
346 Broadway
New York 13, New York

Commanding Officer, ONR Branch Office
495 Summer Street
Boston 10, Massachusetts

Commanding Officer
ONR Branch Office
1000 Geary Street
San Francisco 9, California

Commanding Officer
ONR, Branch Office
John Crerar Library Bldg.
86 East Randolph Street
Chicago 1, Illinois

Commanding Officer
ONR Branch Office
1030 E. Green Street
Pasadena, California

COMMANDING OFFICER
RADC Griffiss Air Force Base
Rome, New York
Attn: Lt. Roger Geesey / RCWID /

Cornell Aeronautical Laboratory
Buffalo 21, New York
Attn: Library

CORNELL UNIVERSITY
Dept. Of Psychology
Ithaca, New York
Attn: Prof. Hochberg

Addresses
(1 copy each)

CORNELL UNIVERSITY
Main Library
Engineering Library

CRANE H. D.
Stanford Research Institute
Computer Laboratory
Menlo Park, California

CRISLER E. H.
Bendix Products Division
Bendix Aviation Corporation
Southbend 20, Indiana

David Taylor Model Basin
Washington 7, D. C.
Attn: Technical Library

DAY, GEORGE (see ONR)

DIBLASI F. P.
Data Processing Systems Staff
Department of State
Washington 25, D. C.

DOLANSKY Prof. L. O.
Northeastern University
360 Huntington Avenue
Boston, Massachusetts

DOMESHEK S., Code 3144
US Naval Training Device Center
Port Washington
Long Island, New York

ELBOURN R. D.
National Bureau of Standards
Washington 25, D. C.

Electronics Research Laboratory
University of California
Berkeley 4, California
Attn: Director

ESTRIN Gerald Prof.
Dept. of Engineering
University of California -LA
Los Angeles 24, California

Addresses
(1 copy each)

FAIRTHORNE R. A.
Ministry of Supply
Royal Aircraft Establishment
South Farnborough
Hants, England

FARLEY Dr. B.
Massachusetts Institute of Technology
Lincoln Laboratory
Lexington 73, Massachusetts

FOERSTER Prof. H. Von
University of Illinois
Electrical Engineering Dept.
Urbana, Illinois

FRAUNFELDER, Mrs. Jane C., Librarian
Pennsylvania Research Associates, Inc.
Suite 508
133 South Thirty-Sixth Street
Philadelphia 4, Pennsylvania

FRIEBURGER H.
Research and Development Division
Veterans Administration
Department of Medicine and Surgery
Washington 25, D. C.

FRY Mr. Bernard M., Deputy Head
Office of Science Information Service
National Science Foundation
1951 Constitution Avenue, N.W.
Washington 25, D. C.

FUCHS, Prof. Wolfgang
Cornell University
Department of Mathematics
Ithaca, New York

FULLER Dr. H.
Laboratory for Electronics, Inc.
1079 Commonwealth Avenue
Boston 15, Massachusetts

Addresses
(1 copy each)

GABELMAN Irving J.
Rome Air Development Center, RCOR
DCS/operations, USAF
Griffiss Air Force Base, New York

GAMBA Prof. A.
Instituto di Fisica dell Universita
Genova, Italy

GIBSON Prof. James J.
Cornell University
Department of Psychology
Ithaca, New York

GEIGER Mr. L. H.
R and D Division SIGRO-6D
Office of Chief Signal Officer
Department of the Army
Washington, D. C.

GIESE J. H.
Aberdeen Proving Ground, BRL
Aberdeen Proving Ground, Maryland
Attn: Chief Computation Lab.

GLEISSNER G. H.
US Naval Weapons Laboratory
Dahlgren, Virginia
Attn: Head, Computation Div.

GLINSKY, George (Professor)
Chairman,
Electrical Engineering Department
University of Ottawa
Ontario, Canada

GOLDMAN Dr. Stanford
Syracuse University
Electrical Engineering Dept.
Syracuse 10, New York

GRANGER Fred P. Jr.
Varo Manufacturing Company
2201 Walnut Street
Garland, Texas

GREEN Bert F. Jr., Room C-345
Massachusetts Inst. of Technology
Lincoln Laboratory
Lexington 73, Massachusetts

Addresses
(1 copy each)

GREENE Peter H.
Committee on Mathematical Biology
University of Chicago
Chicago, Illinois

HAWKINS J. K., Dr.
Aeronutronic
Ford Road
Newport Beach, California

HAY John, Dr.
62 Kensington Avenue
Northampton, Massachusetts

HAYMAN Mr. Harry /RD-375/
Federal Aviation Agency
Bureau of Research and Development
Washington 25, D. C.

HEBB Prof. Donald
McGill University
Department of Psychology
Montreal, P.Q.
Canada

HOCKETT Prof. Charles
Cornell University
Division of Modern Languages
Ithaca, New York

HOLMES W.
Cornell Aeronautical Laboratory
Buffalo 21, New York

HOWERTON Mr. Paul W.
Room 1053 M. Building
Code 163
CIA
Washington 25, D. C.

HUNT, Dr. Earl B.
Univ. of Calif.
Western Management Science Inst.
Grad. School of Business Admin.
Los Angeles 24, California

JOHN Prof. E. R.
University of Rochester
Dept. of Psychology
River Campus Station
Rochester 20, New York

Addresses
(1 copy each)

JOSEPH, Dr. R. D.
Principal Mathematician
Astropower, Inc.
2968 Randolph Street
Costa Misa, California

KAC Prof.
Rockefeller Institute
New York, New York

KAPLAN Sidney
Missile and Surface Radar Division
Radio Corporation of America
Moorestown, New Jersey

KARROLL Joseph E.
Radio Corporation of America
Moorestown, New Jersey

KELLY, Dr. Peter
Astropower, Inc.
2968 Randolph St.
Costa Misa, California

KESTEN Harry
Cornell University
Dept. of Mathematics
Ithaca, New York

KIRON Allan
Office of Research and Development
U. S. Dept. of Commerce
Patent Office
Washington 25, D. C.

KONO, Mr. Ryuichi
Mitsubishi Electric Mfg. Co. Ltd.
Electronics Works
80 Nakano, Minami Shimizu, Amagasaki,
Hyogo Prefecture, Japan

KOLLER, Mr. Herbert R.
Department of Commerce
US Patent Office
Washington 25, D. C.

KULLGREN, Mr. John F.
Department of the Army
Room 2C521 Pentagon
Washington, D. C.

Addresses
(1 copy each)

LANDAHL, Prof. H. D.
University of Chicago
Committee on Mathematical Biology
Chicago, Illinois

LASERFELD, Dr. Azriel
Budd Electronics
43-22 Queens Street
Long Island City 1, New York

LEDLEY, Dr. R. S.
National Biomedical Research
Foundation, Inc.
8600 16th St., Suite 310
Silver Spring, Maryland

LEVINE, Seymour T.
Research Division
Kollsman Instrument Division
80-08 45th Avenue
Elmhurst 73, New York

Lincoln Laboratory
Massachusetts Institute of Technology
Lexington 73, Massachusetts
Attn: Library

LINVILL, Prof. John G.
Stanford University
Electronics Lab.
Stanford, California

LONG, Capt. B. J. (RCWID)
Research Air Development Center
Griffiss Air Force Base, New York

LUCE Duncan R.
Harvard University
Laboratory of Social Relations
Cambridge 38, Massachusetts

LUHN Hans Peter
Yorktown Heights, New York
IBM Research

McCARTHY, Prof. John, 26-007B
Massachusetts Institute of Technology
Cambridge 39, Massachusetts

Addresses
(1 copy each)

McCLURG, Mr. Gregg
Army Research Office OCR and D
Dept. of Army
Code 189
Arlington Hall
Arlington, Virginia

McCULLOCH, Prof. W.
Massachusetts Institute of Technology
Research Laboratory of Electronics
Lexington 73, Massachusetts

MACLEOD, Prof. Robert B.
Cornell University
Department of Psychology
Ithaca, N. Y.

MANDELBROT, Dr. Benoit
IBM Research Center
Yorktown Heights, N. Y.

MARDEN, Mrs. Ethel
National Bureau of Standards
Washington 25, D. C.

MARTI N. F.
Data Instruments Division
Telecomputing Corp.
12838 Saticoy Street
North Hollywood, California

MEDICK J.
Cornell Aeronautical Laboratory
Buffalo 21, New York

MELTON, Prof. Arthur
University of Michigan
Ann Arbor, Michigan

METROPOLIS, Mr. Nicholas, Director
University of Chicago
Institute for Computer Research
Chicago 37, Illinois

MEYER Don
Ohio State University
1314 Kinnear Road
Columbus 12, Ohio

Addresses
(1 copy each)

MINSKY, Dr. Marvin
Massachusetts Inst. of Technology
Research Lab. of Electronics
Cambridge, Mass.

MOOERS Calvin N.
Zator Co.
140½ Mt. Auburn Street
Cambridge 38, Mass.

MORRISON, Prof. Phillip
Cornell University
Department of Physics
Ithaca, N. Y.

MURRAY A. E.
Systems Requirements Dept.
Cornell Aeronautical Laboratory, Inc.
PO Box 235
Buffalo 21, New York

Naval Electronics Laboratory
San Diego 52, California
Attn: Technical Library

Naval Ordnance Laboratory
White Oaks
Silver Spring 19, Maryland
Attn: Technical Library

NEELAND, Mrs. Frances
National Bureau of Standards
Washington 25, D. C.

NEWELL, Dr. Allen
Carnegie Institute of Technology
Graduate School of Industrial Admin.
Pittsburgh 13, Pennsylvania

OETTINGER, Dr. Anthony
Harvard Computation Lab.
Harvard University
Cambridge, Massachusetts

OFFICE OF NAVAL RESEARCH
Resident Representative
University of Rochester
Federal Bldg., Rm. 122
Church and Fitzhugh Sts.
Rochester 14, New York

Addresses
(1 copy each)

Office of Naval Research
Washington 25, D. C.
Attn: Code 455

Office of Technical Services
Technical Reports Section
Department of Commerce
Washington 25, D. C.

OLDS, Dr. James
Department of Psychology
University of Michigan
Ann Arbor, Michigan

PASTA John R.
Division of Research
Atomic Energy Commission
Washington 25, D. C.

PERLIS Alan J.
Director Computation Center
Carnegie Institute of Technology
Pittsburgh, Pennsylvania

PETERSON Gordon
Communications Sciences Lab.
University of Michigan
180 Frieze Building
Ann Arbor, Michigan

PICKUP, Mr. J.
Officer in Charge
US Naval Photographic Interpretation Center
4301 Suitland Road
Suitland, Maryland

PORTER, Dr. C. R.
Psychology Department
Howard University
Washington 1, D. C.

PRYWES, Dr. Noah S.
Moore School of Engineering
University of Pennsylvania
Philadelphia 4, Pennsylvania

Addresses
(1 copy each)

Rabinow Engineering Co., Inc.
7712 New Hampshire Avenue
Washington 12, D. C.

Rand Corporation
1700 Main Street
Santa Monica, California
Attn: Library

RATZ H. C.
University of Saskatchewan
College of Engineering
Saskatoon, Canada

REES, Dean Mina
Hunter College
New York 21, N. Y.

RHODES, Miss Ida
120 Far West
National Bureau of Standards
Washington 25, D. C.

ROSE, Dr. Milton E.
Lawrence Radiation Laboratory
University of California
Berkeley, California

ROSEN, Dr. Charles
Applied Physics Group
Stanford Research Institute
Menlo Park, California

ROSENBLATT, Prof. D.
American University
Department of Mathematics and
Statistics
Washington 6, D. C.

SALPETER, Prof.
Cornell University
Laboratory for Nuclear Studies
Ithaca, New York

SAMSON, Mr. Robert F.
Directorate of Intelligence and
Electronic Warfare
Griffiss Air Force Base
Rome, New York

Addresses
(1 copy each)

SELFRIDGE, Dr. Oliver
Lincoln Laboratory
Massachusetts Institute of Technology
Lexington 73, Massachusetts

SHAPIRO Arthur
NASA
Goddard Space Flight Center
Washington 25, D. C.

SHIMAMOTO, Dr. Yoshio
Brookhaven National Laboratory
Upton, Long Island, New York

SINGER, Prof. J. R.
University of California
Department of Engineering
Berkeley 4, California

SMITH, Mr. J.
Navy Management Office
Data Processing Systems Division
Department of the Navy
Washington 25, D. C.

SOLOMONOFF R. J.
Zator Company
140½ Mt. Auburn
Cambridge 38, Mass.

STANLEY, Mr. Gordon
7685 South Sheridan Ct.
Littleton, Colorado
/Martin/ Denver/

STEIBER Alexander
Juliana van Stolbergham 25
The Hague, Netherlands

STEINBUCH, Prof. Dr.-Ing. K.
Institut für Nachrichtenverarbeitung und
Nachrichtenübertragung
Technische Hochschule Karlsruhe
Kaiserstrasse 12

STEVENS R.
Cornell Aeronautical Laboratory
Buffalo 21, New York

SWANSON D. R.
Thompson Ramo-Woolridge, Inc.
8433 Fallbrook Avenue
Canoga Park, California

Addresses
(1 copy each)

TAYLOR, Dr. W. K.
University College
Anatomy Department
Gower Street
London, W.C.1, England

Technical Information Officer
US Army Signal Research and
Dev. Lab.
Fort Monmouth, New Jersey
Attn: Data Equipment Branch

THOMASIAN, Prof. A. J.
University of California
Institute of Engineering Research
Berkeley, California

THOMPSON, Mendell S.
Library of Congress
Washington 25, D. C.

TRACEY R. A.
Burroughs Corp.
Research Center
Paoli, Pennsylvania

TRUMBULL, Dr. R., Code 454
Office of Naval Research
Washington 25, D. C.

TUNTURI, Dr.
Medical School
University of Oregon
Portland, Oregon

UTTLEY, Dr. A. M.
National Physical Laboratory
Teddington, Mddx.
England

WARE Willis H.
Numerical Analysis Dept.
The Rand Corporation
1700 Main Street
Santa Monica, California

WARHEIT I. A.
International Business Machines, Corp.
1737 L. Street, N. Y.
Washington, D. C.

Addresses

(1 copy each)

WIGINGTON R., Code R42
National Security Agency
Fort George G. Meade, Maryland

WILLIS D. G.
Lockheed Missiles and Space Division
3251 Hanover Street
Palo Alto, California

WILSON Donald F.
Code 5144
Naval Research Laboratory
Washington 25, D. C.

WINKLER, Dr. S.
IBM Corporation
Military Products Division
Owego, New York

WOOSTER, Dr. Harold
Air Force Office of Scientific Research
Washington 25, D. C.

Wright Air Development Division
Electronic Technology Laboratory
Wright Patterson Air Force Base, Ohio
Attn: WWRNEB Computer and Bionics Branch

Yntema, Dr. George
Operations Research, Inc.
8605 Cameron Street
Silver Spring, Maryland

Zschirnt, Dr. H. H.
Air Force Research Division, ARDC
Computer and Mathematical Sciences Lab.,
ARCRC
L. G. Hanscom Field, CRRB
Bedford, Massachusetts

UNCLASSIFIED